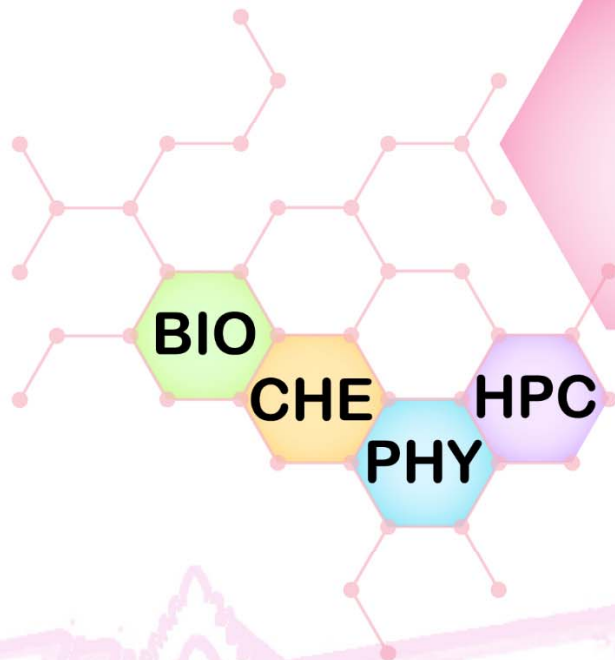




The 22nd International Annual Symposium on Computational Science and Engineering



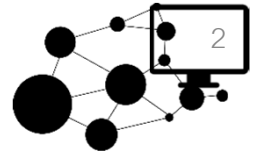
e-PROCEEDINGS



Faculty of Science, Chulalongkorn University
Bangkok, Thailand
Aug 2-3, 2018



WELCOME MESSAGE



On behalf of the Faculty of Science, Chulalongkorn University, I am truly honored and delighted to welcome you to the 22nd International Annual Symposium on Computational Science and Engineering (ANSCSE22). This year the conference is being held during August 2-3, 2018 at Faculty of Science, Chulalongkorn University, Bangkok, Thailand. This conference covers issues on Computational Biology, Chemistry, Physics, Mathematics and High-Performance Computing. I do hope that ANSCSE22 will be a platform to create a stage for exchanging the latest research results and sharing the advanced research ideas about all aspects of Computational Science and Engineering.

As the third largest faculty of the university, we are proud to be one of the best academic and intellectual institution in nation. The Faculty of Science also commits to provide professional services in the form of research consultation, workshops, seminars, national and international conferences, technology transfer and development. Therefore, we are pleased to have the opportunity to host for this event.

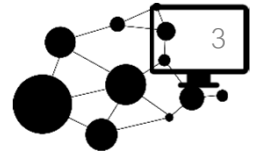
I would like to express my gratitude to the conference organizing committee, sponsors, technical support staffs, and participants who make this event remarkably successful. With your participation, I do believe that this conference will result in future collaborations between universities and research institutions both locally and internationally.

I wish all the success for this conference, and I also wish all of you taken an extra time to enjoy the spectacular and unique beauty of Thailand.



With best wishes,

Professor Dr. Polkit Sangvanich
Dean, Faculty of Science,
Chulalongkorn university

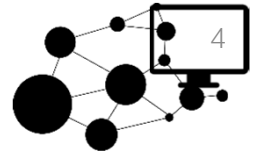


The 22nd session of the International Annual Symposium on Computational Science and Engineering or ANSCSE 22 is hosted by Faculty of Science, Chulalongkorn University. This long continuation of the symposium cannot at all be realized without strong support from host institutions. It also suggested that the community of computational scientists is very well established in Thailand. Usually, there are four parallel sessions with six areas of research. They included computational chemistry, computational biology, computational physics and fluid dynamics, and computer science and high-performance computing. In the future, we might need to include "data science" as one of the research areas, since it is the today growing field. For this year, I would like to thank Chulalongkorn University, the host, for their willingness and consistent effort in putting a tremendous scientific program. This is not the first time that they hosted this event, but the third time. Also, thanks go to our plenary lecturers, Professor David Ruffolo from Mahidol University, Professor Putchong Uthayopas from Kasetsart University, and Professor Ras B. Pandey from University of Southern Mississippi, U.S.A. Last but not least, thanks to our invited speakers and all participants of ANSCSE 22. I hope you all will continue to join and support this annual symposium for the next year.

Associate Professor Dr. Vudhichai Parasuk
President of Computational Science and
Engineering Association (CSEA)



WELCOME MESSAGE

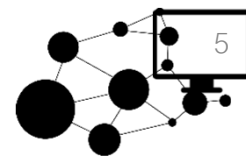


On behalf of the organizing committee, I am honored and delighted to welcome you to the 22nd International Annual Symposium on Computational Science and Engineering (ANSCSE22) at Faculty of Science, Chulalongkorn University.

As a conference chair, I know that the success of the conference depends ultimately on the many people who have worked with us in planning and organizing both the scientific program and supporting arrangements. In particular, we thank the Program Chairs for organizing the technical program, the Program Committee for their thorough and timely reviewing of the papers, our sponsors who have helped us to keep down the costs of ANSCSE22, and all participants who contribute to the progress of scientific research in their field. Recognition should go to the Organizing Committee members who have all worked extremely hard for the details of important aspects of the conference programs and activities.



Professor Dr. Supot Hannongbua
Conference Chair of ANSCSE22



Steering Committee

Asst. Prof. Putchong Uthayopas, Kasetsart University, Thailand

Assoc. Prof. Vudhichai Parasuk, Chulalongkorn University and Acting President of CSEA, Thailand

Prof. Supa Hannongbua, Kasetsart University, Thailand

Honorary Chair

Assoc. Prof. Polkit Sangvanich, Dean of Faculty of Science, Chulalongkorn University, Thailand

Prof. Tirayut Vilanvan, Deputy Dean for Research Affairs, Faculty of Science, Chulalongkorn University, Thailand

Asst. Prof. Sureerat Deowanish, Deputy Dean for Academic Affairs, Faculty of Science, Chulalongkorn University, Thailand

Scientific Committee Chair

Assoc. Prof. Pornthep Sompornpisut, Chulalongkorn University, Thailand

Scientific Committee

Assoc. Prof. Siriporn Jungsuttiwong, Ubon Ratchathani University, Thailand

Asst. Prof. Nawee Kungwan, Chiang Mai University, Thailand

Assoc. Prof. Jiraroj T-Thienprasert, Kasetsart University, Thailand

Asst. Prof. Thanyada Rungrotmongkol, Chulalongkorn University, Thailand

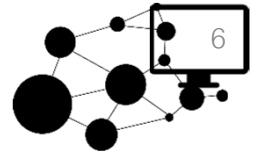
Assoc. Prof. Vejapong Juttijudata, Kasetsart University, Thailand

Asst. Prof. Putchong Uthayopas, Kasetsart University, Thailand

Assoc. Prof. Vara Varavithya, King Mongkut's University of Technology North Bangkok, Thailand

Dr. Supakit Prueksaaron, Thammasat University, Thailand

Dr. Supawadee Namuangruk, National Nanotechnology Center (NANOTEC), NSTDA, Thailand



International Scientific Committee

Prof. Jun Li, Tsinghua University, China

Assoc. Prof. Phornphimon Maitarad, Shanghai University, China

Assoc. Prof. Deva Priyakumar, International Institute of Information Technology, Hyderabad, India

Asst. Prof. Satoru Itoh, Institute for Molecular Science, Japan

Prof. Yasuteru Shigeta, University of Tsukuba, Japan

Assoc. Prof. Norio Yoshida, Kyoshu University, Japan

Prof. Seiji Mori, Ibaraki University, Japan

Assoc. Prof. Hisashi Okumura, Institute for Molecular Science, Japan

Prof. Jen-Shiang K. Yu, National Chiao Tung University, Taiwan

Dr. Kaito Tankahashi, Academia Sinica, Taiwan

Prof. Ras B. Pandey, University of Southern Mississippi, USA

Prof. Eduardo Perozo, University of Chicago, USA

Prof. Michael Green, City College of the City University of New York, USA

Organizing Committee Chair

Prof. Supot Hannongbua, Chulalongkorn University, Thailand

Organizing Committee

Prof. Sirirat Kokpol, Chulalongkorn University, Thailand

Assoc. Prof. Viwat Vchirawongkwin, Chulalongkorn University, Thailand

Asst. Prof. Somsak Pianwanit, Chulalongkorn University, Thailand

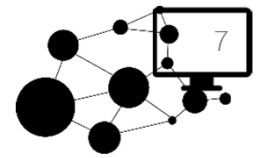
Asst. Prof. Kanet Wongravee, Chulalongkorn University, Thailand

Asst. Prof. Tatiya Chokbunpiam, Ramkhamhaeng University, Thailand

Dr. Nattapong Paiboonvorachat, Chulalongkorn University, Thailand

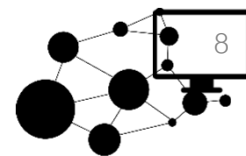
Asst. Prof. Thanyada Rungrotmongkol, Chulalongkorn University, Thailand

TABLE OF CONTENTS



	Page
Welcome Message	2
Committee	5
General Information	8
Conference Map	10
Plenary Lecture	13
List of Invited Speakers	14
Programme	16
e-Proceedings	36
CHE:	
A theoretical study of fluorene based copolymers for solar cell applications, <i>Nuttaporn Janprapa and Chinapong Kritayakornupong</i>	37
Computational Study of Binding Mode of Depsidones in Vascular Endothelial Growth Factor Receptor-2, <i>C. Suksamrarn; P. Saparpakorn and S. Hannongbua</i>	45
PHY:	
Identify Transient Sources from GOTO Sky Survey Data with Clustering Method, <i>W. Yu, R. Yoyponsan; T. Boongoen; J. Mullaney; K. Ulaczyk; U. Sawangwit and A. Eungwanichayapant</i>	52
HPC:	
Loop prevention on Software Defined Network using Adaptive Virtual Tunnel Network, <i>Piyakorn Phanklin; Nuttapol Sermsuksakulchai; Thadthai Szeto; Sirichai Kamnerdlom; Worrapong Arnyong; Suthep Wiwatchaiwong; and Supakit Prueksaroon</i>	64
Resilience flow management on Software-Defined Network using the Directed graph for L2 Loop prevention, <i>Kanjanart Junnawat; Mookdaporn Roekpootaweeporn, and Supakit Prueksaaroon</i>	70
Existence and Approximation of Solutions of Coupled Fractional Order Hybrid Differential Equations, <i>Dussadee Somjaiwang, and Parinya Sa Ngiamsunthorn</i>	76
Sponsors	90

GENERAL INFORMATION



Conference Venue

Mahamakut (MHMK) Building, Faculty of Science, Chulalongkorn University, Bangkok, Thailand

Registration

Registration desk is located in front of the conference room 207 on the 2nd floor of MHMK building.

Registration hours:	Thursday, 2nd August	8:00 - 16:00
	Friday, 3rd August	8:00 - 12:00

Badges

Badges can be picked up on 2nd-3rd August at the registration desk and should be worn for admission to all scientific sessions and the social events.

Workshop

The workshop will take place in 1101/2 Self-Learning Room (Chemistry Library), The 11th floor, MHMK building on Wednesday, 1st August.

Conference Rooms

The conference rooms are 205, 206, 207 and 208 on the 2nd floor of MHMK building.

Plenary and Invited Speakers, Oral Presenters

We kindly ask all speakers to come to the conference room to load/check their presentation at least **20 minutes** prior to their session to ensure the presentation is checked and tested. Technical staffs in the room will assist in uploading and setting up your presentation. Presentations should be provided in a version of Microsoft PowerPoint. If your presentation is in MAC format, it is imperative that this be converted to PC format. Please make a copy of your presentation in your flash drive in order to upload onsite. If speakers wish to use their own laptop, please inform the staff prior to the start of your session for setting up your laptop with the projector.

Poster Session

Poster session is located on the 3rd floor of MHMK building. The poster boards can fit posters up to the A0 size (Width x Height : 84.1 × 118.9 cm, or 33.1 in × 46.8 in) in portrait orientation. Printed posters should be mounted beginning at 8:00 on Thursday 2nd Aug and **MUST** be removed by 18:00 on the same day. Posters are arranged according to research areas. Posters with an odd ID number should be presented from 13:55-14:45. Posters with an even ID number should be presented from 14:45-15:35. For e-Poster, there will be either laptop or TV monitor provided.

Internet Access

To access internet, Chulalongkorn University wireless is available free-of-charge. Please contact IT Staff for internet access account and code.



GENERAL INFORMATION



Lunch

Lunch will be served at the ground floor of MHMK building.

Exhibition

The exhibition is located at the 2nd floor of MHMK building. The “Vendor Session” will be held on 2nd August, 15:45-17:20 at room 206.

Banquet

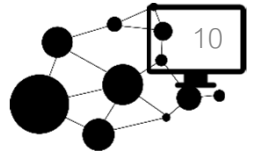
The banquet will take place on 2nd August at Ho Noy, the ground floor of Poosub Noppahawong Na Ayutthaya Building, Faculty of Education.

CU Shuttle Bus

Chulalongkorn University provides free shuttle service for faculty, staff, students, and visitors with safe and convenient transportation to most sites on campus. The shuttle service runs during from Monday to Saturday, 7AM – 7PM.

For more details please visit the website: <https://www.chula.ac.th/en/about/green-university/cu-shuttle-bus/>

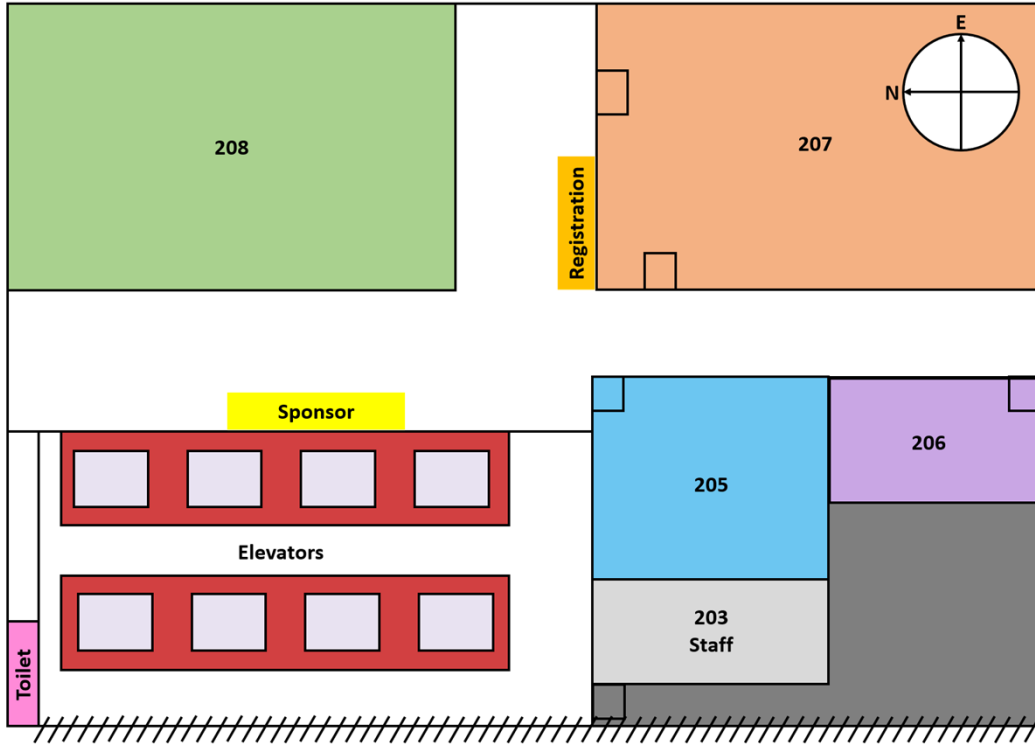




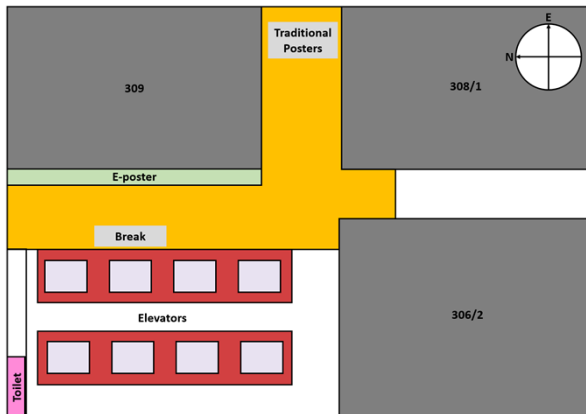
MAP

CONFERENCE ROOM

2nd floor MHMK Building

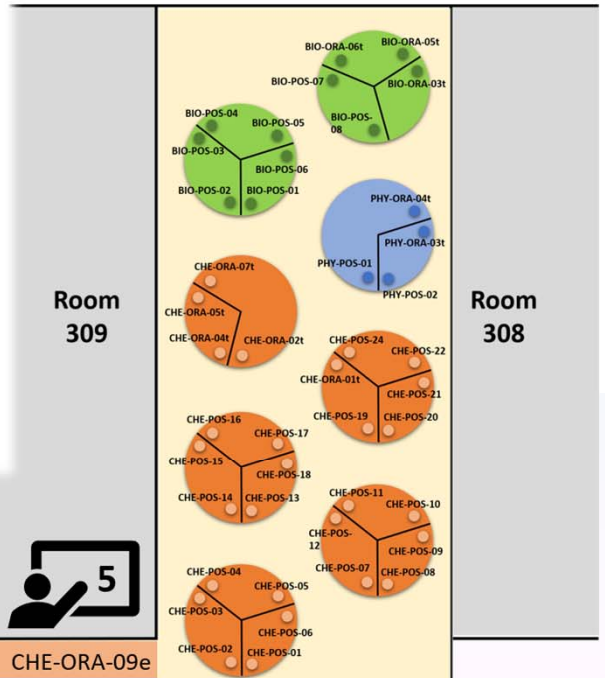


3rd floor MHMK Building



Traditional Posters

CHE PHY BIO HPC

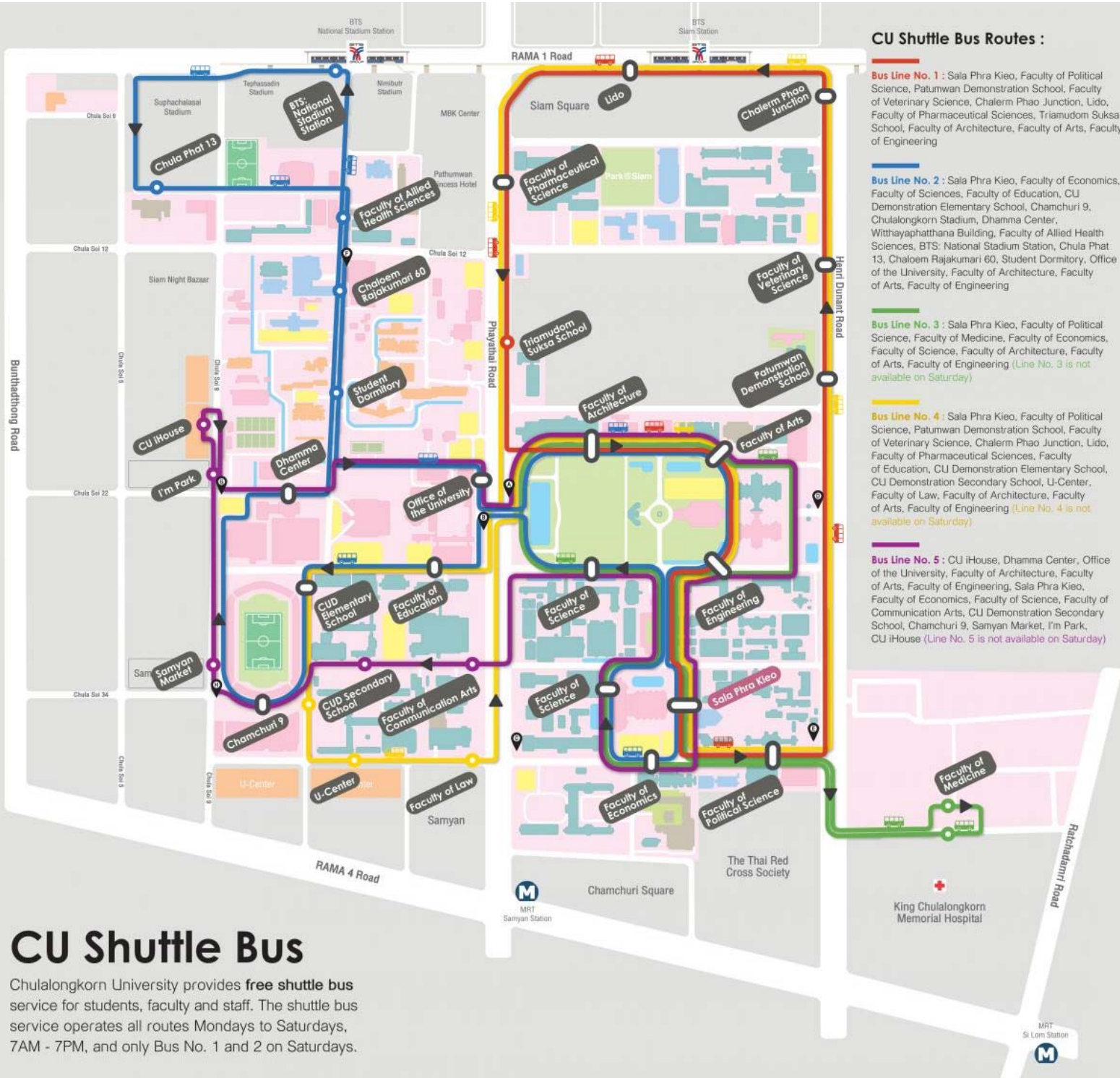


Time	1	2	3	4	5
13:55-14:20	BIO-ORA-01e	BIO-ORA-07e	BIO-ORA-09e	CHE-ORA-03e	CHE-ORA-09e
14:20-14:45	PHY-ORA-05e	PHY-ORA-07e	HPC-ORA-01e	HPC-ORA-03e	HPC-ORA-05e
14:45-15:10	BIO-ORA-02e	BIO-ORA-04e	BIO-ORA-08e	CHE-ORA-10e	CHE-ORA-12e
15:10-15:35	PHY-ORA-02e	PHY-ORA-06e	HPC-ORA-02e	E-Posters	



Conference 2-3 Aug 2018

Chulalongkorn University map link to public transportation

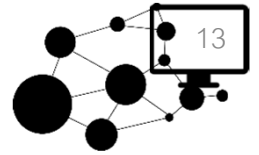


CU Shuttle Bus

Chulalongkorn University provides **free shuttle bus** service for students, faculty and staff. The shuttle bus service operates all routes Mondays to Saturdays, 7AM - 7PM, and only Bus No. 1 and 2 on Saturdays.

BANQUET LOCATION





PL-1: Monte Carlo simulations of energetic particle transport in space, in Earth's atmosphere, and in a cosmic ray detector

David Ruffolo

Department of Physics, Faculty of Science, Mahidol University, Bangkok, Thailand



PL-2: Future of High Performance Computing

Putchong Uthayopas

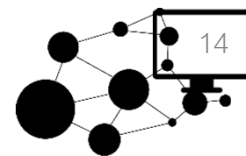
Department of Computer Engineering, Faculty of Engineering, Kasetsart University, Bangkok, Thailand



PL-3: Morphing structures and dynamics by a multigrain approach

Ras B. Pandey

*Department of Physics and Astronomy
University of Southern Mississippi, Hattiesburg, USA*



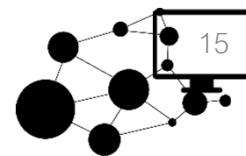
LIST OF INVITED SPEAKERS

Computational Biology, Bioinformatics, Biochemistry and Biophysics

BIO-INV-01	Yasuteru	Shigeta	University of Tsukuba	Japan
BIO-INV-02	Hisashi	Okumura	Institute for Molecular Science	Japan
BIO-INV-03	Satoru G.	Itoh	Institute for Molecular Science	Japan
BIO-INV-04	Michael E	Green	The City College of CUNY	USA
BIO-INV-05	Norio	Yoshida	Kyushu University	Japan
BIO-INV-06	Chia-Ching	Chang	National Chiao Tung University	Taiwan
BIO-INV-07	Tawun	Remsungnen	Khon Kaen University	Thailand
BIO-INV-08	Jen-Shiang K.	Yu	National Chiao Tung University	Taiwan
BIO-INV-09	Sira	Sriswasdi	Chulalongkorn University	Thailand
BIO-INV-10	Chih-Hao	Lu	China Medical University	Taiwan

Computational Chemistry

CHE-INV-01	Seiji	Mori	Ibaraki University	Japan
CHE-INV-02	Tanin	Nanok	Kasetsart University	Thailand
CHE-INV-03	Phornphimon	Maitarad	Shanghai University	China
CHE-INV-04	Kaito	Takahash	Academia Sinica	Taiwan
CHE-INV-05	Pussana	Hirunsit	NANOTEC, NSTDA	Thailand
CHE-INV-06	Paul M.	Gleeson	KMITL	Thailand
CHE-INV-07	Deva U.	Priyakumar	International Institute of Information Technology	India
CHE-INV-08	Thana	Maihom	Kasetsart University	Thailand
CHE-INV-09	Tatiya	Chokbunpiam	Ramkhamhaeng University	Thailand



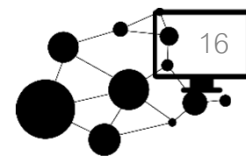
LIST OF INVITED SPEAKERS

Computational Fluid Dynamics and Solid Mechanics

PHY-INV-01	Pakpoom	Reunchan	Kasetsart University	Thailand
PHY-INV-02	Jariyanee	Prasongkit	Nakhon Phanom University	Thailand
PHY-INV-03	Thanayut	Kaewmaraya	Khon Kaen University	Thailand
PHY-INV-04	Udomsilp	Pinsook	Chulalongkorn University	Thailand
PHY-INV-05	Rob	Knoops	Chulalongkorn University	Thailand
PHY-INV-06	Adisak	Boonchun	Kasetsart University	Thailand
PHY-INV-07	Worasak	Sukkabot	Ubon Ratchathani University	Thailand

High Performance Computing, Computer Science, Mathematics and Engineering

HPC-INV-01	Rudklao	Pan-Aram	Electricity Generating Authority of Thailand	Thailand
HPC-INV-02	Monrudee	Liangruksa	NANOTEC	Thailand
HPC-INV-03	Manaschai	Kunaseth	NANOTEC, NSTDA	Thailand
HPC-INV-04	Thiansin	Liamsuwan	Chulabhorn Royal Academy	Thailand



PROGRAMME

Wednesday, 1st August 2018

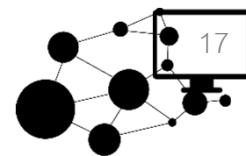
Location: Mahamakut (MHMK) Building, Faculty of Science, Chulalongkorn University

Workshop

Time		Room
08:30-09:00	Registration for Workshop (11 th Floor)	1101/2 Self-Learning Room (Chemistry Library) 11 th Floor
09:00-12:00 (Lecture)	Workshop: Ab Initio Simulation of Reaction Rates and Vibrational Spectra Professor Dr. Kaito Takahashi, Institute of Atomic and Molecular Sciences, Academia Sinica, Taiwan	
13:00-16:00 (Practice)	Demonstration	



Workshop



PROGRAMME

Thursday, 2nd August 2018

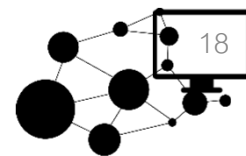
Location: Mahamakut (MHMK) Building, Faculty of Science, Chulalongkorn University

Conference Day 1

Time					Room
08:00-08:30	Registration				2 nd Floor
08:30-08:45	Opening Ceremony Professor Dr. Polkit Sangvanich, Dean of Faculty of Science				207 2 nd Floor
08:45-09:30	Plenary Lecture 1 Title: Monte Carlo simulations of energetic particle transport in space, in Earth's atmosphere, and in a cosmic ray detector Professor Dr. David Ruffolo. Department of Physics, Mahidol University				
09:30-09:40	Group Photo				
09:40-10:00	Coffee Break				2 nd Floor
Oral Presentation 1 (Parallel Sessions)					
Session	Room 208	Room 207	Room 205	Room 206	
	BIO 1	CHE 1	PHY 1	HPC 1	
10:00-12:00	BIO-INV-01 BIO-INV-02 BIO-INV-03	CHE-INV-01 CHE-INV-02 CHE-INV-03	PHY-INV-01 PHY-INV-02 PHY-INV-03	HPC-INV-01 HPC-INV-02	
	BIO-ORA-01e BIO-ORA-02e BIO-ORA-03t	CHE-ORA-01t CHE-ORA-02t CHE-ORA-03e	PHY-ORA-01 PHY-ORA-02e PHY-ORA-03t	HPC-ORA-01e HPC-ORA-02e HPC-ORA-03e	
12:00-13:00	Lunch				Ground Floor
13:00-13:45	Plenary Lecture 2 Title: Future of High Performance Computing Assistant Professor Dr. Putchong Uthayopas, Department of Computer Engineering, Kasetsart University				207 2 nd Floor
13:50-15:40	Poster Session Odd-numbered poster: 13.55-14.45 Even-numbered poster: 14.45-15.35				3 rd Floor
	Coffee Break (Starting at 14:30 on the 3 rd floor)				
Oral Presentation 2 (Parallel Sessions)					
Session	Room 208	Room 207	Room 205	Room 206	
	BIO 2	CHE 2	PHY 2	Special Session	
15:45-17:20	BIO-INV-04 BIO-INV-05	CHE-INV-04 CHE-INV-05	PHY-INV-04 PHY-INV-05	Hewlett Packard Enterprise intel	
	BIO-ORA-04e BIO-ORA-05t BIO-ORA-06t	CHE-ORA-04t CHE-ORA-05t CHE-ORA-06	PHY-ORA-04t PHY-ORA-05e PHY-ORA-06e	DELL EMC	
18:00-20:00	Banquet Location: Ho Noy, Poonsub Noppawong Na Ayutthaya Building (Ground Floor), Faculty of Education				



Overview



PROGRAMME

Friday, 3rd August 2018

Location: Mahamakut (MHMK) Building, Faculty of Science, Chulalongkorn University

Conference Day 2

Time					Room
08:00-09:00	Registration				2 nd Floor
09:00-09:45	Plenary Lecture 3 Title: Morphing Structures and Dynamics by Multi-Grain Computer Simulation Modeling Professor Dr. Ras B. Pandey, University of Southern Mississippi, USA				207 2 nd Floor
09:45-10:00	Coffee Break				2 nd Floor
Oral Presentation 3 (Parallel Sessions)					
Session	Room 208	Room 207	Room 205	Room 206	
	BIO 3	CHE 3	PHY 3	HPC 2	
10:00-11:45	BIO-INV-06 BIO-INV-07 BIO-INV-08	CHE-INV-06 CHE-INV-07	PHY-INV-06 PHY-INV-07	HPC-INV-03 HPC-INV-04	
	BIO-ORA-07e BIO-ORA-08e	CHE-ORA-07t CHE-ORA-08	PHY-ORA-07e PHY-ORA-08	HPC-ORA-04 HPC-ORA-05e	
11:45-13:00	Lunch				Ground Floor
Oral Presentation 4 (Parallel Sessions)					
Session	Room 208	Room 207	Room 205		
	BIO 4	CHE 4	CHE 5		
13:00-14:05	BIO-INV-09 BIO-INV-10 BIO-ORA-09e	CHE-INV-08 CHE-ORA-09e CHE-ORA-10e	CHE-INV-09 CHE-ORA-11 CHE-ORA-12e		
14:30-15:00	Presentation Awards & Closing & Rich Coffee				207

Presentation Code Definition



AAA: BIO = Computational Biology, Bioinformatics, Biochemistry and Biophysics
 CHE = Computational Chemistry
 PHY = Computational Physics, Computational Fluid Dynamics and Solid Mechanics
 HPC = High Performance Computing, Computer Science, Mathematics and Engineering

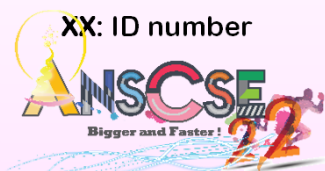
BBB: INV = Invited Speaker
 ORA = Oral Presenter
 POS = Poster Presenter

c: The letter indicates the presenter who is going to present their work in both ORAL and POSTER sessions.

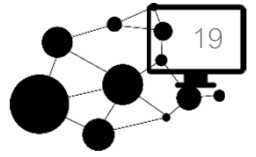
Poster type is indicated as following:

t = Paper printed poster
 e = E-poster

XX: ID number



Overview



PROGRAMME

Thursday, 2nd August 2018

Location: Mahamakut (MHMK) Building, Faculty of Science, Chulalongkorn University

Room 207, MHMK Building, Time 8:00-10:00

Time	
08:00-08:30	Registration
08:30-08:45	Opening Ceremony Welcome Remarks Professor Polkit Sangvanich, Dean of Faculty of Science MC: <i>Thanyada Rungrotmongkol and Tanin Nanok</i>
08:45-09:30	Plenary Lecture 1 Professor Dr. David Ruffolo. Department of Physics, Mahidol University Title: Monte Carlo simulations of energetic particle transport in space, in Earth's atmosphere, and in a cosmic ray detector <i>Chair: Supot Hannongbua, Chulalongkorn University</i>
09:30-09:40	Group Photo
09:40-10:00	Coffee Break

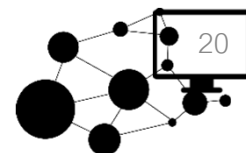
Room 207, MHMK Building

Time	
13:00-13:45	Plenary Lecture 2 Assistant Professor Dr. Putchong Uthayopas, Department of Computer Engineering, Faculty of Engineering, Kasetsart University Title: Future of High Performance Computing <i>Chair: Supa Hannongbua, Kasetsart University</i>



Computational Biology, Bioinformatics,
Biochemistry and Biophysics Session

PROGRAMME



Thursday, 2nd August 2018

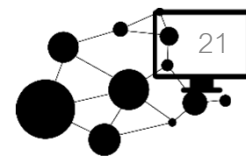
Computational Biology, Bioinformatics, Biochemistry and Biophysics

Session BIO 1			Room 208, MHMK Building
Co-chairs : Yasuteru Shigeta, University of Tsukuba Hisashi Okumura, Institute for Molecular Science			Time 10:00-12:00
Time	Code	Presenter	Title
10:00-10:25	BIO-INV-01	Yasuteru Shigeta University of Tsukuba, Japan	Data-driven Parallel Cascade Selection Molecular Dynamics
10:25-10:50	BIO-INV-02	Hisashi Okumura Institute for Molecular Science, Japan	Simulational studies of A β amyloid fibrils by molecular dynamics method
10:50-11:15	BIO-INV-03	Satoru Itoh Institute for Molecular Science, Japan	Molecular dynamics simulations of a full-length amyloid- β peptide at a hydrophobic/hydrophilic interface
11:15-11:30	BIO-ORA-01e	Panupong Mahalapbutr Chulalongkorn University	Anticancer activity of mansonone G derivatives against human non-small cell lung cancer
11:30-11:45	BIO-ORA-02e	Bodee Nutho Chulalongkorn University	Reaction Mechanism of the Zika Virus NS2B/NS3 Serine Protease with Its Substrate: A QM/MM Study
11:45-12:00	BIO-ORA-03t	Wansiri Innok Thaksin University	The Potential of Interested Leading Alkaloid and Flavonoid Compounds in Thai Herbs against Achetylcholinesterase Inhibitory of Alzheimer's Disease

Session BIO 2			Room 208, MHMK Building
Co-chairs : Michael Green, CCNY : Norio Yoshida, Kyoshu University			Time 15:45-17:20
Time	Code	Presenter	Title
15:45-16:10	BIO-INV-04	Michael Green City College of the City University of New York, USA	Quantum Calculations on the Voltage Sensing Domain of a Voltage Gated Ion Channel
16:10-16:35	BIO-INV-05	Norio Yoshida Kyoshu University, Japan	Theoretical study of biological processes employing statistical mechanics of molecular liquids
16:35-16:50	BIO-ORA-04e	Phakawat Chusuth Chulalongkorn University	The binding of cobratoxin from Naja kaouthia towards nicotinic acetylcholine receptor (nAChR)
16:50-17:05	BIO-ORA-05t	Tadsanee Awang Kasetsart University	Computational studies of the adsorption of human defensin 5 on bacterial membranes
17:05-17:20	BIO-ORA-06t	Channarong Khрутто Chulalongkorn University	Molecular dynamics simulations of M2 channel in phospholipid bilayers with different thickness



Computational Biology, Bioinformatics, Biochemistry and Biophysics Session



PROGRAMME

Thursday, 2nd August 2018

Computational Chemistry

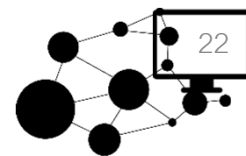
Session CHE 1			
Co-chairs: <i>Kaito Takahashi, Academia Sinica</i> <i>: Supawadee Namungruk, NSTDA</i>			Room 207, MHMK Building Time 10:00-12:00
Time	Code	Presenter	Title
10:00-10:25	CHE-INV-01	Seiji Mori Ibaraki University, Japan	Mechanistic Insights into Metal-Catalyzed Highly Selective Organic Transformation Reactions
10:25-10:50	CHE-INV-02:	Tanin Nanok Kasetsart University	Towards a Molecular Understanding of the Relative Reactivities of ϵ -Caprolactone and L-Lactide in Their Homo- and Copolymerization Using Aluminium Salen-type Initiators: A DFT Study Screen reader support enabled
10:50-11:15	CHE-INV-03	Phornphimon Maitarad, Shanghai University, China	QSAR Study of Phenoxy-imine Catalytic Behavior in Polyethylene Polymerization
11:15-11:30	CHE-ORA-01t	Nuttaporn Janprapa King Mongkut's University of Technology Thonburi	A theoretical study of fluorene based copolymers for solar cell applications
11:30-11:45	CHE-ORA-02t	Rattanawalee Rattanawan Ubon Ratchathani University	Molecular Engineering of D-A Featured Organic Indole Sensitizers for Improving Performance Efficiency of Dye-Sensitized Solar Cells
11:45-12:00	CHE-ORA-03e	Pipat Khongpracha Kasetsart University	Charge Carriers Distribution in Platinum Doped Graphitic Carbon Nitride Quantum Dot

Session CHE 2			
Co-chairs: <i>Deva Priyakumar, IIIT Hyderabad</i> <i>: Pussana Hirunsit, NSTDA</i>			Room 207, MHMK Building Time 15:45-17:20
Time	Code	Presenter	Title
15:45-16:10	CHE-INV-04	Kaito Takahashi Academia Sinica, Taiwan	The Imprint of Electronic Structure on the Reactivity of Linear Carbon Chain Cations
16:10-16:35	CHE-INV-05	Pussana Hirunsit NANOTEC, NSTDA	Theoretical Investigation of CO ₂ Electrochemical Reduction on Cu-based Catalysts: The Effect of Surface Facets and The Role of S Dopant
16:35-16:50	CHE-ORA-04t	Yuwanda Injongkol Ubon Ratchathani University	The mechanism of carbon dioxide hydrogenation to formic acid on Pt-boron nitride nanosheets (Pt-BNNSs): A theoretical study
16:50-17:05	CHE-ORA-05t	Nuttapon Yodsin Ubon Ratchathani University	The theoretical study of catalytic CO ₂ hydrogenation to formic acid over a metal-decorated carbon nanocone
17:05-17:20	CHE-ORA-06	Preeyaporn Poldorn Ubon Ratchathani University	Ag ₇ Au ₆ cluster as a highly active catalyst for CO oxidation: Theoretical study



Computational Chemistry Session

PROGRAMME



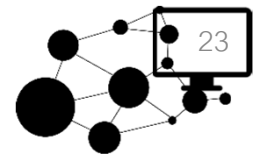
Thursday, 2nd August 2018

Computational Physics, Fluid Dynamic and Solid Mechanics

Session PHY 1 Co-chairs: <i>Thanayut Kaewmaraya, Khon Kaen University</i> <i>: Pakpoom Reunchan, Kasetsart University</i>			Room 205, MHMK Building Time 10:00-12:00
Time	Code	Presenter	Title
10:00-10:25	PHY-INV-01	Pakpoom Reunchan Kasetsart University	Self-trapped hole in BaTiO ₃
10:25-10:50	PHY-INV-02	Jariyane Prasongkit Nakhon Phanom University	First-Principles Study of Two-Dimensional Materials for Nanoelectronics
10:50-11:15	PHY-INV-03	Thanayut Kaewmaraya Khon Kaen University	2D van der Waals Heterostructures for Nanoelectronics
11:15-11:30	PHY-ORA-01	Sujin Suwana Mahidol University	First-Principle Study of Strain-Induced Band Gap Tunability of Two-Dimensional Transition Metal Dichalcogenides MX ₂ (M = Mo, W; X = O, S, Se, Te)
11:30-11:45	PHY-ORA-02e	Abdulmutta Thatribud Prince of Songkla University	Electronic and Optical Properties of Silver Chloride Photocatalyst by First Principles calculation
11:45-12:00	PHY-ORA-03t	Sorayot Chinkanjanarot National Metal and Materials Technology Center	Predicting Coefficient of Linear Thermal Expansion of Carbon Fiber/Graphene Nanoplatelet/EPON862 Hybrid Composites: Multiscale Modeling
Session PHY 2 Co-chairs: <i>Rob Knoops, Chulalongkorn University</i> <i>: Udomsilp Pinsook, Chulalongkorn University</i>			Room 205, MHMK Building Time 15:45-17:20
Time	Code	Presenter	Title
15:45-16:10	PHY-INV-04	Udomsilp Pinsook Chulalongkorn University	Essence of Correlation Energy
16:10-16:35	PHY-INV-05	Rob Knoops Chulalongkorn University	Inflation from Supersymmetry Breaking
16:35-16:50	PHY-ORA-04t	Atipong Malatip National Metal and Materials Technology Center	Matrix Tridiagonalization Methods for 3D Finite Element Analysis of Free Vibration
16:50-17:05	PHY-ORA-05e	Wanfeng Yu Mae Fah Luang University	Identify Transient Sources from GOTO Sky Survey Data with Clustering Method
17:05-17:20	PHY-ORA-06e	Vichayanun Wachirapusanand Chulalongkorn University	Machine Learning system mimicking student's choice in Particle Data Analysis laboratory activity



Computational Physics, Fluid Dynamic and Solid Mechanics Session



PROGRAMME

Thursday, 2nd August 2018

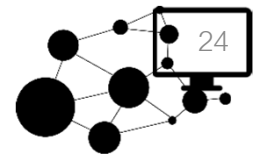
High Performance Computing, Computer Science, Mathematic & Engineering

Session HPC 1 Co-chairs: :		Room 206, MHMK Building Time 10:00-11:35	
Time	Code	Presenter	Title
10:00-10:25	HPC-INV-01	Rudklao Panaram Electricity Generating Authority of Thailand	Mathematics Computing in Environmental Quality for Power Plant
10:25-10:50	HPC-INV-02	Monrudee Liangruksa National Nanotechnology Center, Thailand	Mathematical modeling and analysis of thermal transport for materials design
10:50-11:05	HPC-ORA-01e	Piyakorn Phanklin Thammasat University	Loop prevention on Software Defined Network using Adaptive Virtual Tunnel Network
11:05-11:20	HPC-ORA-02e	Kanjanart Junnawat Thammasat University	Resilience flow management on Software-Defined Network using Directed graph for L2 Loop prevention
11:20-11:35	HPC-ORA-03e	Dussadee Somjaiwang King Mongkut's University	Existence and Approximation of Solutions of Coupled Fractional Order Hybrid Differential Equations



High Performance Computing, Computer Science,
Mathematic & Engineering Session




PROGRAMME



Thursday, 2nd August 2018

Special Vendor Session

Room 206, MHMK Building
Time 15:45-17:15

Time	Code	Presenter	Title
15:45-16:30	-	 	HPE Enterprise Infrastructure for HPC / AI / Deep Learning
16:30-17:15	-		Providing AI and ML Technology That Makes Tomorrow possible, Today

Note: Presentation in Thai



Special Vendor Session



PROGRAMME

Friday, 3rd August 2018

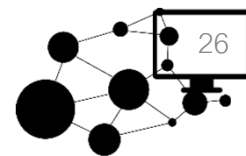
Location: Mahamakut (MHMK) Building, Faculty of Science, Chulalongkorn University

Room 207, MHMK Building

Time	
09:00-09:45	<p>Plenary Lecture 3</p> <p>Professor Ras B. Pandey, University of Southern Mississippi, USA Title: Morphing structures and dynamics by multi-grain computer simulation modeling</p> <p>Chair: <i>Siriporn Jungsutiwong, Ubon Ratchathani University</i></p>



Computational Biology, Bioinformatics,
Biochemistry and Biophysics Session



PROGRAMME

Friday, 3rd August 2018

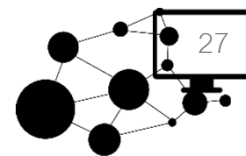
Computational Biology, Bioinformatics, Biochemistry and Biophysics

Session BIO 3 Co-chairs: <i>Chia-Ching Chang, National Chiao Tung University</i> <i>: Chih-Hao Lu, China Medical University</i>			Room 208, MHMK Building Time 10:00-11:45
Time	Code	Presenter	Title
10:00-10:25	BIO-INV-06	Chia-Ching Chang National Chiao Tung University, Taiwan	Structure and conducting mechanism characterization of DNA template guided nickel ion chain
10:25-10:50	BIO-INV-07	Tawun remsungnen Khon Kaen University	Biocompatible MOFs for Drug Delivery: Computational Studies
10:50-11:15	BIO-INV-08	Jen-Shiang K. Yu National Chiao Tung University, Taiwan	Catalytic Roles of Histidine and Arginine in Pyruvate Class II Aldolase
11:15-11:30	BIO-ORA-07e	Kanyani sangpheak Chulalongkorn University	In silico and in vitro studies of chalcones as potent anticancer agents with EGFR kinase
11:30-11:45	BIO-ORA-08e	Kanika Verma Chulalongkorn University	Exploring the Impact of R306C and F270V Mutations in β -Tubulin Structure and Function: A Computational Perspective

Session BIO 4 Co-chairs: <i>Jen-Shiang K. Yu, National Chiao Tung University</i>			Room 208, MHMK Building Time 13:00-14:05
Time	Code	Presenter	Title
13:00-13:25	BIO-INV-09	Sira Sriswasdi Faculty of Medicine, Chulalongkorn University	Toward Next-Generation Neoantigen Prediction with Deep Learning
13:25-13:50	BIO-INV-10	Chih-Hao Lu China Medical University, Taiwan	The relationship between protein function and local structural conservation
13:50-14:05	BIO-ORA-09e	Thapanar Suwanmajo Chiang Mai University	Tunable Signal Processing in Multi-site Phosphorylation Systems via Explicit Enzyme Activation



Computational Biology, Bioinformatics,
Biochemistry and Biophysics Session



PROGRAMME

Friday, 3rd August 2018

Computational Chemistry

Session CHE 3			Room 207, MHMK Building
Co-chairs: <i>Seiji Mori, Ibaraki University</i> <i>: Phornphimon Maitarad, Shanghai University</i>			Time 10:00-11:20
Time	Code	Presenter	Title
10:00-10:25	CHE-INV-06	Matthew Paul Gleeson King Mongkut's Institute of Technology	Application of Computational Methods in Anti-malarial Drug Discovery
10:25-10:50	CHE-INV-07	Deva Priyakumar International Institute of Information Technology, Hyderabad, India	Significance of Urea-Aromatic Interactions in Biology: A Computational Study
10:50-11:05	CHE-ORA-07t	Panyakorn Taweecat* Chulalongkorn University	Molecular dynamics simulations of hyaluronic acid in water
11:05-11:20	CHE-ORA-08	Chartniwat Suksamrarn Kasetsart University	Computational Study of Binding Mode of Depsidones in Vascular Endothelial Growth Factor Receptor-2
Session CHE 4			Room 207, MHMK Building
Chair: <i>Siriporn Jungsutiwong, Ubon Ratchathani University</i>			Time 13:00-13:55
Time	Code	Presenter	Title
13:00-13:25	CHE-INV-08	Thana Maihom Kasetsart University Kamphaeng Saen Campus	Designing Efficient Nanoporous Catalysts for Industrial Chemical Reactions
13:25-13:40	CHE-ORA-10e	Wasut Pornpatcharapong Chiang Mai University	Efficient Two-dimensional Ion Pairing Free Energy Surface Computation with Gaussian Process Regression
13:40-13:55	CHE-ORA-09e	Wiparat Hotarat Chulalongkorn University	Delivery of Alpha-mangostin through biological membrane using cyclodextrins: A molecular dynamics simulation study
Session CHE 5			Room 205, MHMK Building
Chair: <i>Tatiya Chokbunpiam, Ramkhamhaeng University</i>			Time 13:00-13:55
Time	Code	Presenter	Title
13:00-13:25	CHE-INV-09	Tatiya Chokbunpiam Ramkhamhaeng University	Temperature and Gas Loading Induced Structural-Dynamics Properties of Zeolitic Imidazolate Framework-90
13:25-13:40	CHE-ORA-11	Jitrayut Jitonnom Demonstration School of University of Phayao	Computational Modeling of Cationic Metallocene Polymerizations of 2- Oxazoline
13:40-13:55	CHE-ORA-12e	Cangtao Yin Institute of Atomic and Molecular Sciences, Academia Sinica	The reaction between Criegee intermediates and sulfur dioxide: not really barrierless



Computational Chemistry Session



PROGRAMME

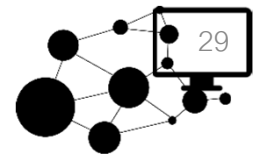
Friday, 3rd August 2018

Computational Physics, Fluid Dynamic and Solid Mechanics

Session PHY 3 Co-chairs: <i>Worasak Sukkabet, Ubon Ratchathani University</i> : <i>Adisak Boonchun, Kasetsart University</i>			Room 205, MHMK Building Time 10:00-12:00
Time	Code	Presenter	Title
10:00-10:25	PHY-INV-06	Adisak Boonchun Kasetsart University	The response of electronic properties of monolayer to elastic strain and the stacking stability of bilayer C2N
10:25-10:50	PHY-INV-07	Worasak Sukkabet Ubon Ratchathani University	Atomistic tight-binding theory in alloy semiconductor nanostructures
10:50-11:05	PHY-ORA-07e	Maneerat Chotsawat Synchrotron Light Research Institute	First-principles study of defects in Bi and Al doped orthorhombic PbZrO3
11:05-11:20	PHY-ORA-08	Wutthikrai Busayaporn Synchrotron Light Research Institute	Surface Structure Determination of TiO ₂ (110)(1x2) Dynamic Scattering of Electrons in LEED-IV



Computational Physics, Fluid Dynamic and Solid Mechanics Session



PROGRAMME

Friday, 3rd August 2018

High Performance Computing, Computer Science, Mathematic & Engineering

Session HPC 2 Co-chairs: :		Room 206, MHMK Building Time 10:00-11:20	
Time	Code	Presenter	Title
10:00-10:25	HPC-INV-03	Manaschai Kunaseth National Nanotechnology Center, Thailand	Shift/Collapse Algorithm for Fast and Scalable Many-Body n-Tuple Computation on Supercomputers
10:25-10:50	HPC-INV-04	Thiansin Liamswan Thailand Institute of Nuclear Technology	Computational Approaches for Pre-Clinical Study of a New Treatment Modality in Radiation Therapy
10:50-11:05	HPC-ORA-04	Pumipat Tongdom Kasetsart University	Differential equations learning from spatial-time series data by the fast iterative shrinkage thresholding algorithm
11:05-11:20	HPC-ORA-05e	Witcha Benjanirat Kasetsart University	Wavelet Gakerin Method for solving Korteweg-de Vries Equation with Neumann Boundary Conditions



High Performance Computing, Computer Science,
Mathematic & Engineering Session



POSTER SESSION

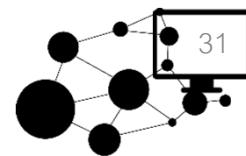
Thursday, 2nd August 2018
13:50-15:40, 3rd Floor, MHMK Building

Printed posters should be mounted beginning at 8:00 on Thursday 2nd Aug and **MUST** be removed by 18:00 on the same day. Posters are arranged according to research areas. There will be e-posters and printed posters.

Posters with an odd ID number should be presented from 13:55-14:45.

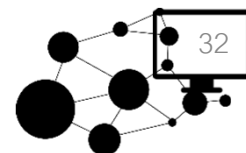
Posters with an even ID number should be presented from 14:45-15:35.





Code	Presenter	Title
BIO-POS-01	Nitchakan Darai Chulalongkorn university	<i>In silico</i> screening of chalcones against Epstein-Barr Nuclear Antigen 1 protein in Epstein-Barr virus.
BIO-POS-02	Jirayu Kammarabutr Chulalongkorn University	In Silico Studies on Potential Compounds against of Viral Hepatitis B Reverse Transcriptase
BIO-POS-03	Sasipha Seetin Kasetsart university	Binding investigation of pyrazine derivative against Glycogen synthase kinase-3 (GSK-3 β) via in silico molecular dynamics simulations
BIO-POS-04	Nayana Bhat Chulalongkorn university	Molecular insights into substrate binding mechanism of Glycerophosphoethanolamine to Glycerophosphodiesterase.
BIO-POS-05	Kowit Hengphasatporn Chulalongkorn University	Homopharma-Based Identification Target of Phenolic Lipid Derivatives Against Dengue Virus Infected Cell
BIO-POS-06	Pitchayathida Mee-udorn Chulalongkorn University	Molecular Dynamics Study on Human Serine Hydroxymethyltransferase with Pyridoxal Phosphate Bound
BIO-POS-07	Peerapong Wongpituk Chulalongkorn University	Effect of Pyridoxal phosphate on Human Serine Hydroxymethyltransferase by Molecular Dynamic Simulation
BIO-POS-08	Mattanun Sangkhawasi Chulalongkorn University	Effect of phenolic compounds as H5N1 influenza A neuraminidase inhibitors by molecular dynamic simulation
BIO-ORA-01e	Panupong Mahalapbutr Chulalongkorn University	Anticancer activity of mansonone G derivatives against human non-small cell lung cancer
BIO-ORA-02e	Bodee Nutho Chulalongkorn University	Reaction Mechanism of the Zika Virus NS2B/NS3 Serine Protease with Its Substrate: A QM/MM Study
BIO-ORA-03t	Wansiri Innok Thaksin University	The Potential of Interested Leading Alkaloid and Flavonoid Compounds in Thai Herbs against Achetylcholinesterase Inhibitory of Alzheimer's Disease
BIO-ORA-04e	Phakawat Chusuth Chulalongkorn University	The binding of cobratoxin from <i>Naja kaouthia</i> towards nicotinic acetylcholine receptor (nAChR)
BIO-ORA-05t	Tadsanee Awang Kasetsart University	Computational Studies of the Adsorption of Human Defensin 5 on Bacterial Membranes
BIO-ORA-06t	Channarong Khрутто Chulalongkorn University	Molecular Dynamics Simulations of M2 Channel in Phospholipid Bilayers with Different Thickness
BIO-ORA-07e	Kanyani Sangpheak Chulalongkorn university	In silico and in vitro studies of chalcones as potent anticancer agents with EGFR kinase
BIO-ORA-08e	Kanika Verma Chulalongkorn University	Exploring the Impact of R306C and F270V Mutations in β -Tubulin Structure and Function: A Computational Perspective
BIO-ORA-09e	Thapanar Suwanmajo Chiang Mai University	Tunable Signal Processing in Multi-site Phosphorylation Systems via Explicit Enzyme Activation

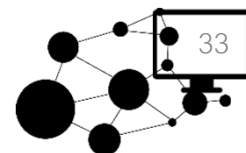
Computational Chemistry Session



Code	Presenter	Title
CHE-POS-01	Rathawat Daengngern King Mongkut's Institute of Technology Ladkrabang	Dynamics Simulation of Excited-State Intramolecular Proton Transfer Reactions of 2,5-bis(2'-benzoxazolyl) hydroquinone
CHE-POS-02	Tinnakorn Saelee Chiang Mai University	Theoretical investigation of Propane Dehydrogenation on Ni(111) surface
CHE-POS-03	Khanittha Kerdpol Chiang Mai University	Replica Exchange Molecular Dynamics Simulations of 2-Hydroxypropyl- β -Cyclodextrin
CHE-POS-04	Panisak Boonamnaj Chulalongkorn University	The pH-Dependent Shaping of Water-filled Crevice in the Hv1 Channel
CHE-POS-05	Rusrina Salaeh Chiang Mai University	Electronic and photophysical properties of derivatives of 2-phenylbenzothiazole and 2-(2'-hydroxyphenyl) benzothiazole: Effect of intramolecular hydrogen bonding
CHE-POS-06	Chattarika Sukpattanacharoen Chiang Mai University	Heteroatom effect on electronic and photophysical properties of 3-hydroxyquinolin-4(H)-one and its derivatives enhancing in the excited-state intramolecular proton transfer processes: A TD-DFT study on substitution effect
CHE-POS-07	Karan Bobuatong Rajamangala University of Technology Thanyaburi	Density functional theory insight towards the design of ionic liquids for CO ₂ capture
CHE-POS-08	Narissa Kanlayakan Chiang Mai University	Path Integral Molecular Dynamics Simulations for Muoniated Thioformaldehyde Radicals
CHE-POS-09	Panita Kongsune Thaksin University	Inhibitory of Influenza H1N1 Hemagglutinin with Flavonoid Compounds from Thai Herbs
CHE-POS-10	Bundet Boekfa Kasetsart University;	An ONIOM study on the 7-hydroxyl-4-methylcoumarin synthesis with H-Beta zeolite
CHE-POS-11	Jakkapan Sirijaraensre Kasetsart University	Effect of Impurities in MgCl ₂ Support for Polymerization of Ethylene with Heterogeneous Ziegler-Natta Catalyst: A DFT Study
CHE-POS-12	Pavee Pongsajanukul Chulalongkorn University	Computational calculation of CO ₂ adsorption in MIL-127(Fe) Metal Organic Framework
CHE-POS-13	Thanawit Kuamit Chulalongkorn university	ELECTRONIC PROPERTIES OF PYRENE ADSORBED ON GRAPHENE NANOFKAKES
CHE-POS-14	Chirawat Chitpakdee National nanotechnology center	Cooperation of Single Co Atom with Defect MoS ₂ as a High Efficient Catalyst for H ₂ O Reaction: A DFT Study
CHE-POS-15	Warin Jetsadawisut, Chulalongkorn university	Molecular Dynamics Simulation of Nanodiscs using Coarse-Grained model
CHE-POS-16	Panichakorn Jaiyong Thammasat University	Computational Insight into Noncovalent Interaction of Solid Polymer Electrolytes on Graphene Surface for Fabrication of Supercapacitor Electrodes

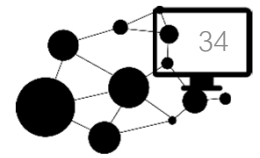


Computational Chemistry Session

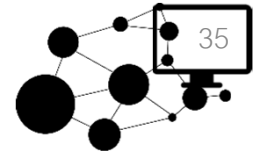


Code	Presenter	Title
CHE-POS-17	Anittha Prasertsab Kasetsart University	Lewis Acid Beta Zeolite Catalyzing the Catalytic Hydrogen Transfer of Furfural to Furfuryl alcohol: Insight from DFT Calculations
CHE-POS-18	Sarawoot Impeng National nanotechnology center	Theoretical investigation on gas sensing properties of a MnN ₄ moiety embedded graphene (MnN ₄ -graphene)
CHE-POS-19	Fadjar Mulya Universitas Gadjah Mada	Design a Better Metalloporphyrin Semiconductor: A Theoretical Studies on the Effect of Substituents and Central Ions
CHE-POS-20	Sunan Kitjaruwankul Kasetsart University	3D-QSAR and molecular docking of xanthone derivatives as HIV-1 reverse transcriptase inhibitors
CHE-POS-21	Sarinya Hadsadee Ubon ratchathani university	D- π -A- π -A system with isoindigo for dye-sensitized Solar cells
CHE-POS-22	Teeranan Nongnual Burapha University	The Spatial Resolution in Fluorescent-Particle Tracking Affected by Motion Blur
CHE-POS-23	Noppakoon Kharmsri Chulalongkorn University	Dimer Interactions of H1V Proton Channel in Resting State by MolecularDynamics Simulations
CHE-POS-24	Suparada Kamchompoo Ubon Ratchathani University	Adsorption of hydrogen sulfide over metal exchanged zeolite clusters: A density functional theory study
CHE-ORA-01t	Nuttaporn Janprapa King Mongkut's University of Technology Thonburi	A theoretical study of fluorene based copolymers for solar cell applications
CHE-ORA-02t	Rattanawalee Rattanawan Ubon Ratchathani University	Molecular Engineering of D-A Featured Organic Indole Sensitizers for Improving Performance Efficiency of Dye-Sensitized Solar Cells
CHE-ORA-03e	Pipat Khongpracha Kasetsart University	Charge Carriers Distribution in Platinum Doped Graphitic Carbon Nitride Quantum Dot
CHE-ORA-04t	Yuwanda Injongkol Ubon Ratchathani University	The mechanism of carbon dioxide hydrogenation to formic acid on Pt-boron nitride nanosheets (Pt-BNNSs): A theoretical study
CHE-ORA-05t	Nuttapon Yodsinn Ubon Ratchathani University	The theoretical study of catalytic CO ₂ hydrogenation to formic acid over a metal-decorated carbon nanocone
CHE-ORA-07t	Panyakorn Taweachat Chulalongkorn University	Molecular dynamics simulations of hyaluronic acid in water
CHE-ORA-09e	Wiparat Hotarat Chulalongkorn University	Delivery of Alpha-mangostin through biological membrane using cyclodextrins: A molecular dynamics simulation study
CHE-ORA-10e	Wasut Pornpatcharapong Chiang Mai University	Efficient Two-dimensional Ion Pairing Free Energy Surface Computation with Gaussian Process Regression
CHE-ORA-12e	Cangtao Yin Academia Sinica	The reaction between Criegee intermediates and sulfur dioxide: not really barrierless

Computational Physics, Fluid Dynamic and Solid Mechanics Session

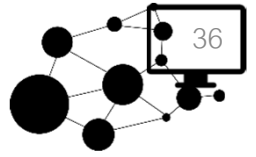


Code	Presenter	Title
PHY-POS-01	Kunwithree Phramrung King Mongkut's University of Technology Thonburi	Meshless local Petrov-Galerkin (MLPG) method for HIV model
PHY-POS-02	Naravadee Nualsaard King Mongkut's University of Technology Thonburi	The Numerical Solution of Fractional Black- Scholes-Schrodinger Equation Using the MLPG Method
PHY-ORA-02e	Abdulmutta Thatribud Prince of Songkla University	Electronic and Optical Properties of Silver Chloride Photocatalyst by First Principles calculation
PHY-ORA-03t	Sorayot Chinkanjanarot National Metal and Materials Technology Center	Predicting Coefficient of Linear Thermal Expansion of Carbon Fiber/Graphene Nanoplatelet/EPON862 Hybrid Composites: Multiscale Modeling
PHY-ORA-04t	Atipong Malatip National Metal and Materials Technology Center (MTEC)	Matrix Tridiagonalization Methods for 3D Finite Element Analysis of Free Vibration
PHY-ORA-05e	Wanfeng Yu Mae fah luang university	Identify Transient Sources from GOTO Sky Survey Data with Clustering Method
PHY-ORA-06e	Vichayanun Wachirapusitanand Chulalongkorn University	Machine Learning system mimicking student's choice in Particle Data Analysis laboratory activity
PHY-ORA-07e	Maneerat Chotsawat Synchrotron Light Research Institute	First-principles study of defects in Bi and Al doped orthorhombic PbZrO ₃



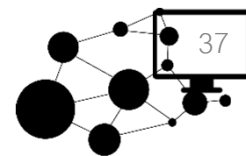
High Performance Computing, Computer Science, Mathematic & Engineering Session

Code	Presenter	Title
HPC-ORA-01e	Piyakorn Phanklin Thammasat University	Loop prevention on Software Defined Network using Adaptive Virtual Tunnel Network
HPC-ORA-02e	Kanjanart Junnawat Thammasat University	Resilience flow management on Software-Defined Network using Directed graph for L2 Loop prevention
HPC-ORA-03e	Dussadee Somjaiwang King Mongkut's University	Existence and Approximation of Solutions of Coupled Fractional Order Hybrid Differential Equations
HPC-ORA-05e	Witcha Benjanirat Kasetsart University	Wavelet Galerkin Method for solving Korteweg-de Vries Equation with Neumann Boundary Conditions



e-PROCEEDINGS





A theoretical study of fluorene based copolymers for solar cell applications

Nuttaporn Janprapa¹, and Chinapong Kritayakornupong^{1,*}

Department of Chemistry, Faculty of Science, King Mongkut's University of Technology Thonburi, Bangkok, 10140, Thailand

** E-mail: corresponding author email; chinapong.kri@kmutt.ac.th; Fax: +66(2)470-8962; Tel. +66(2)470-8962*

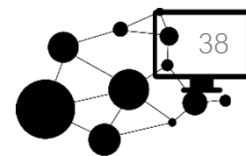
ABSTRACT

The structural, electronic, and charge properties of fluorine polymer (FF)_n and fluorine copolymers (FX)_n (X = Furan (Fu), Pyrrole (Py), Phosphor (Phos), and Para-Phenylene Vinylene (PPV), n = 1-4 repeating unit) were studied using the B3LYP/6-31G(d) method. As the result of structural properties, (FPPV)₄ copolymer shows the planar structure with the dihedral angles close to 180 degree, which corresponds to the smallest band gap of 2.69 eV. In contrast, the (FF)₄ and (FX)₄ structures, when X = Fu, Py, Phos, show the band gap values spanning in the range of 2.78-3.53 eV, which reflect the capacity for light absorption in a wide range. For all (FX)₄ copolymers the reorganization energies of hole (λ_h) are smaller than those of electron (λ_e), indicating better efficiency of hole mobility. As compared to others, the structure of (FPPV)₄ copolymers gives lower value of reorganization energy of hole (λ_h). This means that conducting copolymer between fluorene (F) and para-polyphenylene vinylene (PPV) helps to improve charge carrier transfer rate. Our results demonstrate that the (FPPV)₄ copolymers structure is a candidate for polymer solar cell application as donor materials.

Keywords: Band gap; Copolymer; DFT; Fluorenes; Reorganization energy

INTRODUCTION

Polyfluorene (PFs) has been widely used in light emitting diodes (LEDs) since it has high chemical stability, easy in film formation and better hole transporting property [1]. For polymer solar cell applications, the use of polyfluorene seems to be limited due to its large band gap varying from 2.95 eV to 3.68 eV [2-3]. This leads to a narrow range of light absorption and poor open circuit voltage value. It is well-known that optical and electronic properties of the polyfluorene can be tailored by introducing an effective conjugated unit into the system [4-5]. In experiments, various types of fluorine copolymers including different aromatic unit such as fluorine-thiophene and fluorine-3,4-ethylene dioxythiophene copolymers were synthesized [6-7], presenting a narrow band gap. Since the computer simulation is an effective tool for evaluating



structural and electronic properties of the relevant systems [8-11]. In this study, structural and electronic properties including charge analysis of fluorine (F) copolymer with different aromatic types such as furan (Fu), pyrrole (Py), phenylene (Ph), phosphor (Phos), and (para-phenylene vinylene) (PPV) were investigated by means of the B3LYP/6-31G(d) level of theory.

THEORY AND RELATED WORKS

The parameter to explain the behavior of the charge transfer rate is reorganization energy. The reorganization energy is the geometrical relaxation energy. Small reorganization energy is required for highly efficient transport and charge transfer rate. The neutral, cationic, and anionic forms of (FX)_n copolymers were calculated to estimate the reorganization energy for hole (λ_h) and electrons (λ_e). Their corresponding equations are shown in Eqs. (1) - (2) [12].

$$\lambda_{(hole)} = (E_0^+ - E_0) - (E_+ - E_+^0) \quad (1)$$

$$\lambda_{(electron)} = (E_-^0 - E_-) - (E_0 - E_0^-) \quad (2)$$

$E_0^{+(-)}$ is the energy of cation (anion) calculated with the optimized structure of neutral molecule. $E_{+(-)}^0$ is the energy of neutral molecule calculated at cationic (anion) state. E_0 , E_+ and E_- are the energies of the neutral, cationic, and anionic ground state structures, respectively.

COMPUTATIONAL DETAILS

The chemical structures of the (FF)_n and (FX)_n (X= Fu, Py, Phos, and PPV, n = 1-4 repeating units) investigated in this work are shown in Figure 1. Structures of (FF)_n and (FX)_n oligomers were optimized using the most popular Becke's three-parameter hybrid, B3 with nonlocal correlation of Lee-Yang-Parr, the LYP (B3LYP) method [13], while the basis set 6-31G (d) was applied for all atomic types.

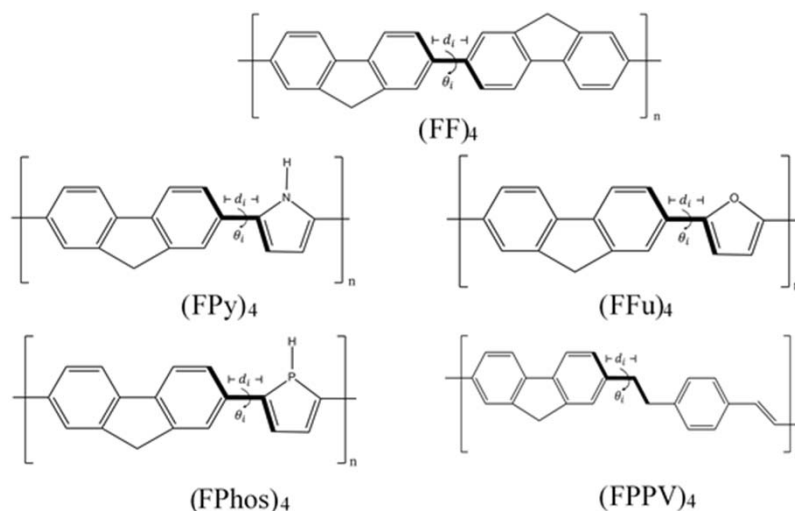


Figure 1. Sketch map of the structures, inter ring bond lengths (d_i) and dihedral angle (θ_i) of $(FF)_n$ and $(FX)_n$ ($X = Fu, Py, Phos,$ and $PPV, n = 1-4$ repeating unit)

To explain electronic properties of $(FF)_n$ structure and $(FX)_n$ copolymers such as HOMO, LUMO, band gap (E_g), ionization potential (IP), electron affinity (EA), and reorganization energy for hole (λ_h) and electrons (λ_e) were also elucidated using the B3LYP/6-31G(d) method. This level of theory has been successfully applied in other relevant systems [14-16]. Moreover, HOMO, LUMO, and band gap obtained from B3LYP functional are better agreement with the experimental observations than those calculated by CAM-B3LYP method [17]. Hence, B3LYP method is adequate for this study. All calculations were performed using Gaussian 03 package [18] with the default temperature and pressure of 298.15 K and 1 atm, respectively.

RESULTS AND DISCUSSION

Structural properties

The optimized geometrics of the $(FF)_n$ and $(FX)_n$ ($X = Fu, Py, Phos,$ and $PPV, n = 1-4$ repeating units) calculated by the B3LYP/6-31G(d) method are displayed in Figure 2. The structural parameters of the $(FF)_n$ and $(FX)_4$ copolymers are listed in Table 1. The inter-ring distances of the $(FF)_4, (FFu)_4, (FPy)_4, (FPhos)_4,$ and $(FPPV)_4$ are 1.483, 1.454, 1.459, 1.463, and 1.463 Å, respectively. It is clearly seen that the C-C inter-ring distances of $(FX)_4$ copolymers with different monomer (X) unit are decreased compared to that of $(FF)_4$ copolymers. The short inter-ring distances (d_i) show the facilitation of electron delocalization, which is highly desirable for an effective charge transport. In addition, the average dihedral angle values obtained from the $(FX)_4$ are ranging from 154.1° to 178.0° . This reflects a higher planarity of the $(FFu)_4, (FPy)_4, (FPhos)_4,$ and $(FPPV)_4$ copolymers in comparison with $(FF)_4$ copolymers (See Fig. 2). As the results, the $(FPPV)_4$ copolymer structure shows a better delocalization of electrons, indicating higher conductive properties.

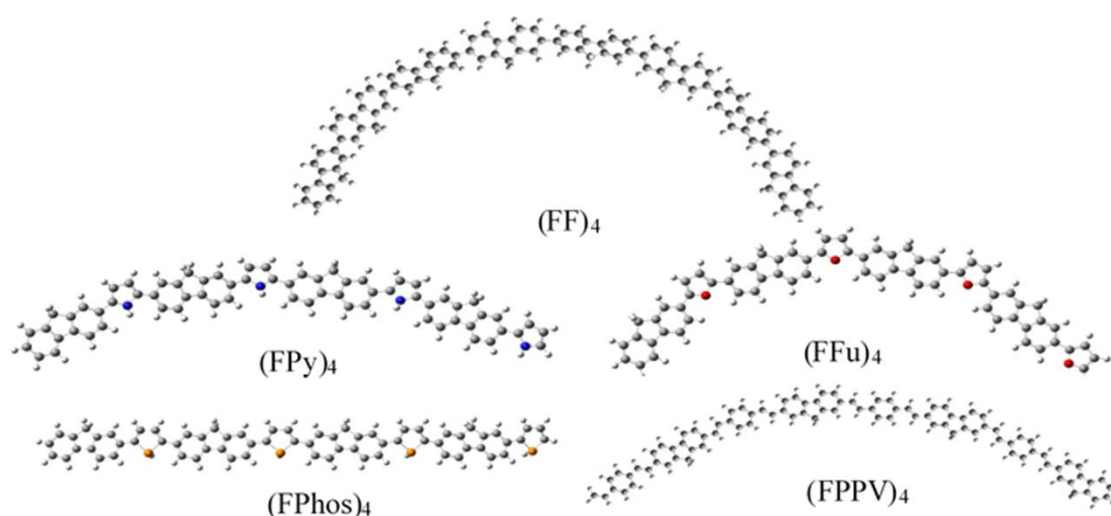


Figure 2. Optimized structures of $(FF)_4$ and $(FX)_4$ ($X = \text{Fu, Py, Phos, and PPV}$) copolymers at the ground state at B3LYP/6-31G(d) method.

HOMO, LUMO, and Band gaps

Electronic properties of $(FF)_n$ and $(FX)_n$ copolymers are listed in Table 1. For $(FF)_n$ structure, the band gaps are 4.16, 3.71, 3.58, and 3.53 eV for $(FF)_1$, $(FF)_2$, $(FF)_3$, and $(FF)_4$ structures, respectively. The band gap value of $(FF)_4$ is consistent with the experimental result (3.68 eV) [6]. This means that the B3LYP/6-31G(d) method is adequate for describing electronic properties in our systems. In the cases of copolymers $(FX)_n$, the number of monomeric unit increased as the band gap decreased proving a result of higher π -electrons delocalization the backbone of $(FX)_n$. The band gap values are 3.53, 3.10, 2.94, 2.78, and 2.69 eV obtained for $(FF)_4$, $(FPy)_4$, $(FFu)_4$, $(FPhos)_4$, and $(FPPV)_4$, respectively. It is noted that $(FPPV)_4$ structure gives the lowest band gap value. This is in consistent well with the structural data. The lowest band gap value of $(FPPV)_4$ reflects a broader solar absorption range.

Table1. Structural parameters (inter-ring bond lengths and dihedral angle) and electronic properties (HOMO, LUMO, E_g , IP, and EA) of the $(FF)_4$ and $(FX)_4$ ($X = \text{Fu, Py, Phos, and PPV}$) copolymers obtained by the B3LYP/6-31G(d) level of theory.

Structure	inter-ring bond lengths (Å)	dihedral angle (°)	E_{HOMO} (eV)	E_{LUMO} (eV)	E_{gap} (eV)	IP (eV)	EA (eV)
$(FF)_n$							
n=1	1.484	142.68	-5.35	-1.19	4.16	6.47	0.13
n=2	1.483	142.66	-5.14	-1.44	3.71	5.94	0.68
n=3	1.483	142.77	-5.09	-1.51	3.58	5.73	0.90
n=4	1.483	142.62	-5.07	-1.55	3.53	5.61	1.03

(FFu)_n							
n=1	1.457	179.76	-5.22	-1.11	4.12	6.61	-0.23
n=2	1.454	179.94	-4.83	-1.54	3.29	5.82	0.58
n=3	1.454	179.97	-4.72	-1.67	3.05	5.52	0.89
n=4	1.454	178.47	-4.67	-1.73	2.94	5.36	1.06
(FPy)_n							
n=1	1.462	154.64	-5.01	-0.90	4.11	6.37	-0.42
n=2	1.460	156.06	-4.68	-1.27	3.41	5.63	0.35
n=3	1.460	156.05	-4.59	-1.39	3.19	5.36	0.64
n=4	1.459	156.23	-4.55	-1.45	3.10	5.21	0.80
(FPhos)_n							
n=1	1.465	152.69	-5.34	-1.50	3.85	6.62	0.25
n=2	1.464	153.74	-4.97	-1.87	3.10	5.87	1.01
n=3	1.463	153.95	-4.87	-1.99	2.88	5.60	1.28
n=4	1.463	154.10	-4.82	-2.04	2.78	5.45	1.44
(FPPV)_n							
n=1	1.463	180.00	-5.16	-1.67	3.49	6.32	0.55
n=2	1.462	180.00	-4.89	-1.96	2.92	5.69	1.18
n=3	1.462	178.69	-4.82	-2.06	2.76	5.45	1.43
n=4	1.462	178.20	-4.79	-2.10	2.69	5.32	1.56

Ionization Potentials and Electron Affinities

The ionization potential values (IPs) and electronic affinity values (EAs) explain the value of energy barrier for injecting and transporting rates for electron and hole. Low ionization potential indicates occurrence of hole injections from anode to hole transport material, while the high electronic affinity demonstrates easily injected electrons from cathode to electron transport layer. The ionization potential (IPs) and electron affinity (EAs) of all molecules are summarized in Table 1. As listed in Table 1, the energies required to create a hole in the polymer are 5.61, 5.36, 5.21, 5.45, and 5.32 eV, whereas the extraction of an electron from anion requires 1.03, 1.06, 0.80, 1.44, and 1.56 eV for (FF)₄, (FFu)₄, (FPy)₄, (FPhos)₄, and (FPPV)₄, respectively. The smaller IPs of (FPy)₄, (FFu)₄, (FPhos)₄, and (FPPV)₄ copolymers than (FF)₄ revealed the increment of hole injection. For electron affinities, all selected (FX)₄ copolymers can easily injected electrons to acceptor materials with the trend of the (FPPV)₄ > (FPhos)₄ > (FFu)₄ > (FF)₄ > (FPy)₄. This is very ideal for the process of an effective charge transfer which could produce the higher efficiency of polymer solar cells.

Reorganization energies

The calculated reorganization energies for the hole and electron are listed in Table 2 and depicted in Figure 3. The results obtained for (FF)₄, (FFu)₄, (FPy)₄, (FPhos)₄, and (FPPV)₄ copolymers showed $\lambda_{\text{hole}} < \lambda_{\text{electron}}$, suggesting that hole mobility was higher than electron mobility. The (FPPV)₄ copolymers showed lower λ_{hole} compared to

(FF)₄, confirming that the (FPPV)₄ copolymers improved the conductivity of the holes. It indicates that their polymers are good candidates for hole transport materials. In addition, low reorganization energy values were pronounced from the calculated complexes demonstrating high charge transfer rate. The high hole transport for donors contributes to enhance the charge transport efficiency leading to increased open circuit voltage and fill factor.

Table 2. Calculated molecular reorganization energy of the (FF)₄ and (FX)₄ (X = Fu, Py, Phos, and PPV) copolymer obtained by B3LYP/6-31G(d) level of theory.

Structure	λ_{hole}	$\lambda_{\text{electron}}$	λ_{total}
(FF) ₄	0.090	0.127	0.217
(FFu) ₄	0.128	0.191	0.319
(FPy) ₄	0.135	0.139	0.274
(FPhos) ₄	0.176	0.224	0.399
(FPPV) ₄	0.079	0.086	0.165

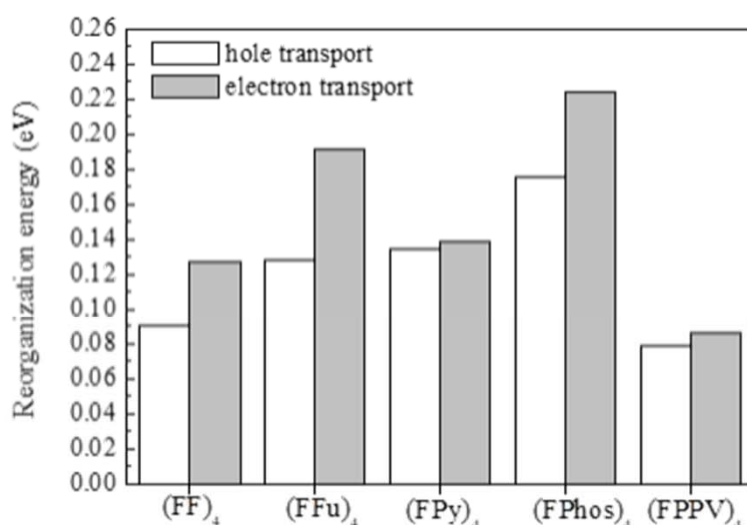
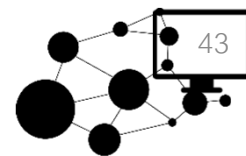


Figure 3. Reorganization energy for hole and electron of (FF)₄ and (FX)₄ (X = Fu, Py, Phos, and PPV) copolymers obtained by the B3LYP/6-31G(d) method.

CONCLUSION

The density functional theory (DFT) was performed for evaluating structural and electronic properties of (FF)_n and (FX)_n (X = Fu, Py, Phos, and PPV, n = 1-4 repeating units) copolymers. The results show that (FPPV)₄ copolymers has the dihedral angles nearly 180 degree, which represents a more planarity compared to (FF)₄ copolymer. The calculated band gap energies of (FF)₄ and (FX)₄ copolymers are found in the range of 2.69 to 3.53 eV. It appears that the (FPPV)₄ structure gives the



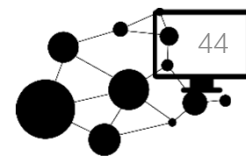
smallest band gap value of 2.69 eV. Moreover, the reorganization energy for the hole of (FPPV)₄ copolymer is lower than other (FX)₄ copolymers. As the results, the (FPPV)₄ copolymer is a potential hole transport material for photovoltaic solar cells.

ACKNOWLEDGMENTS

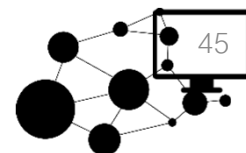
This work was supported by grants of Petchra Pra Jom Klao Doctoral Scholarship Academic for Ph.D. Program at KMUTT (Grant No. 04/2557). The computation resources of computational chemistry research unit at department of chemistry, KMUTT.

REFERENCES

- [1] Chen, S.-A., Lu, H.-H., and Huang, C.-W., Eds.: U. Scherf and D. Neher), Springer Berlin Heidelberg, Berlin, Heidelberg, 2008, 49-84.
- [2] Wu, W.C., Liu, C.L., and Chen, W.C., *Polymer*, 2006, **47**, 527-538.
- [3] Bundgard, E., and Krebs, F.C., *Sol. Energy Mater. Sol. Cells*, 2007, **91**, 954-985.
- [4] Cheng, Y.J., Yang, S.H., and Hsu, C.S., *Chem. Rev.*, 2009, **109**, 5868-5923.
- [5] Liu, B., Yu, W.L., Lai, Y.H., and Huang, W., *Chem. Mater*, 2001, **13**, 1984-1991.
- [6] DeLeeuw, D.M., Simenon, M.M.J., Brown, A.R., and Einerhand, R.E.F., *Synth. Met*, 1997, **87**, 53-59.
- [7] Casseiro, S. M., Zanlorenzi, C., Atvars, T. D. Z., Santos, G., Fonseca, F. J., and Akcelrud, L., *J. Lumin*, 2013, **134**, 670-677.
- [8] Xiao, S., Stuart, A.C., Liu, S., Zhou, H., and You, W., *Adv. Func. Mat.*, 2010, **20**, 635-643.
- [9] Pappenfus, T. M., Schmidt, J.A., Koehn, R.E., and Alia, J.D, *Macromolecules*, 2011, **44**, 2354-2357.
- [10] McCormick, T.M., Bridges, C.R., Carrera, E.I., DiCarmino, P.M., Gibson, G.L., Hollinger, J., Kozycz, L.M., and Seferos, D.S., *Macromolecules*, 2013, **46**, 3879-3886.
- [11] Ku, J., Lansac, Y., and Jang, Y. H., *J. Phys. Chem. C*, 2011, **115**, 21508-21516.
- [12] Hutchison, G.R., Ratner, M.A., and Marks, T.J., *J. Am. Chem. Soc.*, 2005, **127**, 2339-2350.
- [13] Lee, C., Yang, W., and Parr, R.G., *Physical Review B*, 1988, **37**, 785-789.
- [14] Yang, L., Feng, J.-K., and Ren, A.-M., *Polymer*, 2005, **46**, 10970-10981.
- [15] Ling, L., and Lagowski, J.B., *Polymer*, 2013, **54**, 2535-2543.
- [16] Sanchez-Bojorge, N.A., Rodriguez-Valdez L.M., and Flores-Holguin N., *J Mol Model*, 2013, **19**, 3537-3542.
- [17] McCormick, T.M., Bridges, C.R., Carrera, E.I., DiCarmino, P.M., Gibson, G.L., Hollinger, J., Kozycz, L.M., and Seferos, D.S., *Macromolecules*, 2013, **46**, 3879-3886.



[18] Frisch, M. J.; Trucks, G. W.; Schlegel, H. B.; Scuseria, G. E.; Robb, M. A.; Cheeseman, J. R.; Montgomery, Jr., J. A.; Vreven, T.; Kudin, K. N.; Burant, J. C.; Millam, J. M.; Iyengar, S. S.; Tomasi, J.; Barone, V.; Mennucci, B.; Cossi, M.; Scalmani, G.; Rega, N.; Petersson, G. A.; Nakatsuji, H.; Hada, M.; Ehara, M.; Toyota, K.; Fukuda, R.; Hasegawa, J.; Ishida, M.; Nakajima, T.; Honda, Y.; Kitao, O.; Nakai, H.; Klene, M.; Li, X.; Knox, J. E.; Hratchian, H. P.; Cross, J. B.; Bakken, V.; Adamo, C.; Jaramillo, J.; Gomperts, R.; Stratmann, R. E.; Yazyev, O.; Austin, A. J.; Cammi, R.; Pomelli, C.; Ochterski, J. W.; Ayala, P. Y.; Morokuma, K.; Voth, G. A.; Salvador, P.; Dannenberg, J. J.; Zakrzewski, V. G.; Dapprich, S.; Daniels, A. D.; Strain, M. C.; Farkas, O.; Malick, D. K.; Rabuck, A. D.; Raghavachari, K.; Foresman, J. B.; Ortiz, J. V.; Cui, Q.; Baboul, A. G.; Clifford, S.; Cioslowski, J.; Stefanov, B. B.; Liu, G.; Liashenko, A.; Piskorz, P.; Komaromi, I.; Martin, R. L.; Fox, D. J.; Keith, T.; Al-Laham, M. A.; Peng, C. Y.; Nanayakkara, A.; Challacombe, M.; Gill, P. M. W.; Johnson, B.; Chen, W.; Wong, M. W.; Gonzalez, C.; and Pople, J. A.; Gaussian 03. Gaussian, Inc., Wallingford CT, 2004.



Computational Study of Binding Mode of Depsidones in Vascular Endothelial Growth Factor Receptor-2

C. Suksamrarn¹, P. Saparpakorn^{1,2} and S. Hannongbua^{1,2,C}

¹Department of Chemistry, Faculty of Science, Kasetsart University, Bangkok, Thailand

²Center for Advanced Studies in Nanotechnology and Its Applications in Chemical, Food and Agricultural Industries, KU institute for Advanced Studies, Kasetsart University, Bangkok 10900, Thailand

^CE-mail: fscisph@ku.ac.th; Fax: +66 2 562 5555 ext 647671; Tel. +66 2 562 5555 ext 647541

ABSTRACT

Colon cancer is one of the most common types of cancer and leading causes of death worldwide. There are a number of proteins involved in molecular pathway causing colon cancer. Vascular endothelial growth factor receptor-2 (VEGFR-2), a protein controlling the formation of new blood vessel, is an interesting protein target in colon cancer treatment. Depsidones are compounds containing two aromatic rings joined by an ester bond and an ether bond. These are found as secondary metabolite in lichens. In this research fourteen depsidones, isolated from the fungus *Chaetomium brasiliense*, were theoretical studied in order to understand insight into their binding affinity to VEGFR-2. Geometrical optimized structures of all depsidones were performed based on density functional theory at M062X/6-31G(d) level of theory. The structures of two major forms of each depsidone were observed. Then, molecular docking between depsidones and VEGFR-2 were investigated by using GOLD. From the docking results, all depsidones showed similar binding mode except one depsidone – it also gave highest fitness score and formed strong hydrogen bond with Glu917 and Cys919 amino acid residues.

Keywords: Anti-cancer, depsidone, vascular endothelial growth factor receptor-2, molecular docking, density functional theory

INTRODUCTION

Colon cancer is one of the most common types of cancer and leading causes of death worldwide. More than one million people develop colon cancer each year, with over 600,000 patients dying of the disease annually. A number of proteins involved in molecular pathway causing colon cancer were found. Vascular endothelial growth factor receptor-2 (VEGFR-2), is an interesting protein target in colon cancer treatment [1]. VEGFR-2, found at human vascular endothelium, controls angiogenesis, the formation of new blood vessel. If angiogenesis is out of balance, cancer occurs [2]. At the tyrosyl groups in the protein kinase domain, VEGFR-2 catalyzes autophosphorylation reaction, the transfer of phosphate group from adenosine triphosphate (ATP) to other protein receptors [3]. There are several FDA-approved anti-colon cancer drugs such as sorafenib and regorafenib. As VEGFR-2 inhibitors, these drugs bind VEGFR-2 at protein kinase domain. However, these drugs contain unwanted side effects, such as hand-foot skin reaction, diarrhea, fatigue, hypothyroidism, anorexia,



hypertension and nausea [4]. In this work, we theoretically studied fourteen depsidones (1 – 14), a group of compounds containing two aromatic rings joined by an ester bond and an ether bond, to know their potential to be anti-colon cancer drug candidate. Molecular docking approach was applied to investigate the binding orientation and of depsidones in VEGFR-2 and also interactions between depsidones and this protein, in order to evaluate the binding. The structures of these depsidones are shown in Figure 1. Depsidones are natural products isolated from the fungus *Chaetomium brasiliense* by Kanokmedhakul, S. *et al.* in 2009 [5].

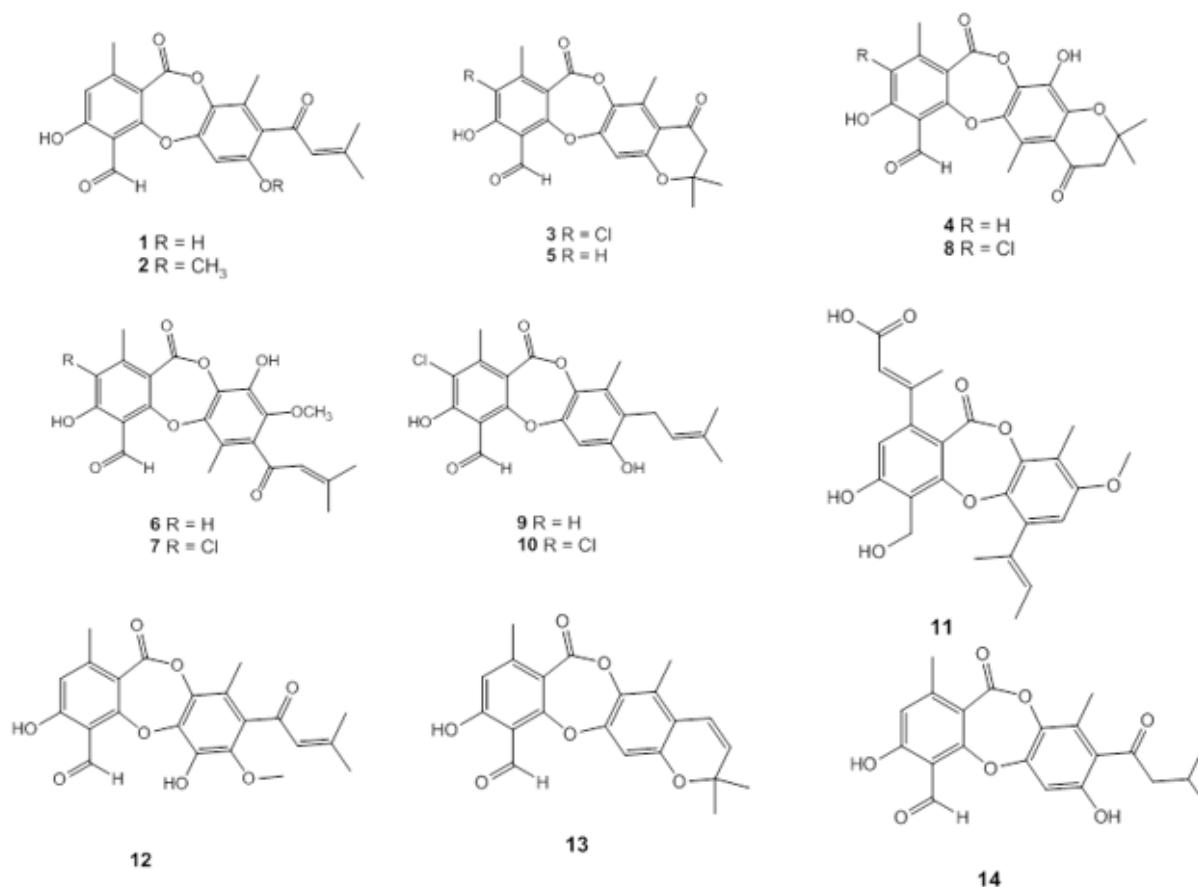


Figure 1. Structure of depsidones 1 – 14 [5]

METHODOLOGY

Three dimensional structures of depsidones

First, by observing the three dimensional structures of the depsidones, due to non-planarity of the middle seven-membered ring, there are two possible different isomers. According to the X-ray crystallographic structures of some depsidones found in nature such as pannarin, 2-cholounginol, niludin [6,7], it can be confirmed that the three dimensional structure of depsidones exist in two distinguish forms, in this work, the “down” and “up” form, are focused as shown in Figure 2.

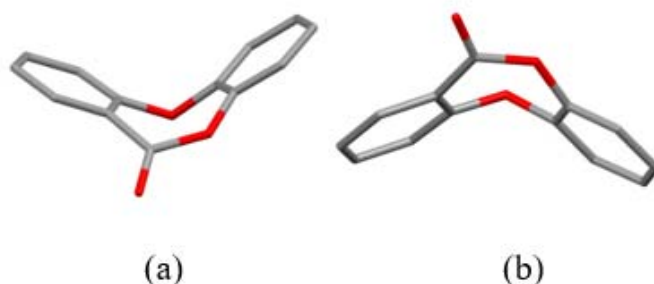


Figure 2. (a) “Down” form (b) “Up” form of depsidones

Geometry optimization and quantum chemical calculations

Chemical structures of the fourteen depsidones in both form were constructed using GaussView 5.0 program and were then optimized at M062X/6-31G(d) level using Gaussian 09 program [8]. Then energy calculations of the geometry optimized depsidones (in both forms) were done at M062X/6-31G(d), M062X/6-31G(d,p), M062X/6-31+G(d,p), M062X/6-31++G(d,p), M062X/6-311G(d,p), M062X/6-311+G(d,p) and M062X/6-311++G(d,p) for comparison on structural parameters.

Molecular docking calculations

To generate the binding mode of the fourteen depsidones and two known VEGFR-2 inhibitors, sorafenib, as docking reference, and regorafenib in VEGFR-2, molecular docking calculation using GOLD 5.2.2 program were done. Goldscore as scoring function was applied. The initial coordinates of VEGFR-2 were obtained from the X-ray crystallographic structure available in the protein databank (PDB). The PDB code of the chosen VEGFR-2 structure, with high resolution of 2.03 Å, is 4ASD. The water molecules were removed from the original protein structure. All hydrogen atoms were added to the protein. The protein structure and the ligands were treated to be rigid and flexible, respectively.

The three-dimensional grid box with size $10 \times 10 \times 10$ Å was centered on the original protein data bank ligand. Genetic algorithm (GA) was used as searching algorithm; the number of GA run was set to 100. The distinct conformational clusters were generated using root mean square deviations (RMSD) tolerance of 1.5 Å.

RESULTS AND DISCUSSION

Structural stability

The calculated energy different of the depsidones in both forms by using various basis sets are shown in Table 1. The results revealed that all depsidones except 6 and 7 in each forms are not significantly different in stability. For compound 6 and 7, since “down” forms showed some six-membered-ring intramolecular hydrogen bonds which are not observed in “up” forms, depicted in Figure 2. As shown in Table 1,

there are slight energy difference between both forms – the “down” forms are mostly little more stable the “up” forms.

Table 1. Calculated energy different of the depsidones in both forms

compound	ΔE (kcal/mol)*						
	basis set						
	6-31G(d)	6-31G(d,p)	6-311G(d)	6-311G(d,p)	6-31+G(d,p)	6-31++G(d,p)	6-311++G(d,p)
1	0.13	0.12	0.17	0.15	0.14	0.13	0.16
2	0.14	0.14	0.20	0.19	0.14	0.16	0.18
3	0.00	0.00	0.00	0.00	0.00	0.00	0.00
4	0.00	0.00	0.02	0.01	0.02	0.02	0.03
5	0.00	0.00	0.00	0.00	0.00	0.00	0.00
6	4.10	4.13	4.15	4.26	3.75	3.74	3.65
7	4.18	4.21	4.23	4.33	3.84	3.80	3.72
8	0.00	0.00	0.00	0.00	0.00	0.00	0.00
9	0.10	0.10	0.06	0.06	0.08	0.07	0.07
10	0.11	0.11	0.08	0.07	0.11	0.11	0.10
11	0.00	0.00	0.00	0.00	0.00	0.00	0.00
12	0.18	0.17	0.23	0.22	0.16	0.18	0.23
13	0.00	0.00	0.00	0.00	-0.02	0.00	0.00
14	1.50	1.46	1.65	1.59	1.81	1.81	1.91

* $\Delta E = E_{\text{“Up form”}} - E_{\text{“Down form”}}$

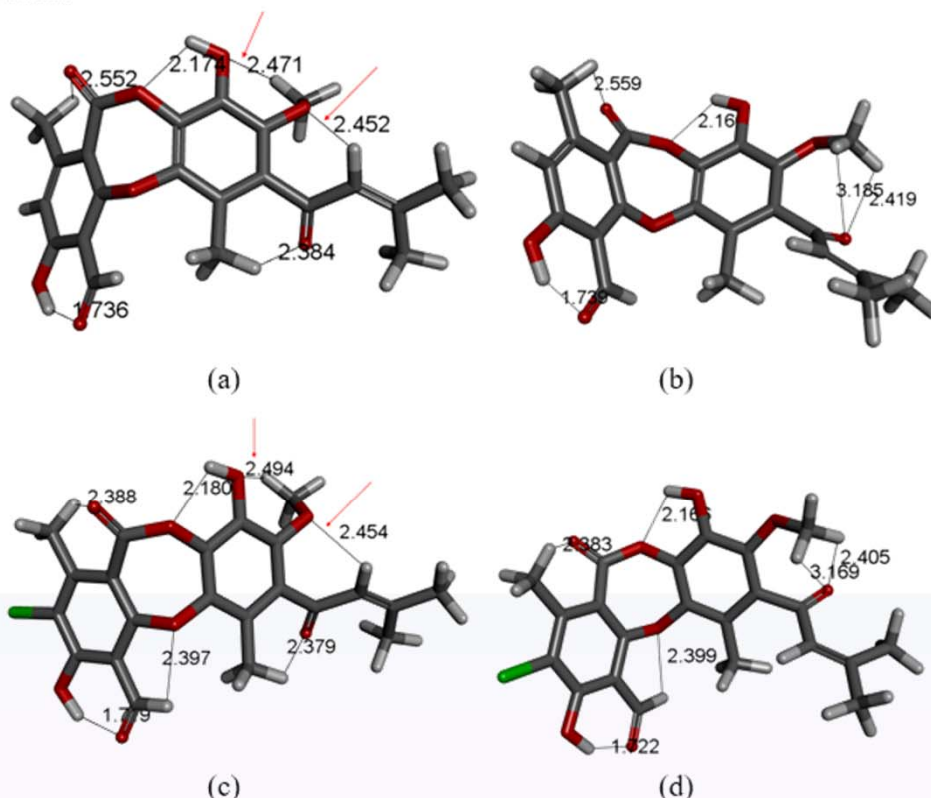


Figure 3. The three-dimensional structures of optimized (a) 6 in “down” form, (b) 6 in “up” form, (c) 7 in “down” form, and (d) 7 in “up” form. The numbers indicate hydrogen bond distances in angstrom. The arrows point to the 6-membered-ring hydrogen bond that found only in “down” form.

Binding mode of the depsidones in VEGFR-2

Before performing molecular docking simulation, the RMSD of heavy atoms in sorafenib, as docking reference, were obtained in the value of 0.439 Å. This value indicates that this molecular docking performance is validated. The Goldscore of 14 depsidones in both form and known VEGFR-2 inhibitors were collected, as shown in Table 2.

Table 2. Goldscore of known VEGFR-2 inhibitors and 14 depsidones

compound	Goldscore	compound	Goldscore	compound	Goldscore
sorafenib	90.1	5 down	47.68	10 down	52.57
regorafenib	90.5	5 up	45.59	10 up	54.89
1 down	50.41	6 down	54.37	11 down	45.96
1 up	52.72	6 up	53.27	11 up	51.09
2 down	52.42	7 down	53.17	12 down	53.32
2 up	53.26	7 up	50.33	12 up	54.33
3 down	50.16	8 down	49.54	13 down	51.32
3 up	45.43	8 up	53.4	13 up	46.23
4 down	46.32	9 down	53	14 down	53.07
4 up	52.64	9 up	58.37	14 up	53.59

Among the 14 depsidones, 9 in “up” form gave the highest Goldscore. The binding position of all ligands in VEGFR-2 is illustrated in Figure 4. All depsidones except 9 in “up” form bind VEGFR-2 in the same location, whereas 9 in “up” form bind VEGFR-2 in another location, near to the sorafenib and regorafenib.

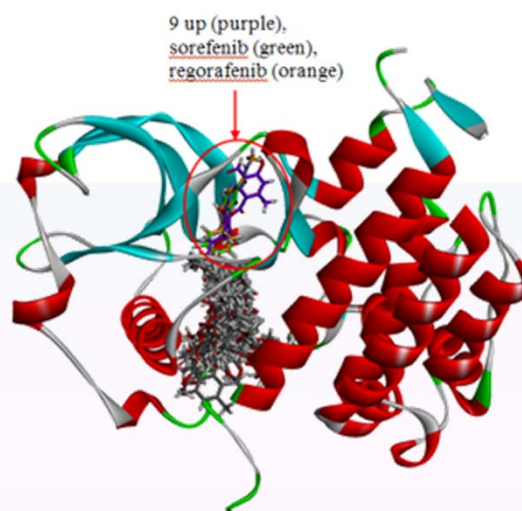


Figure 4. binding position of all ligands in VEGFR-2

The possible interactions between ligands and VEGFR-2 including hydrogen bonding, hydrophobic interaction, and π - π interaction were investigated. The H-bond interaction between ligands and surrounding amino acids are shown in Figure 5. For sorafenib, regorafenib and 9 in “up” form, the similar interactions to Leu840, Val848, Ala866, Lys868, Glu885, Val899, Glu917, Cys919, Leu1035, Cys1045 are found. Sorafenib and regorafenib also form the interaction similar to Lys920, Leu1019, His1026, Ile1044 and Asp1046. The interaction to Val916 is found in regorafenib and the 9 in “up” form. The interaction to Phe1047 is found in sorafenib and the 9 in “up” form. In the further study, molecular dynamics study will be performed to investigate specific interactions between compound 9 in “up” conformation and each surrounding amino acid residues.

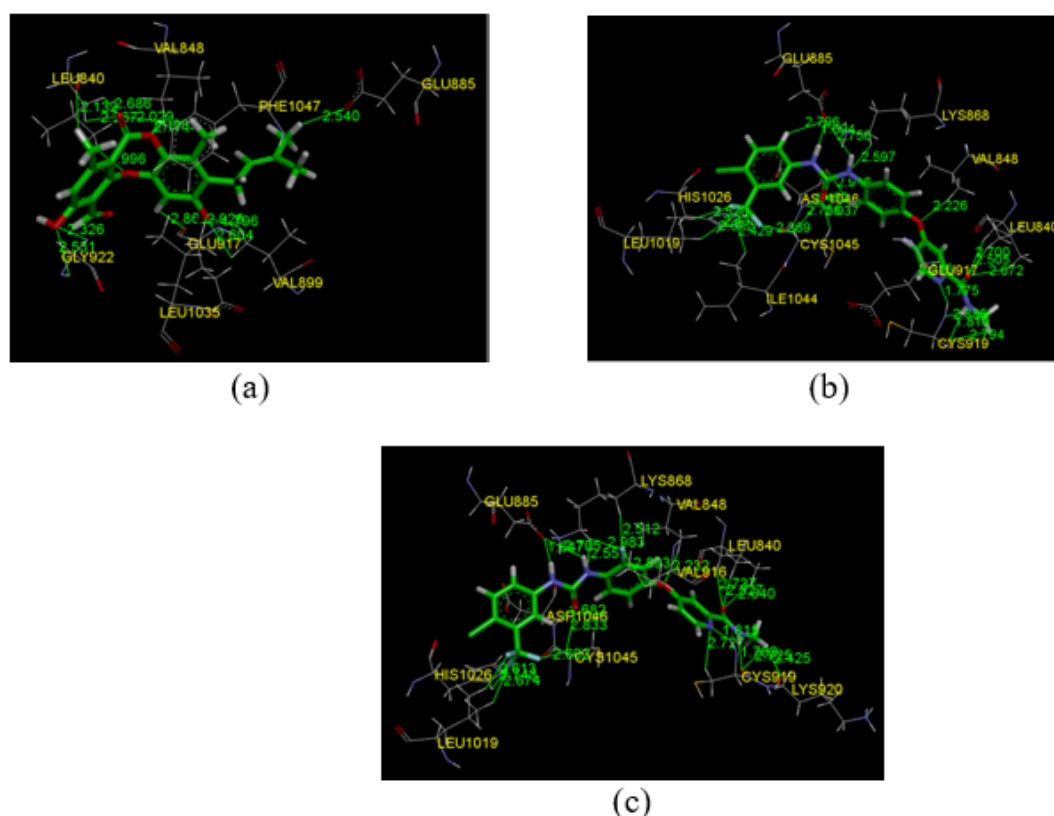
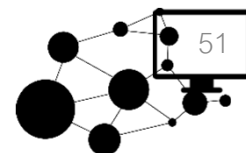


Figure 5. Hydrogen bonds between (a) 9 in “up” form, (b) sorafenib, (c) regorafenib and VEGFR-2, depicted with the green lines. The numbers indicate distance of the hydrogen bonds in angstrom.

CONCLUSION

The binding mode of 14 depsidones (in “up” and “down” forms) in vascular endothelial growth factor receptor-2 were studied by molecular docking simulations. Compound 9 in “up” form showed the different binding mode from other depsidones.

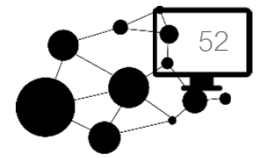


ACKNOWLEDGMENTS

The authors thanks Professor Dr.Somdej Kanokmedhakul for valuable information of depsidones. C.S. is grateful to the Junior Science Talent Project (JSTP) from the National Science and Technology Development Agency (NSTDA) of Thailand for a scholarship. Research supporting from the Thailand Research Fund (DBG5980001) is gratefully acknowledged. Laboratory of Computational and Applied Chemistry (LCAC) at the Department of Chemistry, Faculty of Science, Kasetsart University is acknowledged for research facilities.

REFERENCES

- [1] Weng, W., Feng, J., Qin, H., Ma, Y., *Int. J. Cancer*, 2015, **136**, 493-502.
- [2] Holmes, K., Roberts, O. L., Thomas, A. M., Cross, M. J., *Cell. Signal.*, 2007, **19**, 2003-2012.
- [3] Roskoski Jr., R. *Biochem. Biophys. Res. Comm.*, 2008, **375**, 287-291.
- [4] Galun, D. Srdic-Rajic, T. Bogdanovic, A. Loncar, Z. Zuvella, M. J. *Hepatocell. Carcinoma*. 2017, **4**, 93-103.
- [5] Khumkomkhet, P., Kanokmedhakul, S., Kanokmedhakul, K., Hahnvajanawong, C., Soyong, K., *J. Nat. Prod.*, 2009, **72**, 1487-1491.
- [6] Blaser, D., Stoeckli-Evans, H., *Acta Cryst.*, 1991, **47**, 2624-2626.
- [7] Kawahara, N., Nakajima, S., Satoh, Y., Yamazaki, M., Kawai, K. *Chem. Pharm. Bull.* 1088, **36** (6), 1970-1975.
- [8] Frisch, M. J., Trucks, G.W., Schlegel, H.B., et al. Gaussian 09, Revision A.02. Wallingford, CT: Gaussian, Inc.; 2009.



Identify Transient Sources from GOTO Sky Survey Data with Clustering Method

W. Yu¹, R. Yoyponsan², T. Boongoen³, J. Mullaney⁴, K. Ulaczyk⁵, U. Sawangwit⁶
and A. Eungwanichayapant^{1C}

¹*School of Science, Mae Fah Luang University, Chiang Rai, 57100 Thailand*

²*Department of Physics, Faculty of Science, Chiang Mai University, Chiang Mai, 50200 Thailand*

³*School of Information Technology, Mae Fah Luang University, Chiang Rai, 57100 Thailand*

⁴*Department of Physics and Astronomy, University of Sheffield, Sheffield S10 2TN, UK*

⁵*The University of Warwick, Coventry CV4 7AL, UK*

⁶*National Astronomical Research Institute of Thailand, Chiang Mai, 50180 Thailand*

^C*E-mail: anant@mfu.ac.th; Fax: +66 5 391 6777; Tel. +66 5 391 6782*

ABSTRACT

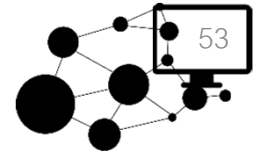
The Gravitational-wave Optical Transient Observer (GOTO) Sky Surveys project's primary objective is to identify optical counterparts to gravitational wave (GW) events. It will achieve this by surveying the region of the sky covered by the GW event error-circle and identifying all transient sources within that region. A key aspect of achieving this goal is GOTO's repeated survey of the night sky to build up a set of recent reference images to compare against. The large amounts of imaging data produced by GOTO every night will be processed and analyzed in order to classify 40-million detected source. It is impossible for humans to conduct this task alone and it is therefore recognized that developing machine learning algorithms to assist with this task is an important component of the project. In this proceeding, we focus on the problem of classifying transient events, which is made more challenging due to the extreme imbalance of the data, whereby the number of identified sources is very large compared to the number of true transient sources. In order to solve these shortcomings, clustering methods such as Kmeans, Agglomerative and DBSCAN were introduced and their results were evaluated with several clustering indices. We will discuss the results and their applications within the GOTO project at the meeting.

Keywords: Gravitational-wave detectors, Sky survey, Transient source detection, Data clustering, Imbalance data.

INTRODUCTION

The detection of the gravitational waves by the Laser Interferometer Gravitational-Wave Observatory (LIGO) [1] in 2016 was a major scientific discovery, especially in the fields of physics and astronomy. This event provides further evidence of Einstein's theory of relativity, which is one of the pillars of modern physics. In astronomy, it also provided a new tool for "hearing" some of the Universe's most extreme phenomena such as the collision of two massive black holes or neutron stars that cause ripples space-time.





In addition to gravitational waves, it is natural to expect that electromagnetic (EM) waves are also produced by such extreme events. “Seeing” the EM waves associated with gravitational wave events (particularly those involving at least one neutron star) can provide more information which can help us to understand existing physics or perhaps even discover new physics associated with such extreme events. The EM waves produced by these events are likely only produced for a short period of time, presenting only a short window during which astronomers must first detect, measure and then discriminate these transient events from other transients such as novae, supernovae, tidal disruption flares, etc [2]. Over the next few years, astronomers must therefore become adept at rapidly identifying and classifying transient events.

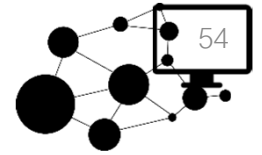
The Gravitational-wave Optical Transient Observer (GOTO) is a ground-based observatory that attempts to detect transient sources over the whole sky using an array of four 0.5 m aperture, wide-field optical telescopes, which can respond to alerts generated by the LIGO and Virgo gravitational wave detectors. GOTO is an international collaboration led by University of Warwick of UK and Monash University of Australia. Its current facility is housed at La Palma, Canary Island and is capable of delivering roughly 400 images per night, with each image containing, on average, roughly 20,000 astronomical sources. To classify transient and non-transient sources with such a large volume of images, machine learning is the most promising option.

Classification is the first application of machine learning we have explored to analyze the GOTO dataset. Because of the extremely imbalance nature of the dataset, however, the standard classification methods are not sufficient to reach the desired level of precision and recall. This work proposes a method to improve classification by identifying clusters within the parameter space of GOTO data that provides different learning contexts, enabling us to follow this up with different treatments, and thereby breaking a difficult imbalanced problem to into smaller, yet simpler, ones.

THEORY AND RELATED WORKS

Machine learning has been adopted in many astronomy studies, most commonly as a means to identify and classify sources in astronomical data. To date, most of these works have utilized so call “supervised learning” as the primary classification process. Examples include: the detection of point-source transients and moving objects in the Dark Energy Survey Supernova (DES-SN) by using the “Random Forest” technique [3] and the application of machine learning classification to the photometric supernova [4] and SDSS transient survey images [5]. The effectiveness of supervised learning depends critically on the training dataset. The most successful applications rely on training data that has relatively low amounts of imbalance between source and noise. However, some situations suffer extreme levels of imbalance, such as the classification of true transient sources from artefacts and noise





in wide-area sky surveys. When such large levels of imbalanced datasets cannot be avoided, supervised learning may not be sufficient and more input from other types of machine learning may be required [6].

Such high levels of imbalance is present in the data collected by the GOTO project. One attempt to solve this problem has been to apply the SMOTE technique [7], which increased the minority population (i.e., true transients) by simulating additional source data. Here, we tackle the problem by taking another approach. Instead of performing classification directly to the dataset, we clustered the dataset to get a useful pattern of the data and utilize that pattern to improve the quality of classification.

COMPUTATIONAL DETAILS

Machine learning techniques that have previously been used to analyse astronomical data have included: data collection and handling, data normalization, data preparation, Principle Component Analysis (PCA), cluster analysis and evaluation. For the aims of this paper, we have tried several typical clustering methods including KMeans, Agglomerative and DBSCAN. In order to justify the appropriate number of clusters that best represent a natural data structure, we apply the technique of clustering model evaluation. For this study, and following clustering indices that have been widely adopted in previous studies, we investigate the use of the Silhouette coefficients (SC) and Calinski-Harabaz (CH) indices. These indices are exploited to determine the best clustering method and setting for this dataset. Note that the implementation of the clustering algorithms and the calculation of the aforementioned quality indices are conducted by the scikit-learn [8] python library.

Data Acquisition

In order to investigate the possibility of using clustering to help analyse GOTO data while the telescope was still under construction (and thus prior to any data being obtained), we instead relied on simulated GOTO images. Another benefit of using the simulated data is that we know which sources in the images are “true” transients (since we put them into the data “by-hand”). We generated the GOTO image with the “SkyMaker” software [9] that can simulate observed astronomical images of stars and galaxies, including the complicating factors such as background noise and the point spread functions (PSF).

There are two database that are used to generate sources in our simulated GOTO images. The USNO CCD Astrograph Catalog (UCAC) was used for stars brighter than 17th magnitude while the Sloan Digital Sky Survey (SDSS) was used for galaxies and stars fainter than 17th magnitude. We queried these databases for all sources that would be covered by a single observation of one GOTO telescope. In addition to the source list, key characteristics of the telescope, such as the saturation level of the pixels (65,535), the zeropoint of the

telescope (the magnitude of a star that would result in one count per second; 23.5), pixel size (1.24 arcsecond per pixel), and CCD size in pixels (8176x6132) were also provided to SkyMaker. Finally, we allowed the PSF size to vary randomly from between 0.8 to 3 arcseconds to simulate the effects of the varying atmosphere on the PSF.

To simulate transient sources, we simulate two observations of a given patch of sky and inject new sources in the second observation. The injected sources are placed at random positions across the simulated image with magnitudes selected randomly from between 14 to 19. These images are processed using the LSST software stack [10], with the output from the stack forming the input of our clustering process.

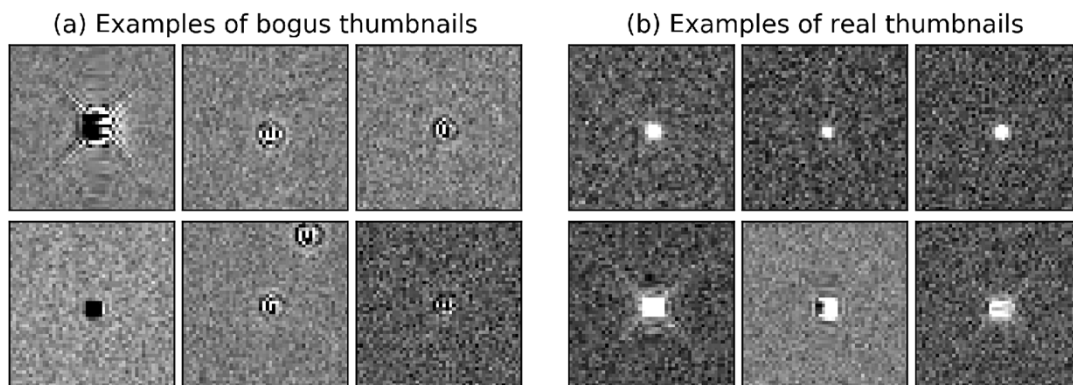


Figure 1. Image examples of bogus and real sources

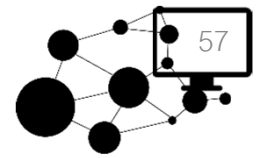
Data Preparation

The original dataset presented in this research contains a total of 7,891 records with 29 attributes. Each record has a variable flag that indicates whether it is a transient source (flag=1) or not (flag=0).

Table 1: All features from data extraction of the image difference.

Features Name	Description	Informative
Id	Identification number of objects	No
RA	Right ascension of objects	No
DEC	Declination of objects	No
SdssCentroid_x	x- component in pixel coordinate	No
SdssCentroid_y	y- component in pixel coordinate	No
PSF_flux	The brightness within the PSF of the camera	Yes
PSF_flux_Sigma	A measure of the uncertainty associated with PSF_Flux	Yes

DipoleFit_Flux	The brightness that he appearance positive pixels next to negative pixels and arise due to imprecisions in the difference imaging process.	Yes
DipoleFit_Flux_Pos	The brightness of the positive part of the dipole	Yes
DipoleFit_Flux_Pos_Sigma	A measure of the uncertainty associated with DipoleFit_Flux_Pos	Yes
Psf_Dipole_Flux_Neg	The brightness of the negative part of the dipole within the PSF of the camera	Yes
Psf_Dipole_Flux_Neg_Sigma	A measure of the uncertainty associated with Psf_Dipole_Flux_Neg	Yes
Psf_Dipole_Flux_Pos	The brightness of the positive part of the dipole within the PSF of the camera	Yes
Psf_Dipole_Flux_Pos_Sigma	A measure of the uncertainty associated with Psf_Dipole_Flux_Pos	Yes
DipoleFit_Flux_Neg	The brightness of the negative part of the dipole	Yes
DipoleFit_Flux_Neg_Sigma	A measure of the uncertainty associated with DipoleFit_Flux_Neg	Yes
Variable_Flag	Flag indicates type of sources either transient or non-transient	Yes
Psf_Dipole_Flux_Pos_x	x-component in pixel coordinate of positive flux	No
Psf_Dipole_Flux_Pos_y	y-component in pixel coordinate of positive flux	No
Psf_Dipole_Flux_Neg_x	x-component in pixel coordinate of negative flux	No
Psf_Dipole_Flux_Neg_y	y-component in pixel coordinate of negative flux	No
Psf_Dipole_Flux_x	x-component in pixel coordinate of positive flux	No
Psf_Dipole_Flux_y	y-component in pixel coordinate of positive flux	No
DipoleFit_Flux_Pos_x	x-component in pixel coordinate of positive flux	No
DipoleFit_Flux_Pos_y	y-component in pixel coordinate of positive flux	No
DipoleFit_Flux_Neg_x	x-component in pixel coordinate of positive flux	No
DipoleFit_Flux_Neg_y	y-component in pixel coordinate of positive flux	No
DipoleFit_Flux_x	x-component in pixel coordinate of positive flux	No
DipoleFit_Flux_y	y-component in pixel coordinate of positive flux	No



Data Cleaning

There are 1,902 records that have missing values. Considering the missing values and high-dimensional space, we choose to first preprocess prior to performing any further analysis. There are several methods to deal with the missing values such as simply “Deleting” the record or “Interpolating” to estimate the missing data. In this work we chose to delete all records that have missing values. Therefore, from the original 7,891 we retain 5,989 records for further analysis, where 5,973 belong to class 0 and 16 belong to class 1.

Data Transformation

After cleaning the data, the next step is the selection of the features to provide to the learning model. We know that not all features are informative. For example, in this case, the features referring to the (x,y) coordinate of the sources were considered not informative. Table 1 shows that 18 non-informative features were excluded from the computation and 11 informative features were included. The feature named “variable flag” was not used as input to the model but reserved for checking the quality of the clustering results.

Data Normalization

There are many techniques to normalize data prior to supplying it to the learning model. From our trials, the best normalization for this dataset is the normalization in vector space model [11]. In this technique, a record j with n features is considered to be n dimensional vectors. All features are considered as basis vectors and the value, x_j , in each feature is the component of the basis vector. We normalized these vectors by their Euclidean norm:

$$\hat{x}_j = (x_1, x_2, \dots, x_n)^T / \sqrt{(x_1^2 + x_2^2 + \dots + x_n^2)}_j$$

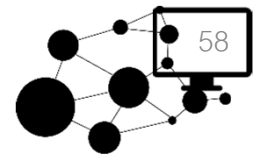
PCA

Principal component analysis (PCA) is a statistical analysis method that converts the dimensions of the dataset to a new set of orthogonal and uncorrelated dimensions. This technique was used to reduce the 11 original input attributes to a smaller number of output principal components. By comparing the eigenvalues of attributes covariance matrix or contribution rates of each eigenvector (i.e., which are scores of each principal component contribution data set), we selected 2 suitable principal components to represent the data. The contribution rates of the first (pc1) and the second principal component (pc2) are 76.5% and 16.9% respectively. This implies that the variance from these two components capture more than 90% of the variance of all 11 original input attributes, meaning the new two-dimensional parameter space is a good representation of the original dataset.

Clustering Techniques

We applied the standard data clustering algorithms which are based on different assumptions of clusterings:





- Kmeans is a representative for the partitioning methods
- Agglomerative is a representative for the hierarchical methods
- DBSCAN is a representative for the density based methods

All of these methods were applied to the GOTO data whose dimensions have been reduced via PCA. The data were clustered with the choice of cluster numbers ranging from 2 to 8. Then, the corresponding results are assessed against the identified quality indices to identify the most appropriate clusters.

Clustering Index

We chose 2 clustering indices to evaluate the quality of the clustering results:

- *Silhouette Coefficients (SC)*: The calculation of the coefficient is based on two mean distances, which are the distance within the cluster (a) and the distance between nearest clusters (b). The Silhouette coefficient is defined as

$$s = \frac{(b - a)}{\text{Max}(a, b)},$$

which lies with the range of $[-1, 1]$. If the Silhouette score is close to 1, the cluster will be very compact and clearly separated from the nearest cluster.

- *Calinski-Harabaz (CH) Index*: CH index is the ratio of the dispersion within the cluster to the dispersion between the clusters:

$$s(k) = \frac{\text{Tr}(B_k) / (k - 1)}{\text{Tr}(W_k) / (N - k)},$$

where N is a number of samples, k is a number of clusters, B_k is the covariance matrix between clusters, and W_k is the covariance matrix within each cluster. This index does not have a fixed range; instead, a higher index corresponds to a better quality of the cluster.

Note that both measurement methods can be performed without knowledge of the ground truth classes, which satisfy the original purpose of this study and, therefore, make it more applicable to the real-world situation.

RESULTS AND DISCUSSION

After clustering the GOTO data using the cluster numbers between $k=2$ to 8 with the aforementioned three methods, we consider their performance in the context of the above indices. Specific to the SC metric, the comparison of SC scores achieved by different methods is shown in Figure 2. The measures for Kmeans and Agglomerative are similar to each other and are always higher than those of DBSCAN. Given this observation, Kmeans and Agglomerative are more suitable for the GOTO data. These results also show that $k=3$

provides the best clustering for Kmeans and Agglomerative, whereas the best k for DBSCAN (the weaker of the two methods) is 3.

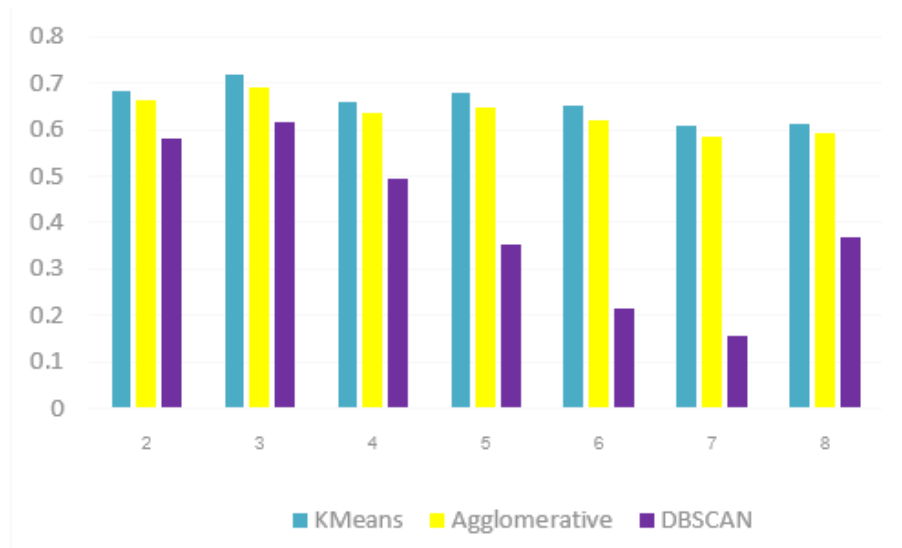


Figure 2. Silhouette coefficients comparison of Kmeans clustering, Agglomerative clustering and DBSCAN clustering.

Similarly, the comparison using CH index (see Figure 3) also suggests that Kmeans and Agglomerative perform better than DBSCAN. The CH index also indicates that Kmeans always performs better than the corresponding Agglomerative method. If we only consider CH index, $k=8$ is the best option for both Kmeans model and Agglomerative, while $k=3$ is the most appropriate for DBSCAN.

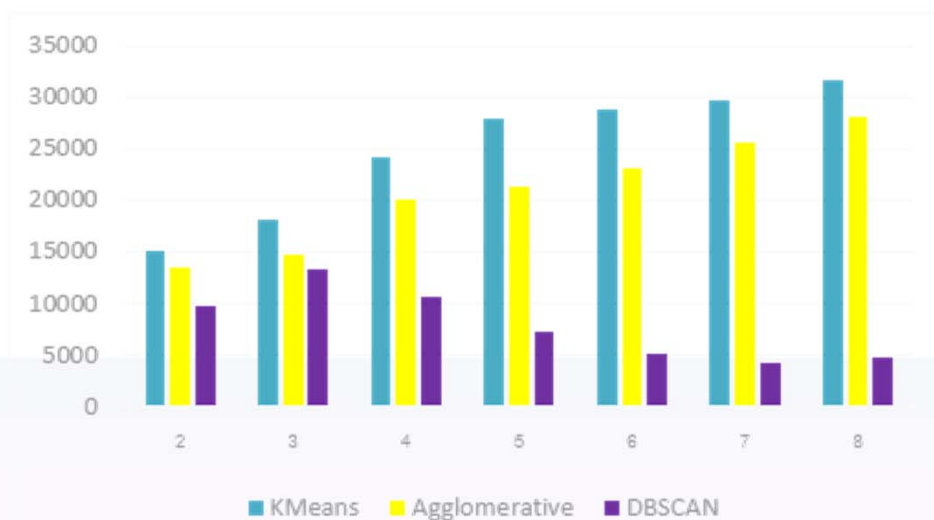


Figure 3. Calinski-Harabaz index scores comparison of Kmeans clustering, Agglomerative clustering, and DBSCAN clustering.

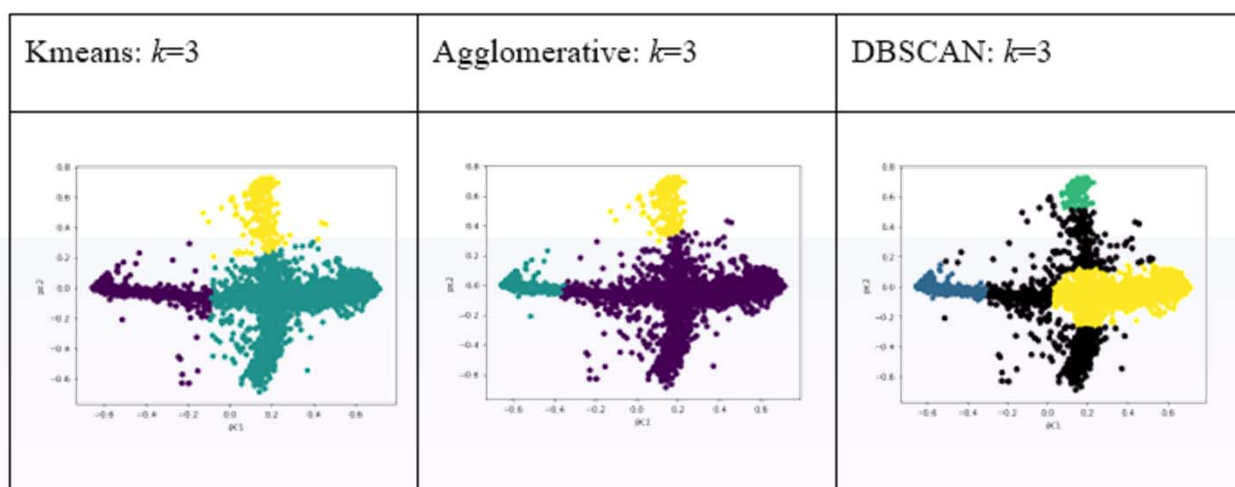
There are several points that we can learn from Figure 2 and 3. The SC and CH measures obtained by Kmeans and Agglomerative show a similar trend. For the

Agglomerative method, we applied ward linkage that minimizes the variance of the clusters being merged. This linkage strategy will select the representatives from each cluster and decide which pair is the closest and therefore should be merged. These cluster-specific samples must be close to the centroid of the cluster and have a tendency to form a convex cluster. Provided with this insight, Kmeans and Agglomerative generally give the similar cluster results.

Comparing the SC and CH scores of Kmeans and Agglomerative, we notice an inconsistency of the best k from both indices. The SC gave the best $k=3$ but the CH index gave $k=8$. By contrast, DBSCAN shows a more consistent outcome with both indices, with $k=3$ providing the highest scores with both SC and CH index. Therefore, DBSCAN will still be considered here to provide an alternative finding, even though its scores are low in all cases compared with the other two. It must to be noted here that both SC and CH index are distance-based evaluations and so can be biased toward the Kmeans and Agglomerative, which are distance-based clustering methods. Evidence of this can be observed in both Figure 2 and 3 which show that the indices for Kmeans and Agglomerative are always higher than that for DBSCAN. This, again, highlights how it might be too early to justify ruling-out DBSCAN for clustering analysis of GOTO data.

We have discussed the results of clustering evaluation by only considering clustering indices. On this basis, we introduction of scatter plots can be used to further asses the pros and cons of the five clustering models. Table 1 and Table 2 show the five best clustering model scatter plots in two-dimensional space. Within each scatter plot different colors or shapes refer to the points belonging to different clusters.

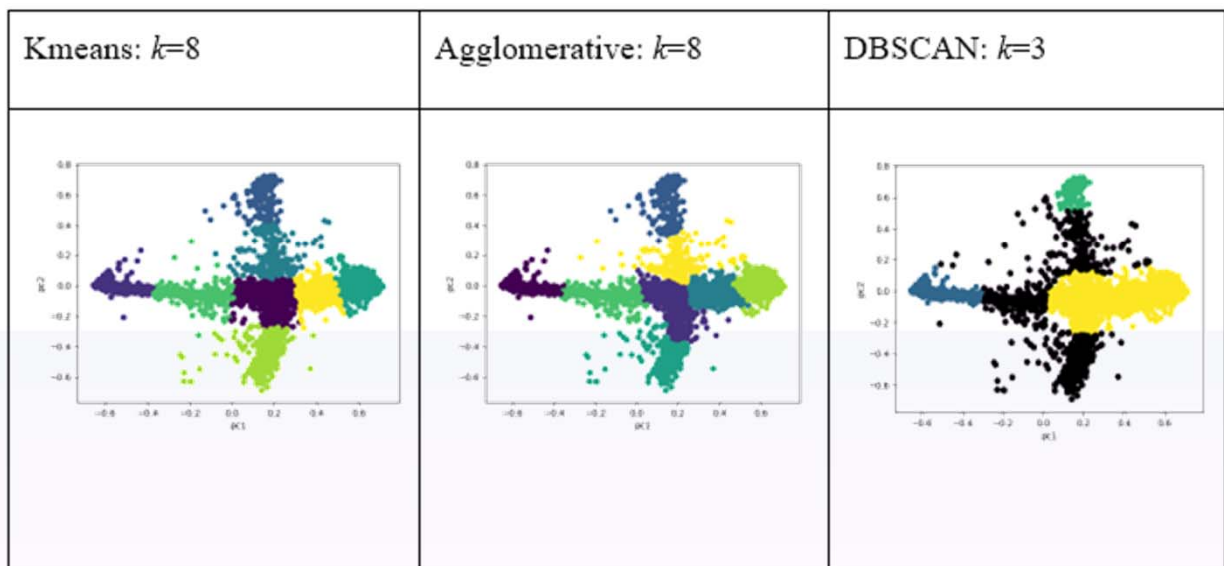
Table 1: The best clustering model scatter plots in two-dimensional space, where x-axis is principal component 1,y-axis is principal component 2.



	Transient	Non-Transient	T:N Ratio	Transient	Non-Transient	T:N Ratio	Transient	Non-Transient	T:N Ratio
Cluster 1	12	471	2.55e-2	5	3429	1.46e-3	2	2147	9.32e-4
Cluster 2	2	3216	6.22e-4	2	2104	9.51e-4	9	363	2.48e-2
Cluster 3	2	2286	8.75e-4	9	440	2.05e-2	0	2755	0
Outlier							5	708	7.06e-3

The information from Table 1 shows that all the clustering methods that we use can reduce the degree of imbalance within the dataset. For example, Kmeans and Agglomerative have one cluster and DBSCAN has one cluster that increase the Transient to Non-Transient ratios (T:N Ratio) to the degree that the standard J48 classification method can achieve Precision better than 80% for this dataset [7] when the original T:N Ratio is worse than $8e-3$. Moreover, DBSCAN produces one cluster in particular that contains only 2755 Non-Transient. This kind of cluster will help us to tackle the imbalance problem by screening out the Non-Transient data from the dataset.

Table 2 The best clustering model scatter plots in two-dimensional space, where x-axis is principal component 1, y-axis is principal component 2.

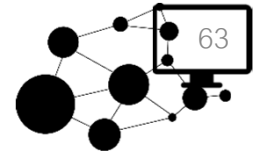


	Transient	Non-Transient	T:N Ratio	Transient	Non-Transient	T:N Ratio	Transient	Non-Transient	T:N Ratio
Cluster 1	2	2095	9.55e-4	2	2104	9.51e-4	2	2147	9.32e-4
Cluster 2	0	940	0	0	713	0	9	363	2.48e-2
Cluster 3	9	407	2.21e-2	9	440	2.05e-2	0	2755	0
Cluster 4	3	240	1.25e-2	0	971	0			
Cluster 5	2	298	6.71e-3	2	250	8e-3			
Cluster 6	0	883	0	0	262	0			
Cluster 7	0	248	0	0	989	0			
Cluster 8	0	862	0	3	244	1.23e-2			
Outlier							5	708	7.06e-3

On the other hand, if we believe the best k from the CK index and extract information as shown in Table 2, then Kmeans with $k=8$ has only 1 cluster with a T:N Ratio of more than $8e-3$ and 4 clusters that have only 2,933 Non-Transient sources. Agglomerative with $k=8$ has 2 clusters that the ratio more than $8e-3$ and 2935 Non-Transients from 4 clusters that can be screened out. Finally, DBSCAN with $k=3$ has 1 cluster that the ratio more than $8e-3$ and 2755 Non-Transient from one cluster to remove.

CONCLUSION

The extremely imbalance nature of the GOTO dataset is the main factor that effects the precision of classification. To improve the classification performance, we need to find a hidden pattern in the dataset and use it to identify a more focused group for classification and removing the noise. We achieved this by applying PCA to the normalized dataset with the selected features. Several standard clustering methods from difference clustering strategies were then applied to the dataset. As a result, all of the clustering methods that we used can find clusters that we can then use to reduce the level of imbalance within the data, allowing us to classify sources more effectively.

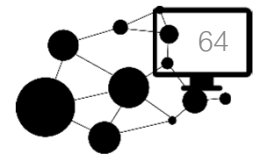


ACKNOWLEDGMENTS

This work was supported by Newton Fund (STFC-NARIT).

REFERENCES

- [1] B. P. Abbott et al., “Observation of gravitational waves from a binary black hole merger,” *Phys. Rev. Lett.*, vol. 116, no. 6, pp. 1–16, 2016.
- [2] A. Rau et al., “Exploring the Optical Transient Sky with the Palomar Transient Factory,” *Publ. Astron. Soc. Pacific*, vol. 121, no. 886, pp. 1334–1351, 2009.
- [3] D. A. Goldstein et al., “AUTOMATED TRANSIENT IDENTIFICATION IN THE DARK ENERGY SURVEY,” *Astron. J.*, vol. 150, no. 3, p. 82, Aug. 2015.
- [4] M. Lochner, J. D. McEwen, H. V. Peiris, O. Lahav, and M. K. Winter, “Photometric Supernova Classification With Machine Learning,” 2016.
- [5] L. du Buisson, N. Sivanandam, B. A. Bassett, and M. Smith, “Machine learning classification of SDSS transient survey images,” *Mon. Not. R. Astron. Soc.*, vol. 454, no. 2, pp. 2026–2038, 2015.
- [6] D. E. Wright et al., “A transient search using combined human and machine classifications,” vol. 10, no. July, pp. 1–10, 2017.
- [7] A. B. Tabacolde et al., “Transient Detection Modelling for Gravitational-wave Optical Transient Observer (GOTO) Sky Survey,” in *Proceedings of the 2018 10th International Conference on Machine Learning and Computing*, 2018, pp. 384–389.
- [8] F. Pedregosa et al., “Scikit-learn: Machine Learning in Python,” *J. Mach. Learn. Res.*, vol. 12, pp. 2825–2830, 2011.
- [9] E. Bertin, “SkyMaker: astronomical image simulations made easy”, *MmSAI*, 80, 422, 2009
- [10] J. Bosch et al., The Hyper Suprime-Cam software pipeline, *PASJ*, 70, 5, 2018
- [11] G. Salton, A. Wong, and C.-S. Yang, “A Vector Space Model for Automatic Indexing,” *Mag. Commun. ACM*, vol. 18, no. 11, pp. 613–620, 1975.



Loop prevention on Software Defined Network using Adaptive Virtual Tunnel Network

Piyakorn Phanklin¹, Nuttapol Sermsuksakulchai¹, Thadthai Szeto², Sirichai Kamnerdlo², Worrapong Arnyong², Suthep Wiwatchaiwong^{2,C}, and Supakit Prueksaroon^{1,C}

¹Department of Computer Engineering, Faculty of Engineering,
Thammasat University, Pathum Thani, Thailand

²CS Loxinfo Public Co., Ltd, CW Tower, 90 Ratchadapisek Road, Huai Khwang, Bangkok, 10310

^CE-mail: thepsp@csloxinfo.net, psupakit@engr.tu.ac.th

ABSTRACT

Nowadays, Cloud data center is very high complexity and requires a lot of network devices. The automate networking systems and centralize management system is needed to meet customer's expectations. Loop is a most common problem in general and enterprise network. Spanning tree protocol (STP) is a standard loop detection and recovery by drop some network links to remove the loop. All network switches require pre-configuration manually. Software-Defined Networking (SDN) has solved this problem. With SDN, the control plane is removed from the network device's hardware and implements it in software call SDN controller instead. With the OpenFlow protocol, SDN controller centrally controls routing, network operation and each network device can be configured centrally. OpenDaylight has a feature to prevent loop called Loop remover that imitates technique from STP. Loop remover has a limitation of best path selection. In this paper, we used OpenDaylight as SDN controller and operated features called Virtual Tenant Network (VTN). VTN provides the multi-tenant virtual network on an SDN controller for single physical network resources. VTN can reduce the investment for each physical tenant network, simplifies design, implement and operate the entire complex network. Although the network is designed on VTN, the data is still transferred over the physical network which can be a complicated network and cause a loop on SDN. This paper, we develop our loop prevention system based on VTN application. We provide automate loop prevention and routing management by calculating the best path by using Dijkstra's Algorithm. The packages flow generates by SDN and VTN application automatically.

Keywords: SDN, VTN, Loop, OpenDaylight.

INTRODUCTION

Growing Enterprise Network and Enterprise Data Center make networking complex and requires a lot of network devices and cause the loop in the network. Layer 2 loop is usually occurring in general and enterprise network which is the state that the switch sends a frame to the network and infinitely loop in the system. The loop creates broadcast storms cause the whole network to meltdown and lead to the failure of network communication, multiple copies of unicast frame may be delivered to a destination host so the waste of processing occurs, and





media access control (MAC) database instability because of the same source MAC address could be seen on multiple ports.

Spanning tree protocol (STP) [1] is standard loop detection and recovery by dropping some network links to remove the loop. But the STP enabled path is not the best path. As shown in Figure 1, STP uses an algorithm that calculates the best loop-free path (Path A) but Path B is the best path from Switch B to Switch C.

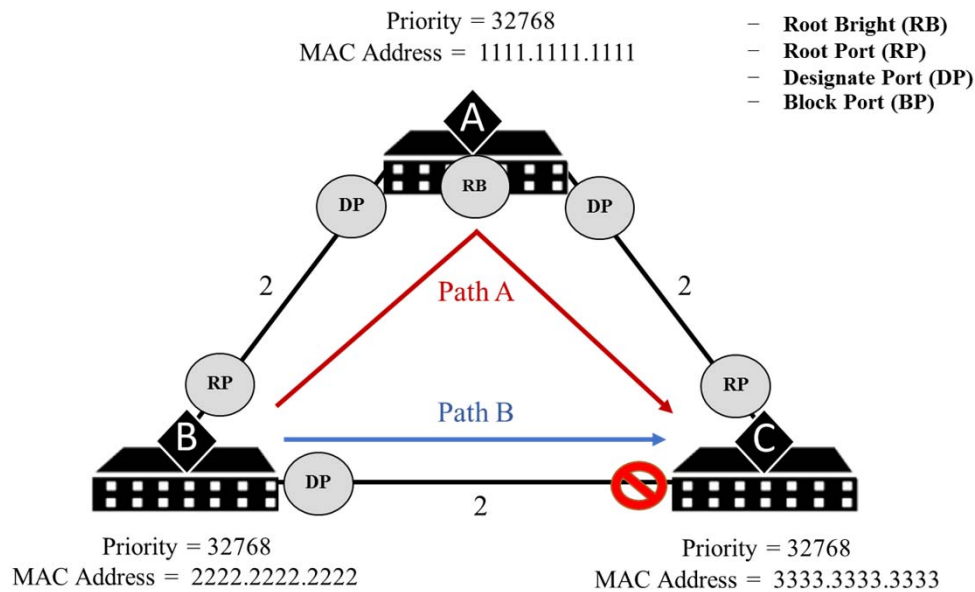
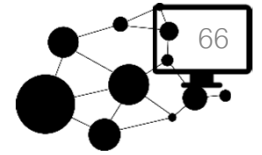


Figure 1. Example Network to Illustrate STP

Software-defined networking (SDN) is a network architecture that centralized in software-based SDN controllers. SDN controller provides a single control plane and centrally controls routing, network operation and each network device can be configured centrally. In traditional network architecture, the control plane is response for configuration of the device that depending on device vendor causes limitations of network management and an error configuring network device which may impact the network. The control plane is responsible for deciding how to forward the received data and also in SDN network. But in SDN network, there is a single control plane to centrally controls routing, network operation and each network device can be configuration centrally by SDN Controller. The centralized management on the SDN Controller will allow the device to make the same standard decisions so network administrators can respond quickly to changing business needs that do not need to directly manage the network device. And it also handles the flow entries more effectively and flexible. In addition, the ordinary switches that support the OpenFlow [3] that can be used in SDN network, no need to use Enterprise switches. The Application Programming Interfaces (API) that resides in between the application layer and control layer is the northbound API, which SDN controller used it to communicate to the applications. And southbound API is used to communicate between the SDN controller, OpenFlow switches, and routers of the network. The southbound API serves as the OpenFlow or alternative protocol specification so that the network can be programmed with OpenFlow protocol on the SDN controller. We used OpenDaylight [2] controller as the SDN controller platform to unified control across a network of different network devices. Virtual Tenant Network (VTN) [4] is an application that provides



the multi-tenant virtual network for single physical network resources with complete separation of a logical plane from the physical plane. The VTN can reduce the investment for each physical tenant network, simplifies design, implement and operate the entire complex network. Although users can define network on VTN, the data is still transferred over the underlying physical network which can be a complicated network and cause a loop on SDN.

In this paper, we provide automate loop prevention and routing management by calculating the best path by using Dijkstra's algorithm based on VTN mechanism.

THEORY AND BACKGROUND TECHNOLOGIES

The network loop

The loop states that the switch sends frames to the network and infinitely loop in the system. Loop on Data Link Layer (or switching loop) occurs in networks when there is more than one path between two endpoints. Loop creates broadcast storms, switch forwarded broadcast messages by switches out every port and other switches will repeatedly rebroadcast the broadcast messages flooding the network. Because the Data Link Layer's frame header does not support a time to live (TTL) field, if the frame is sent into a looped topology, the result is an infinite loop in the network.

The loop can cause misleading entries in a switch's MAC database and can cause endless unicast frames to be broadcast throughout the network. A loop can make a switch receive the same broadcast frames on two different ports, and alternately associate the sending MAC address with the one or the other port. It may then incorrectly direct traffic for that MAC address to the wrong port, effectively causing this traffic to be lost, and even causing other switches to incorrectly associate the sender's address with a wrong port as well.

Spanning Tree Protocol

In a legacy network with loops, The IEEE 802.1D Spanning Tree Protocol (STP), a standard layer-2 protocol, is used to construct spanning tree to prevent the packet broadcast storm problem to remove the loop. If STP detect a loop, it will be truncated to a unique path or a single path to the node by disabling some network links. When the STP feature is enabled, the switch will send a special frame to exchange information across bridges and detect loops in a network topology. This special frame is called the BPDU (Bridge Protocol Data Unit) and relayed by every bridge in the network with this format as shown in Figure 2.

Protocol identifier (2 bytes)	Version (1 byte)	Message type (1 byte)	Flags (1 byte)	Root ID (8 bytes)	Root path cost (4 bytes)	Bridge ID (8 bytes)	Port ID (2 bytes)	Message age (2 bytes)	Maximum age (2 bytes)	Hello time (2 bytes)	Forward delay (2 bytes)
----------------------------------	---------------------	--------------------------	-------------------	----------------------	-----------------------------	------------------------	----------------------	--------------------------	--------------------------	-------------------------	----------------------------

Figure 2. BPDU Frame Format

Virtual Tenant Network (VTN)

Typically, the network is configured as a silo and it needed a huge investment in networking and operating expenses. Because network device is installed for each tenant and cannot be shared resources with others.

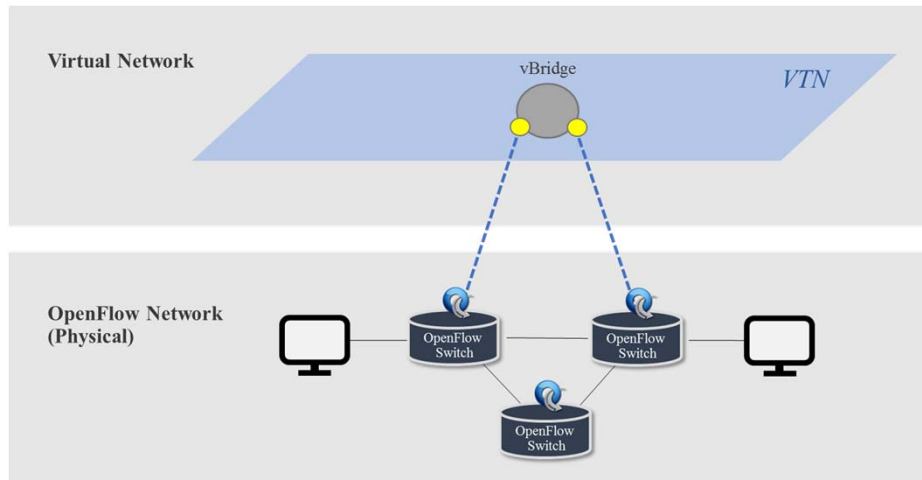


Figure 3. Example Network to Illustrate VTN

VTN is a network application that provides the multi-tenant virtual network on an SDN controller. The virtual tenant can be used to support each virtual network and can be shared on a physical network with others. This reducing cost and managing network resources better through the use of visualizations for SDN management. Once users design virtual network on VTN and map to the physical network then configured on the individual OpenFlow switch leveraging SDN control protocol without having to physically set up network devices. VTN hide the entire complex underlying physical network, users can design virtual network on VTN without knowing the topology of the physical network. The illustration of VTN logical view as shown in Figure 3.

EXPERIMENTAL AND DEVELOPMENT DETAILS

In this work, we used the OpenDaylight that enable VTN application. The controller can provide multiple tenants that support virtual networks on the physical network. The VTN will automatically generate flow entries on all OpenFlow switches, once the switches connect to the controller. The VTN flow entries are pushed to the individual OpenFlow switches. We develop a program to manage the loop free on datalink layer. The program used a VTN mechanism to detect the topology and generate new flow automatically when topology changed. The flowchart to the program shown in Figure 4. Although the network is based on VTN, the data is still transferred while loop occurs on SDN. From the flowchart, the original topology that generated by VTN was saved in case of the initial state. The VTN managed loop-free by using STP protocol. The running topology is loading to compare with the original topology to find the link different or link failure. We provide automate shortest path selection by overwriting the VTN flow table. The Dijkstra's algorithm use a shortest path algorithm. To calculating a cost for best path, the program generates the end to end flows based on the combination of two performance metrics: the average latency and the port bandwidth of every OpenFlow switches. When the topology changed, VTN generates new flow entries in automatic and recalculate the best path again.

In our experiment, program developed by Python. The program leveraging the northbound by REST API to transfer data to OpenDaylight controller and our program. The standard JSON format was used. The HTTP methods provide the operations, such as create, read, update, and delete that can perform to the controller. The users cannot configure a flow

by themselves, the program generated flow entries automatically. We install on the IBM x3100 Intel Xeon E3-1230v2 3.3GHz memory 32GB harddisk 1TB and gigabit Ethernet. We have three OpenFlow switches model HP 5130-24G and HP 3800-24G. The OpenDaylight version Beryllium was used. The user interface of our program as shown in Figure 5. Our experiments show that program can achieve well loop detection and automate loop-free with the shortest path as a requirement.

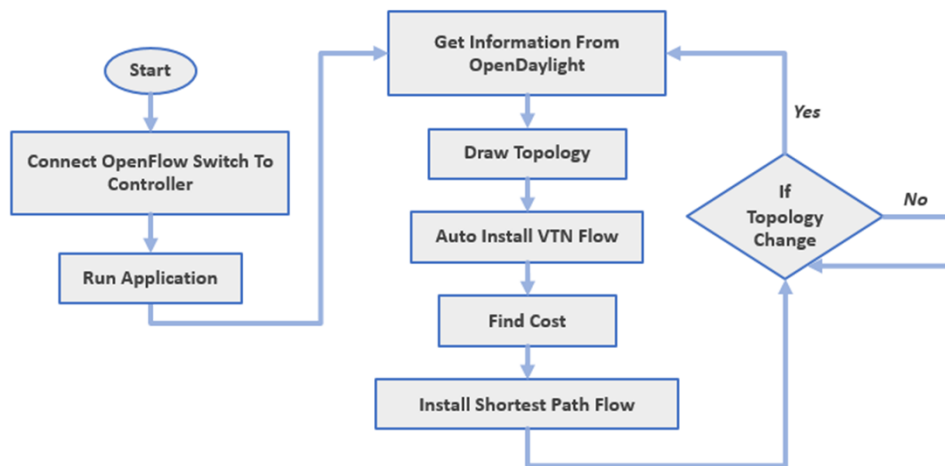


Figure 4. Flowchart of the program

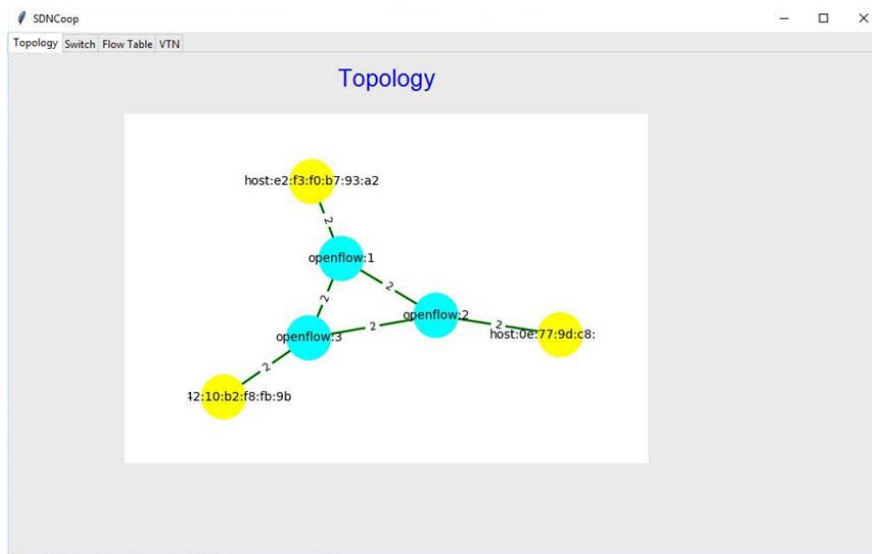
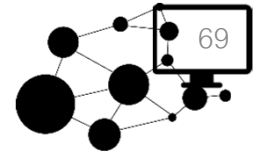


Figure 5. the program user interface

CONCLUSION

A solution has been proposed to overcome the SDN loop problem. We develop automated loops prevention and shortest path routing management. Our program can automatically generate flow entries over VTN application and calculate the best path by using Dijkstra's Algorithm based on average latency and port bandwidth. The program doesn't allow manage by manual, which it cause of loop problem on SDN network. The program allows the users to define multiple virtual networks on a single physical network that improves the resource allocation efficiency.

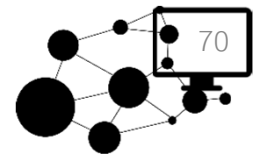


ACKNOWLEDGMENTS

The authors acknowledge Thailand Research Fund (TRG5780062), CS Loxinfo Public Co., Ltd. and faculty of Engineering, Thammasat University that have contributed to the research results and reported within this paper.

REFERENCES

- [1] *IEEE 802.1D spanning tree protocols*, The Institute of Electrical and Electronics Engineers (IEEE), 9 Jun. 2004. available online at <https://ieeexplore.ieee.org/document/1309630/>
- [2] *OpenDaylight controller*, The OpenDaylight Foundation, available online at <https://www.opendaylight.org/>
- [3] *OpenFlow Switch Specification*, Open Networking Foundation, Jun. 2012.
- [4] Shreyansh, J., *Understanding OpenDaylight VTN and the Redirection Function*, NEC Technologies India Pvt. Ltd., available online at https://events.static.linuxfound.org/sites/events/files/slides/OpenDaylight_VTN_Redirection_Shreyansh_201504_0.pdf



Resilience flow management on Software-Defined Network using the Directed graph for L2 Loop prevention

Kanjanart Junnawat, Mookdaporn Roekpootaweeporn, and Supakit Prueksaaron^C

*Department of Computer Engineering, Faculty of Engineering, Thammasat University,
Pathum Thani, Thailand*

^CE-mail: psupakit@engr.tu.ac.th

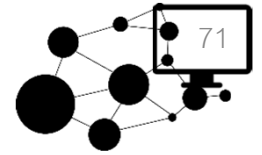
ABSTRACT

In large-scale data centers that are dealing with thousands of computer servers, storages, and network switches. The network problem happens regularly from many factors such as hardware malfunction, human errors and software errors. The network loop is a one of the common problem that is occurring from human error. To prevent this problem, normal data center run a Spanning Tree Protocol (STP) that will drop some network links to eliminate network loop with specific conditions. However, network management in large-scale datacenter very difficult and high complexity. Because their network consist of many network switch's brands and it requires a special command to management. Software-Defined Network (SDN) solve these problems by a separate operation of control plane and data plane. The control plane is a part of packets flow control and policies management. The second part is the data plane by performs the packet forwarding. SDN required to centralize management called controller to act as software control plane. Opendaylight (ODL) is the most popular SDN controller and support interfacing with GUI and REST API. ODL supported standard loop detection and prevention by using Spanning Tree Protocol (STP). STP provides a mechanism to drop some network link to evade network loop. To control the network flow and forwarding direction cannot possible when using STP. In this work, we extended our program to the detect loop in SDN network and provide dynamic forwarding flow to every Openflow switches. The Directed graph technique is used as loop detection. Program provides the normal flow and end to end flow in case of loop occurred. The end to end flows are based on Dijkstra's algorithm to select the shortest path.

Keywords: SDN, VTN, Loop, OpenDaylight.

INTRODUCTION

In a Software Defined Network (SDN), the behavior of the underlying switches is determined globally, by a controller which dictates the local rules each switch should use to direct packets it encounters. This centralized control is a best significant benefit of SDNs, but also a source of potential pitfalls. In an SDN network, the SDN switch called OpenFlow switch, it allows to write network operating systems that can accommodate suites of applications which work together on the controller to make the network run smoothly. Using such a system we can write the program that works in tandem to perform different functions in a network such as a network visualization, traffic analysis, or traffic simulation. The SDN switch has less functionality and these switches forwarding of packets based on the policies in its flow tables. The SDN controller performs to distribute flow to every switch and these switches perform



forwarding of packets accordingly. If there are not matching policies found, then these switches communicate to its controller regarding the arrived packet. The controller then instructs flow entries to every switch from source to destination and provide the path for the communication. There is three types of application programming interface (API) in SDN. These interfaces are North Bound interface, South Bound interface, and East-West interface. The communications between an SDN controller to all switches are done through the secure channel, Transport Layer Security. Examples of different well-known controllers are NOX, POX, Beacon, OpenDay light, Floodlight, Ryu, Trema, ONOS, Juniper Contrail etc.

The SDN framework design to solve the complex problem in the large-scale datacenter. For example, consider the problem of routing consistency. When the routing instructions sent to switches are generated by complex chains of modules it can become difficult or impossible to provide theoretical guarantees that the network will avoid certain types of bad behavior. The loops are a potential problem in a computer network, which are cyclical paths through the switches that can block some packets to never leave the network. This sort of behavior can lead to increased latency, power consumption, and can possibly be targeted for attack.

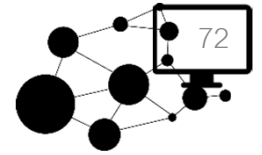
In [1], Kazemian et. al. tackled this problem on static (not software defined) networks using a theoretical model that they call Header Space Analysis. Unfortunately, their framework does not extend to dynamic, Software Defined Networks. Thus, following their work, we have developed the program for detecting loops on functioning OpenFlow networks and built an application that can detect looping behavior in networks, but also prevent in real time and discover the shortest path. By monitoring a network from SDN controller, we can verify that every new flow table entry and every withdrawn entry will not cause any packets to loop in the network for a relatively small amortized cost. Our application can be customized to make controllers refuse to install flow table entries by using REST API.

The objective of our paper is to emphasize loop free in SDN, discover the shortest path possible and identify an alternative path during link down. The proposed approach designed using OpenDaylight controller and industrial OpenFlow switches.

BACKGROUND AND RELATED WORKS

The framework of Header Space Analysis, presented in [1], provides a geometric interpretation of packet flows in networks. The authors begin by modeling packets as points in a discrete geometric space and define operators characterizing how a packet moves and is transformed through a network. By then constructing these functions for real functioning networks, they can build a model of the network that can be queried for properties like “Does user A communicate with user B?” or “is there any packet that user C can send through switch D that will not leave the network?”. In our work, we extend this framework to a graph theoretic one, which allows us to consider dynamic rule insertions and deletions over time much more simply.

Discovering the network topology is an important issue in SDN. One of the well-known loop free techniques is Spanning Tree Protocol (STP). STP protocol help to block the redundant paths when the network has more than one path to the same destination. During the main path is used, the reserve path was blocked by the root node. On the other hand, if main path down, STP will enable reservation path. STP find the path by sending BPDU to every switch in



network and BPDUs consist of bridge id, port id, root id and path cost. STP has a few disadvantages to efficient the network path and utilizes the bandwidth during the loop occurred.

Jmal et al. [2] Explained shortest path routing mechanism using POX controller. Pakzad et al. [3] proposed efficient topology discovery with the minimum number of Packet-Out events from the controller to the switches. Link failure is a common phenomenon in any networks. In [4] [5], the authors presented to handle link failure and provide failure recovery in OpenFlow protocol in SDN networks.

PROPOSED APPROACH

In this section, we will show how to model a whole network by using a Directed graph. Directed graph (Digraph) is dynamic algorithms to help us compute port to port reachability in our network. Digraph is a graph that has a set of vertices connected by edges, where the edges have a direction associated with them. The aim of this work we used Digraph for loop detection. From Figure 1, (a) the direction of the vertex of link between node 0 and 2 and self-looping of node 3. (b) show the circular looping. Digraph can detect loop by when a direction of edge can reach to parent node or itself then this topology has a loop in it. We use depth-first search algorithm to prevent backtracking on the same path.

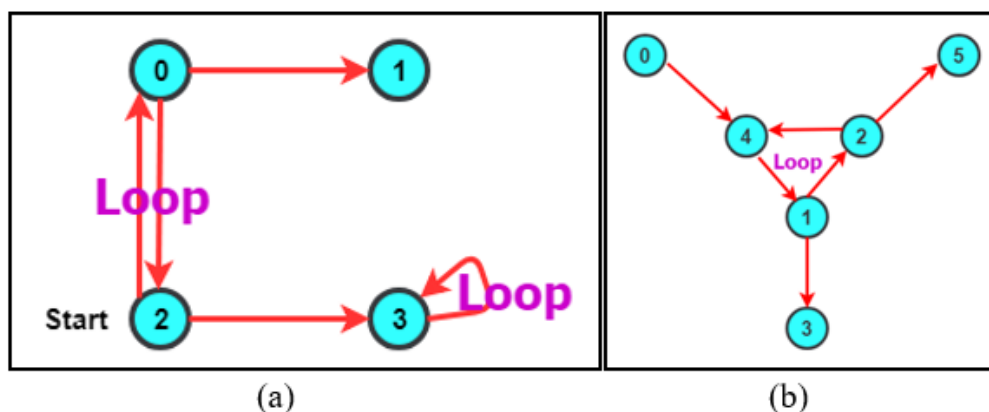


Figure 1. Example of loop detection in the Directed graph algorithms

Normally, Directed Graph Algorithm use number from 0 to amount of nodes to represent all nodes then our program requires a hostname conversion to a number as shown in Figure 2.

allnodes[host:66:48:b8:17:58:06]:	0
allnodes[openflow:1]:	1
allnodes[openflow:2]:	2
allnodes[host:b2:8d:d4:74:e4:9e]:	3
allnodes[openflow:3]:	4
allnodes[host:ea:5f:0c:86:ac:4e]:	5

Figure 2. Convert hostname to number

We use Dijkstra's Algorithm to find the shortest path by using cost that calculates from port utilization and port bandwidth. The equation of link's cost as shown in equation (1)

$$\text{Cost} = \frac{1}{\text{Bandwidth} \times (1 - \text{Utilization})} \quad (1)$$

From the link's cost that calculation from Dijkstra's Algorithm. The program start calculates the path from source to destination. The new flow entry put to the controller flow table by replacing the old one. Finally, packets travel from source to destination address correctly. The flowchart of our work as shown in Figure 3.

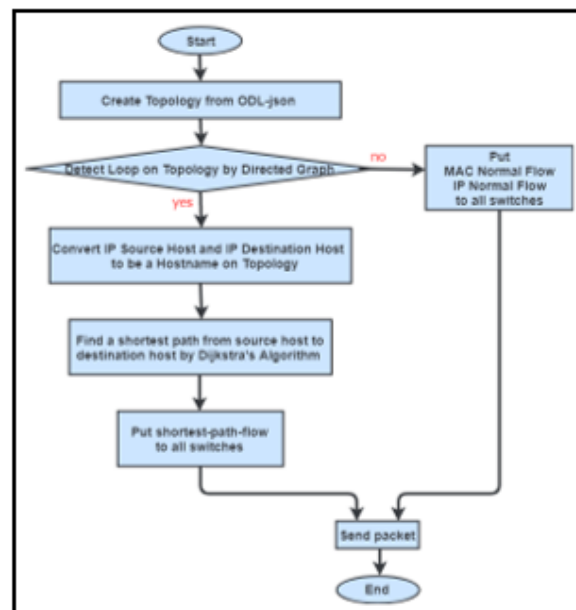
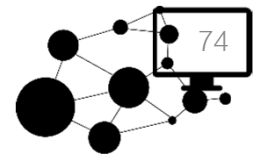


Figure 3. Flowchart of the program

EXPERIMENTAL DETAIL AND RESULTS

In order to verify that our algorithms are sufficiently efficient to run on functioning SDNs, we have developed our algorithm for loop detection in Python and run on both simulated environment and real environment for testing flow rule installations. OpenDaylight version Beryllium SR4 used as SDN controller. ODL features such as odl-resconf, odl-mdsal-apidocs, odl-dlax-all and odl-l2switch-switch are enabled. The program interfaces as shown in figure 4.

In our simulation, we based on Mininet that is a network emulator which creates a network of virtual hosts, switches and links. Mininet hosts run on standard Linux network software, and network switches support OpenFlow and SDN features. We simulate networks with a certain number of switches and clients per switch. The switches are first arranged in a ring with a port attached between every switch and its immediate neighbors. We then add ports between every pair of unconnected switches with a probability given by random. This test imitates real network environment and is intended to make loops thus forcing our program to do as much work as possible to handle our random rule insertions.



In our real environment, we used two HP switches model 5130-24G and HP switch model 3800-24G to evaluate our program. The three switches connect for looping in the delta pattern. We add ports between the unconnected pair by random also. Our program maintenance and backtracing are the most intensive tasks needed to be done. Given this network topology, program calculates the shortest path between end to end clients properly.

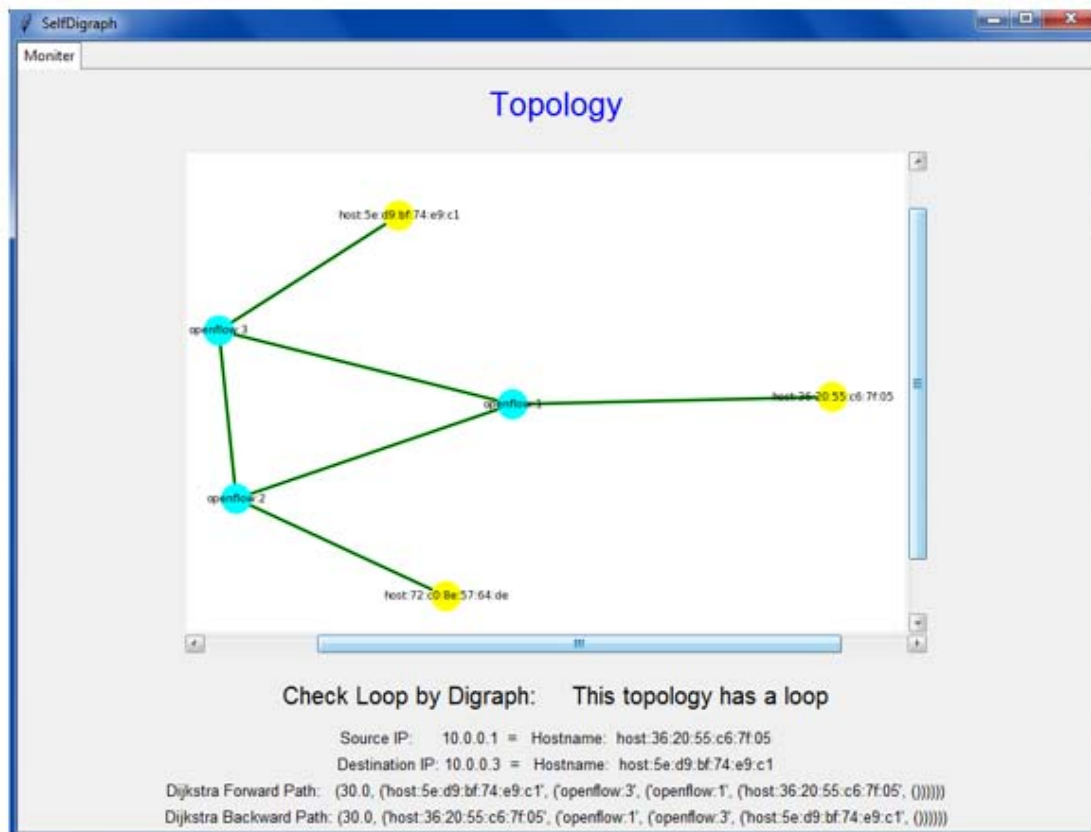


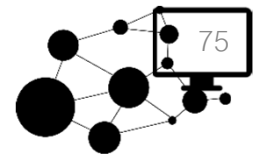
Figure 4. Program user interface

CONCLUSION

For any SDN network, loop detection and recovery are an important issue. The proposed algorithms are work as an event handler for the controller. Our program can automatically loop detection and prevention on SDN network. It used Directed graph algorithm to detect the loop and it used Dijkstra's algorithm to discovery the shortest path. We maintained the flow table to find the path and alternative paths. We used a minimum intermediate node path for communication. Our next plan is loop detection and prevention in large-scale network with supported link aggregation.

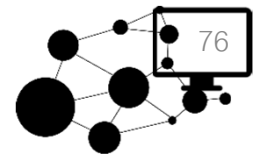
CONCLUSION

The authors acknowledge Thailand Research Fund (TRG5780062), CS Loxinfo Public Co., Ltd. and faculty of Engineering, Thammasat University that have contributed to the research results and reported within this paper.



REFERENCES

- [1] Peyman Kazemian, George Varghese, Nick McKeown. Header Space Analysis: Static Checking for Networks. In Proceedings of 9th USENIX Symposium on Networked Systems Design and Implementation (NSDI), 2012.
- [2] Jmal, R.; Chaari Fourati, L., "Implementing shortest path routing mechanism using Openflow POX controller," Networks, Computers and Communications, The 2014 International Symposium on , vol., no., pp.1,6, 17-19 June 2014
- [3] Pakzad, F.; Portmann, M.; Wee Lum Tan; Indulska, J., "Efficient topology discovery in software defined networks," Signal Processing and Communication Systems (ICSPCS), 2014 8th International Conference on, vol., no., pp.1,8, 15-17 Dec. 2014
- [4] Sharma, S.; Staessens, D.; Colle, D.; Pickavet, M.; Demeester, P., "Fast failure recovery for in-band OpenFlow networks," Design of Reliable Communication Networks (DRCN), 2013 9th International Conference on the , vol., no., pp.52,59, 4-7 March 2013
- [5] Sharma, S.; Staessens, D.; Colle, D.; Pickavet, M.; Demeester, P., "Enabling fast failure recovery in OpenFlow networks," Design of Reliable Communication Networks (DRCN), 2011 8th International Workshop on the , vol., no., pp.164,171, 10-12 Oct. 2011
- [6] Chinnawat Nualta, Chanon Taupachit, Nawin Somyat, Wachira Promsaka Na Sakolnakorn, and Supakit Prueksaaron, "Spinner: Automatic Failure Detection and Recovery," The 5th International Conference on Engineering, Energy and Environment, pp 107-112, 1-3 November 2017.
- [7] Saha, Anish Kumar, Koj Sambyo, and C.T Bhunia. "Topology Discovery, Loop Finding and Alternative Path Solution in POX Controller", Proceedings of the International MultiConference of Engineers and Computer Scientists 2016 Vol II, IMECS 2016, March 16 - 18, 2016, Hong Kong.



Existence and Approximation of Solutions of Coupled Fractional Order Hybrid Differential Equations

Dussadee Somjaiwang, and Parinya Sa Ngiamsunthorn^C

*Department of Mathematics, Faculty of Science, King Mongkut's University of Technology Thonburi,
126 Pracha Uthit Road, Bang Mod, Thung Khru, Bangkok, Thailand
E-mail: parinya.san@kmutt.ac.th; Fax: +66 2 428 4025; Tel. +66 2 470 8828*

ABSTRACT

We study the existence of solutions of coupled fractional hybrid differential systems with order $0 < \alpha < 1$. The existence result is proved by constructing a sequence that approximates the coupled solution based on the coupled fixed point theorem of Dhage (2015). We also illustrate the result by numerical computation example.

Keywords: Hybrid differential equations, Caputo fractional derivative, Coupled fixed point, Approximation of solutions.

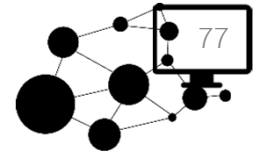
INTRODUCTION

Several real-world problems can be solved based on mathematical models in various areas such as natural sciences, social sciences, economics and humanities. These mathematical models are usually formulated in terms of ordinary differential equations, partial differential equations and neural network etc. Fractional order differential equations are the generalization of the class of ordinary differential equations. It has been interested by many researchers in recent years. Fractional order differential equations have been frequently used in epidemic model [1 – 7], physics [8 – 11], economics [12 – 14], biological systems [15, 16] and engineering [17]. One important type of differential equation which involves a perturbation term of derivatives is the hybrid differential equation. The details of this type of equation can be found, for example, in [18, 19]. Recently, hybrid differential equations have been used in modelling biological systems [20 – 24]. However, it is quite difficult to obtain analytical solutions of fractional hybrid differential equations. In such case, many researchers tend to analyze the solutions numerically or study existence results by using the theory of fixed point. In our previous work [25], the existence and approximation of solution are proved for fractional hybrid differential equations

$$\begin{aligned} \frac{d^\alpha}{dt^\alpha} [x(t) - f(t, x(t))] &= g(t, y(t)) & t \in J = [t_0, t_0 + a] \\ x(t_0) &= x_0 \end{aligned} \quad (1)$$

where the caputo fractional derivative of order $0 < \alpha < 1$ is concerned.

In this work, we extend the problem (1) to consider the coupled systems of fractional order differential equation which is important in biosciences, and other applications. There are several works on the coupled systems of fractional order differential equations, for example, [26 – 28]. Our focus is to prove the existence and approximation of solution of coupled fractional order differential systems of the form



$$\begin{aligned}
 \frac{d^\alpha}{dt^\alpha}[x(t) - f(t, x(t))] &= g(t, y(t)) & t \in J = [t_0, t_0 + a] \\
 x(t_0) &= x_0 \\
 \frac{d^\alpha}{dt^\alpha}[y(t) - f(t, y(t))] &= g(t, x(t)) & t \in J = [t_0, t_0 + a] \\
 y(t_0) &= y_0.
 \end{aligned} \tag{2}$$

The result of this work is proved based on coupled fixed point theorem of Dhange [32]. The results obtained both existence and approximation of solution which can be used in numerical computation. In the next section, we introduce basic concepts of Caputo fractional order differential equations. Section 3 is devoted for the proof of the existence and approximation result. Finally, in Section 4, we give a numerical example for solutions of coupled fractional hybrid differential systems.

THEORY AND RELATED WORKS

Suppose $a > 0$ and $t_0 \geq 0$ are given. We denoted by $J = [t_0, t_0 + a]$ for the closed and bounded interval in \mathbb{R} . The set of all continuous functions $x : J \rightarrow \mathbb{R}$ is denoted by $C(J, \mathbb{R})$. It is well known that the set $C(J, \mathbb{R})$ forms a Banach space with respect to the supremum norm $\| \cdot \|$ defined by

$$\|x\| = \sup_{t \in J} |x(t)|$$

for $x \in C(J, \mathbb{R})$.

We next give the definition of Caputo fractional derivative used in the differential system (2). Here, we study the coupled fractional hybrid ordinary differential equation (2) when the perturbation term $f \in C(J \times \mathbb{R}, \mathbb{R})$, $g \in C(J \times \mathbb{R}, \mathbb{R})$ and the initial data $x_0, y_0 \in \mathbb{R}$. The Caputo fractional order derivative can be stated as follows.

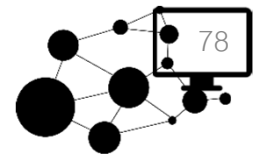
Definition 2.1 Let $\alpha > 0$, we define the left Caputo fractional derivative of order α as

$$D^\alpha f(t) = \begin{cases} \frac{1}{\Gamma(n-\alpha)} \int_a^t (t-s)^{n-\alpha-1} D^n f(s) ds, & n-1 < \alpha < n \\ \frac{d^n}{dt^n} f(t) & , \alpha = n \in \mathbb{N} \end{cases} \tag{3}$$

where $n \in \mathbb{N}$ such that $n - 1 < \alpha < n$ and $D = d/dt$.

Definition 2.2 The Riemann-Liouville fractional integral of order $\alpha > 0$ is defined as

$$I^\alpha f(t) = \frac{1}{\Gamma(\alpha)} \int_a^t (t-\tau)^{\alpha-1} D^n f(\tau) d\tau, \tag{4}$$



provided that the integral is pointwise defined on $[0, \infty)$.

Lemma 2.1 Let $\alpha > 0$. The Caputo type fractional order differential equation

$$\frac{d^\alpha}{dt^\alpha} y(t) = 0 \quad (5)$$

has a solution of the form

$$y(t) = c_0 + c_1 t + c_2 t^2 + \dots + c_{n-1} t^{n-1}, \quad (6)$$

where $c_i \in \mathbb{R}$, $i = 0, 1, \dots, n-1$ ($n = [\alpha] + 1$). Here $[\alpha]$ is the integral part of α .

Lemma 2.2 For $\alpha > 0$ and $y \in C^n[0, T]$, we have

$$I^\alpha \frac{d^\alpha}{dt^\alpha} y(t) = y(t) + c_0 + c_1 t + \dots + c_{n-1} t^{n-1}, \quad (7)$$

for some $c_i \in \mathbb{R}$, $i = 0, 1, 2, \dots, n-1$ ($n = [\alpha] + 1$).

In this works, we study mild solution of the coupled system as described by the definition below.

Definition 2.3 We say that a function $(x, y) \in E \times E$ is a solution of the coupled fractional hybrid differential equation (2) if the following integral equations hold

$$\begin{aligned} x(t) &= f(t, x(t)) + x_0 - f(t_0, x_0) + \int_{t_0}^t \frac{(t-s)^{\alpha-1}}{\Gamma(\alpha)} g(s, y(s)) ds, \quad t \in J \\ y(t) &= f(t, y(t)) + y_0 - f(t_0, y_0) + \int_{t_0}^t \frac{(t-s)^{\alpha-1}}{\Gamma(\alpha)} g(s, x(s)) ds, \quad t \in J \end{aligned} \quad (8)$$

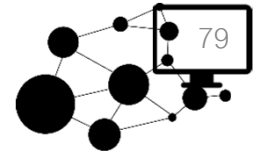
To investigate the existence of solutions, we consider the Banach space $C(J, \mathbb{R})$ equipped with a partially order relation $x \preceq y$ given that $x(t) \leq y(t)$ for all $t \in J$ whenever $x, y \in C(J, \mathbb{R})$.

We shall collect some results of coupled fixed point theory in partially ordered metric space.

Let (E, \preceq) be a partially ordered set and let d be a metric on E so that (E, \preceq, d) is a partially ordered metric space.

The space E is said to be regular if, for any nondecreasing (respectively, nonincreasing) sequence $\{x_n\}_{n \in \mathbb{N}}$ in E such that the sequence $x_n \rightarrow x$ as $n \rightarrow \infty$, we have $x_n \preceq x^*$ (respectively, $x_n \succeq x^*$) for all $n \in \mathbb{N}$. In particular, the space $C(J, \mathbb{R})$ is regular [29].

We may consider the product space $E \times E$ as a metric space under the metric d^* given by



$$d^* ((x, y), (w, z)) = d(x, w) + d(y, z),$$

for $(x, y), (w, z) \in E \times E$. We introduce a partial order as follows. For $(x_1, x_2), (y_1, y_2) \in E \times E$, we have

$$(x_1, x_2) \preceq (y_1, y_2) \leftrightarrow x_1 \preceq y_1 \text{ and } x_2 \succeq y_2.$$

From the above definition of partial order, it follows that the triplet $(E \times E, \preceq, d^*)$ is also a partially ordered metric space.

Let $T : E \times E \rightarrow E$ and consider the coupled mapping,

$$T(x, y) = x \quad \text{and} \quad T(y, x) = y.$$

We call a point $(x^*, y^*) \in E \times E$ a coupled solution or coupled fixed point for the coupled mapping if it satisfies

$$T(x^*, y^*) = x^* \quad \text{and} \quad T(y^*, x^*) = y^*.$$

For any $(x, y) \in E \times E$,

Definition 2.4 [30] Let $T : E \times E \rightarrow E$ be an operator. Then T is partially continuous at a point $(a, b) \in E \times E$ if for any $\varepsilon > 0$ there is $\delta > 0$ such that

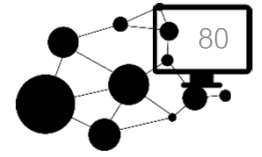
$$d^*(T(x, y), T(a, b)) < \varepsilon$$

whenever (x, y) is comparable to (a, b) and

$$d^*((x, y), (a, b)) < \delta.$$

The operator T is partially continuous on $E \times E$ if it is partially continuous at every point of $E \times E$. It is easily seen that if $T : E \times E \rightarrow E$ is partially continuous, then it is continuous on every totally ordered set or chain in $E \times E$.

Definition 2.5 [30] An operator $T : E \times E \rightarrow E$ is said to be mixed monotone if $T(x, y)$ is nondecreasing in x for each $y \in E$ and nonincreasing in y for each $x \in E$ under the order relation \preceq in E .



Note that if $T : E \times E \rightarrow E$ is mixed monotone, then it is a nondecreasing mapping on $E \times E$ under the order relation \preceq defined in $E \times E$.

Definition 2.6 [31] An operator $T : E \times E \rightarrow E$ is partially compact if $T(C_1, C_2)$ is a relatively compact subset of E for any chains C_1 and C_2 in E .

Definition 2.7 [30] Let E be a nonempty set equipped with an order relation and a metric d . The order relation and the metric d are said to be compatible whenever the following condition holds: if $\{x_n\}_{n \in \mathbb{N}}$ is a monotone sequence in E for which a subsequence $\{x_{n_k}\}_{k \in \mathbb{N}}$ of $\{x_n\}_{n \in \mathbb{N}}$ converges to x^* , then the whole sequence $\{x_n\}_{n \in \mathbb{N}}$ converges to x^* . Similarly, if $(E, \preceq, \|\cdot\|)$ is a partially ordered normed linear space, the order relation and the norm $\|\cdot\|$ are said to be compatible whenever the order relation and the metric d induced by the norm $\|\cdot\|$ are compatible.

Theorem 2.1 [32] Let (E, \preceq, d) be a regular partially ordered complete metric space. Suppose that the metric d and the order relation are compatible in every compact chain C of E .

Let $T : E \times E \rightarrow E$ be an operator satisfying mixed monotone, partially continuous and partially compact conditions. If there exist $x_0 \in E$ and $y_0 \in E$ such that $x_0 \preceq T(x_0, y_0)$ and $y_0 \succeq T(y_0, x_0)$, then T has a coupled fixed point (x^*, y^*) . In addition, the sequences x_n and y_n defined by

$$\begin{aligned}x_n &= T(x_{n-1}, y_{n-1}) = T^n(x_0, y_0) \\y_n &= T(y_{n-1}, x_{n-1}) = T^n(y_0, x_0)\end{aligned}$$

converge monotonically to x^* and y^* , respectively.

Next we state the assumptions to obtain the existence and approximation of solution of (2).

Assumption 1

A1 The functions $f : J \times \mathbb{R} \rightarrow \mathbb{R}$ and $g : J \times \mathbb{R} \rightarrow \mathbb{R}$ are continuous.

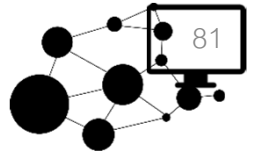
A2 f is nondecreasing in x for each $t \in J$ and $x \in \mathbb{R}$.

A3 There exists a constant $M_f > 0$ such that $0 \leq |f(t, x)| \leq M_f$ for all $t \in J$ and $x \in \mathbb{R}$.

B1 g is nonincreasing in x for each $t \in J$ and $x \in \mathbb{R}$.

B2 There exists a constant $M_g > 0$ such that $0 \leq |g(t, x)| \leq M_g$ for all $t \in J$ and $x \in \mathbb{R}$.

B3 There exists a lower coupled solution $(u, p) \in C(J, \mathbb{R}) \times C(J, \mathbb{R})$ of (2), that is,



$$\begin{aligned}
 \frac{d^\alpha}{dt^\alpha} [u(t) - f(t, u(t))] &\leq g(t, p(t)) & t \in J = [t_0, t_0 + a] \\
 u(t_0) &\leq x_0 \in \mathbb{R} \\
 \frac{d^\alpha}{dt^\alpha} [p(t) - f(t, p(t))] &\geq g(t, u(t)) & t \in J = [t_0, t_0 + a] \\
 p(t_0) &\geq y_0 \in \mathbb{R}
 \end{aligned} \tag{9}$$

EXISTENCE AND APPROXIMATION OF SOLUTIONS

In this section, we give a proof of the existence and approximation result for mild solutions of coupled fractional order hybrid differential equations.

Theorem 3.1 Suppose that all assumptions in (A1)–(A3) and (B1)–(B3) holds. Then the coupled fractional hybrid differential equation (2) has a solution $x^* : J \rightarrow \mathbb{R}$ and $y^* : J \rightarrow \mathbb{R}$. Moreover, the iterative sequence of approximations x_n and y_n for $n = 1, 2, \dots$, defined by

$$\begin{aligned}
 x_{n+1}(t) &= f(t, x_n(t)) + x_0 - f(t_0, x_0) + \int_{t_0}^t \frac{(t-s)^{\alpha-1}}{\Gamma(\alpha)} g(s, y_n(s)) ds, \\
 y_{n+1}(t) &= f(t, y_n(t)) + y_0 - f(t_0, y_0) + \int_{t_0}^t \frac{(t-s)^{\alpha-1}}{\Gamma(\alpha)} g(s, x_n(s)) ds, \\
 x_1(t) &= u(t) \\
 y_1(t) &= p(t)
 \end{aligned}$$

converge monotonically to x^* and y^* respectively.

Proof By choosing the partially ordered Banach space $E = C(J, \mathbb{R})$, we turn the problem of finding solution of (2) into finding a coupled fixed point solution of the operator

$T : E \times E \rightarrow E$ where

$$T(x, y)(t) = f(t, x(t)) + x_0 - f(t_0, x_0) + \int_{t_0}^t \frac{(t-s)^{\alpha-1}}{\Gamma(\alpha)} g(s, y(s)) ds \quad t \in J.$$

We verify that the conditions in Theorem 2.1 are satisfied.

Step I: Firstly, we prove that T is a mixed monotone operator on $E \times E$.

For any $y \in E$ and $x_1 \leq x_2$ in E , we obtain from assumption (A2), that

$$\begin{aligned}
 T(x_1, y)(t) &= f(t, x_1(t)) + x_0 - f(t_0, x_0) + \int_{t_0}^t \frac{(t-s)^{\alpha-1}}{\Gamma(\alpha)} g(s, y(s)) ds, \\
 &\leq f(t, x_2(t)) + x_0 - f(t_0, x_0) + \int_{t_0}^t \frac{(t-s)^{\alpha-1}}{\Gamma(\alpha)} g(s, y(s)) ds, \\
 &= T(x_2, y)(t)
 \end{aligned}$$

for all $t \in J$. Therefore, the operator T is also nonincreasing in y . Thus T is a mixed monotone operator T on $E \times E$.

Step II: In this step, we show that the operator T is partially continuous mixed monotone operator on $E \times E$.

For this, let $\{X_n\}_{n \in \mathbb{N}} = (x_n, y_n)$ be a monotone nondecreasing sequence in a chain $C = C_1 \times C_2$ of $E \times E$ such that $X_n = (x_n, y_n) \rightarrow (x, y) = X$ and $X_n \leq X$ for all $n \in \mathbb{N}$. We obtain from the dominated convergence theorem that

$$\begin{aligned}
 \lim_{n \rightarrow \infty} (TX_n)(t) &= \lim_{n \rightarrow \infty} \left(f(t, x_n(t)) + x_0 - f(t_0, x_0) + \int_{t_0}^t \frac{(t-s)^{\alpha-1}}{\Gamma(\alpha)} g(s, y_n(s)) ds, \right) \\
 &= \lim_{n \rightarrow \infty} f(t, x_n(t)) + \lim_{n \rightarrow \infty} x_0 - \lim_{n \rightarrow \infty} f(t_0, x_0) + \lim_{n \rightarrow \infty} \int_{t_0}^t \frac{(t-s)^{\alpha-1}}{\Gamma(\alpha)} g(s, y_n(s)) ds \\
 &= f(t, x(t)) + x_0 - f(t_0, x_0) + \lim_{n \rightarrow \infty} \int_{t_0}^t \frac{(t-s)^{\alpha-1}}{\Gamma(\alpha)} g(s, y(s)) ds \\
 &= T(X)(t)
 \end{aligned}$$

for each $t \in J$. This implies that $T X_n$ converges to $T X$ pointwise on J and the convergence is monotonic by the property of g . Next, we show that $T\{X_n\}_{n \in \mathbb{N}}$ is equicontinuous in E .

Let $t_1, t_2 \in J = [t_0, t_0 + a]$ such that $t_1 < t_2$. We have

$$\begin{aligned}
 &|T(X_n)(t_2) - T(X_n)(t_1)| \\
 &= \left| f(t_2, x_n(t_2)) - f(t_1, x_n(t_2)) + \int_{t_0}^{t_2} \frac{(t_2-s)^{\alpha-1}}{\Gamma(\alpha)} g(s, y_n(s)) ds - \int_{t_0}^{t_1} \frac{(t_1-s)^{\alpha-1}}{\Gamma(\alpha)} g(s, y_n(s)) ds \right| \\
 &\leq \left| f(t_2, x_n(t_2)) - f(t_1, x_n(t_1)) \right| + \left| \int_{t_0}^{t_2} \frac{(t_2-s)^{\alpha-1}}{\Gamma(\alpha)} g(s, y_n(s)) ds - \int_{t_0}^{t_1} \frac{(t_2-s)^{\alpha-1}}{\Gamma(\alpha)} g(s, y_n(s)) ds \right| \\
 &\quad + \left| \int_{t_0}^{t_1} \frac{(t_2-s)^{\alpha-1}}{\Gamma(\alpha)} g(s, y_n(s)) ds - \int_{t_0}^{t_1} \frac{(t_1-s)^{\alpha-1}}{\Gamma(\alpha)} g(s, y_n(s)) ds \right| \\
 &= \left| f(t_2, x_n(t_2)) - f(t_1, x_n(t_1)) \right| + \left| \int_{t_1}^{t_2} \frac{(t_2-s)^{\alpha-1}}{\Gamma(\alpha)} g(s, y_n(s)) ds \right| \\
 &\quad + \left| \frac{1}{\Gamma(\alpha)} \int_{t_0}^{t_1} [(t_2-s)^{\alpha-1} - (t_1-s)^{\alpha-1}] g(s, y_n(s)) ds \right| \\
 &\leq \left| f(t_2, x_n(t_2)) - f(t_1, x_n(t_1)) \right| + \frac{M_g}{\Gamma(\alpha)} \int_{t_1}^{t_2} |(t_2-s)^{\alpha-1}| ds + \frac{M_g}{\Gamma(\alpha)} \int_{t_0}^{t_1} |(t_2-s)^{\alpha-1} - (t_1-s)^{\alpha-1}| ds
 \end{aligned}$$

$$= |f(t_2, x_n(t_2)) - f(t_1, x_n(t_1))| + \frac{M_g}{\Gamma(\alpha)} a^{\alpha-1} (t_2 - t_1) + \frac{M_g}{\Gamma(\alpha)} \int_{t_0}^{t_2} |(t_2 - s)^{\alpha-1} - (t_1 - s)^{\alpha-1}| ds$$

$$\rightarrow 0,$$

as $t_2 - t_1 \rightarrow 0$ uniformly for all $n \in \mathbb{N}$, since f is continuous for all $t \in J$ and bounded. This implies that $T X_n \rightarrow T X$ uniformly. Therefore, T is partially continuous on $E \times E$.

Step III: Next we need to prove operator T is partially compact mixed monotone operator.

Let C_1 and C_2 be chains in E . We shall show that $T(C_1 \times C_2)$ is a relatively compact subset of E , that is, to show that $T(C_1 \times C_2)$ is uniformly bounded and equicontinuous in E . Let $x \in C_1$ and $y \in C_2$ be arbitrary. We have by hypothesis (A3) and (B2) that

$$|T(x, y)(t)| = \left| f(t, x(t)) + x_0 - f(t_0, x_0) + \int_{t_0}^{t_1} \frac{(t_1 - s)^{\alpha-1}}{\Gamma(\alpha)} g(s, x_n(s)) ds \right|$$

$$\leq M_f + |x_0 - f(t_0, x_0)| + \frac{M_g}{\Gamma(\alpha)} \int_{t_0}^{t_1} (t_1 - s)^{\alpha-1} ds$$

$$\leq M_f + |x_0 - f(t_0, x_0)| + \frac{M_g}{\Gamma(\alpha + 1)} (t_1 - t_0)^\alpha$$

$$= M_f + |x_0 - f(t_0, x_0)| + \frac{M_g}{\Gamma(\alpha + 1)} a^\alpha =: K$$

for all $t \in J$. Hence, we obtain $\|T(x, y)\| \leq K$ for all $x \in C_1$ and $y \in C_2$. This means $T(C_1 \times C_2)$ is uniformly bounded. We next show that $T(C_1 \times C_2)$ is equicontinuous. Taking $t_1, t_2 \in J$ and $t_2 > t_1$, then for any $m \in T(C_1 \times C_2)$, there exist $x \in C_1$ and $y \in C_2$ such that $m = T(x, y)$. We have

$$|m(t_2) - m(t_1)|$$

$$= \left| f(t_2, x(t_2)) - f(t_1, x(t_2)) + \int_{t_0}^{t_2} \frac{(t_2 - s)^{\alpha-1}}{\Gamma(\alpha)} g(s, y(s)) ds - \int_{t_0}^{t_1} \frac{(t_1 - s)^{\alpha-1}}{\Gamma(\alpha)} g(s, y(s)) ds \right|$$

$$\leq \left| f(t_2, x(t_2)) - f(t_1, x(t_1)) \right| + \left| \int_{t_0}^{t_2} \frac{(t_2 - s)^{\alpha-1}}{\Gamma(\alpha)} g(s, y(s)) ds - \int_{t_0}^{t_1} \frac{(t_2 - s)^{\alpha-1}}{\Gamma(\alpha)} g(s, y(s)) ds \right|$$

$$+ \left| \int_{t_0}^{t_1} \frac{(t_2 - s)^{\alpha-1}}{\Gamma(\alpha)} g(s, y(s)) ds - \int_{t_0}^{t_1} \frac{(t_1 - s)^{\alpha-1}}{\Gamma(\alpha)} g(s, y(s)) ds \right|$$

$$= \left| f(t_2, x(t_2)) - f(t_1, x(t_1)) \right| + \left| \int_{t_1}^{t_2} \frac{(t_2 - s)^{\alpha-1}}{\Gamma(\alpha)} g(s, y(s)) ds \right|$$

$$+ \left| \frac{1}{\Gamma(\alpha)} \int_{t_0}^{t_1} [(t_2 - s)^{\alpha-1} - (t_1 - s)^{\alpha-1}] g(s, y_n(s)) ds \right|$$

$$\begin{aligned}
 &\leq |f(t_2, x_n(t_2)) - f(t_1, x(t_1))| + \frac{M_g}{\Gamma(\alpha)} \int_{t_1}^{t_2} |(t_2 - s)^{\alpha-1}| ds + \frac{M_g}{\Gamma(\alpha)} \int_{t_0}^{t_2} |(t_2 - s)^{\alpha-1} - (t_1 - s)^{\alpha-1}| ds \\
 &= |f(t_2, x(t_2)) - f(t_1, x(t_1))| + \frac{M_g}{\Gamma(\alpha)} a^{\alpha-1} (t_2 - t_1) + \frac{M_g}{\Gamma(\alpha)} \int_{t_0}^{t_2} |(t_2 - s)^{\alpha-1} - (t_1 - s)^{\alpha-1}| ds \\
 &\rightarrow 0,
 \end{aligned}$$

as $t_2 - t_1 \rightarrow 0$ uniformly for $(x, y) \in C_1 \times C_2$ since f is continuous for all $t \in J$. This means that $T(C_1 \times C_2)$ is equicontinuous. It follows that $T(C_1 \times C_2)$ is relatively compact. Hence, T is partially compact.

Step IV: By hypothesis (B3), the fractional hybrid equation (2) has a lower coupled solution (u, p) defined on J , that is,

$$\begin{aligned}
 \frac{d^\alpha}{dt^\alpha} [u(t) - f(t, u(t))] &\leq g(t, p(t)) & t \in J = [t_0, t_0 + a] \\
 u(t_0) &\leq x_0 \in \mathbb{R} \\
 \frac{d^\alpha}{dt^\alpha} [p(t) - f(t, p(t))] &\geq g(t, u(t)) & t \in J = [t_0, t_0 + a] \\
 p(t_0) &\geq y_0 \in \mathbb{R}
 \end{aligned}$$

By formulating as a coupled solution, we have that

$$\begin{aligned}
 u(t) &\leq f(t, u(t)) + x_0 - f(t_0, x_0) + \int_{t_0}^t \frac{(t-s)^{\alpha-1}}{\Gamma(\alpha)} g(s, p(s)) ds, \\
 p(t) &\geq f(t, p(t)) + y_0 - f(t_0, y_0) + \int_{t_0}^t \frac{(t-s)^{\alpha-1}}{\Gamma(\alpha)} g(s, u(s)) ds,
 \end{aligned}$$

for $t \in J$. It follows that u satisfies the operator inequality $u \leq T(u, p)$ and $p \geq T(p, u)$.

Thus, we conclude that the operator T satisfies all conditions in Theorem 2.1. Then the operator $x = T(x, y)$ and $y = T(y, x)$ has a coupled solution (x, y) . Moreover, we can construct an approximation of a coupled solutions (x, y) as sequences x_n and y_n which converge monotonically to x and y , respectively. This completes the proof.

NUMERICAL EXAMPLE

We provide an example of coupled hybrid fractional differential equations in this section. In particular, we show that our main result can be applied to obtain an approximate sequence for a solution by using numerical computation.

Example 4.1 Consider the following coupled hybrid fractional differential system

$$\begin{aligned}
 \frac{d^\alpha}{dt^\alpha} [x(t) - \sqrt{5 + \tanh(x(t))}] &= g(t, y(t)), & t \in J = [0, 1] \\
 x(0) &= 0 \\
 \frac{d^\alpha}{dt^\alpha} [y(t) - \sqrt{5 + \tanh(y(t))}] &= g(t, x(t)), & t \in J = [0, 1] \\
 y(0) &= 2,
 \end{aligned} \tag{10}$$

where

$$g(t, x) = \begin{cases} \frac{1}{e^x} & x \geq 0, \\ 1 & x < 0. \end{cases}$$

It is clear that f and g are continuous functions on $J \times \mathbb{R}$. The functions on J . The conditions (A1) and (B1) are satisfied. The assumptions (A2),(A3), (B2) and (B3) are also true since because the function $f(t, x) = \sqrt{5 + \tanh(x)}$ is nondecreasing and it is bounded by $M_f = \sqrt{6}$ that is,

$$0 \leq |f(t, x)| \leq \sqrt{6}.$$

For the function g is nonincreasing bounded by $M_g = 1$, that is,

$$0 \leq |g(t, x)| \leq M_g = 1,$$

for all $t \in \mathbb{R}$ and $x, y \in \mathbb{R}$. Finally, in this example, we can choose a lower couple solution for assumption (B3) as $u(t) = 0$ and $p(t) = 3.5$ for all $t \in [0, 1]$ as

$$\begin{aligned} 0 &\leq f(t, u(t)) + x_0 - f(t_0, x_0) + \int_{t_0}^t \frac{(t-s)^{\alpha-1}}{\Gamma(\alpha)} g(s, p(s)) ds, \\ &\leq \frac{t^\alpha}{e^{3.5} \Gamma(\alpha+1)} \end{aligned}$$

and

$$\begin{aligned} 3.5 &\geq f(t, p(t)) + y_0 - f(t_0, y_0) + \int_{t_0}^t \frac{(t-s)^{\alpha-1}}{\Gamma(\alpha)} g(s, u(s)) ds \\ &= \sqrt{5 + \tanh(3.5)} + 2 - \sqrt{5 + \tanh(2)} + \frac{t^\alpha}{\Gamma(\alpha+1)}, \end{aligned}$$

for $t \in [0, 1]$. Then $(u(t), p(t)) = (0, 3.5)$ is a lower coupled solution. Since all assumptions are satisfied, we conclude from our main result in Theorem 2.1 that (10) has a solution $x : [0, 1] \rightarrow \mathbb{R}$ and $y : [0, 1] \rightarrow \mathbb{R}$ which is a limit of the monotone sequence x_n and y_n , $n = 1, 2, \dots$ defined by

$$\begin{aligned} x_{n+1}(t) &= f(t, x_n(t)) + x_0 - f(t_0, x_0) + \int_{t_0}^t \frac{(t-s)^{\alpha-1}}{\Gamma(\alpha)} g(s, y_n(s)) ds, \\ y_{n+1}(t) &= f(t, y_n(t)) + y_0 - f(t_0, y_0) + \int_{t_0}^t \frac{(t-s)^{\alpha-1}}{\Gamma(\alpha)} g(s, x_n(s)) ds, \end{aligned}$$

for all $t \in [0, 1]$,

The iterative sequence for the solution of (10) can be numerically computed as shown in Figure 1-3. Here, we compute the fractional order derivative when $\alpha = 0.25, 0.5,$ and $= 0.75$ and apply the trapezoidal rule with step size 0.002 for iteration scheme of the sequence x_n . Furthermore, we use the error between iterates $\|x_{n+1} - x_n\|$ as a criterion to stop the iteration when its value is less than 0.0017 since the exact explicit solutions are not available. The numerical results illustrate that the sequence of approximate solutions x_n and y_n converges monotonically.

CONCLUSION

We establish the existence result for solutions of coupled fractional order hybrid differential systems based the existence result for solutions of coupled fractional order hybrid differential Which is useful for numerical computation. In particular, we obtain sequences of functions that monotonically converge too solutions.

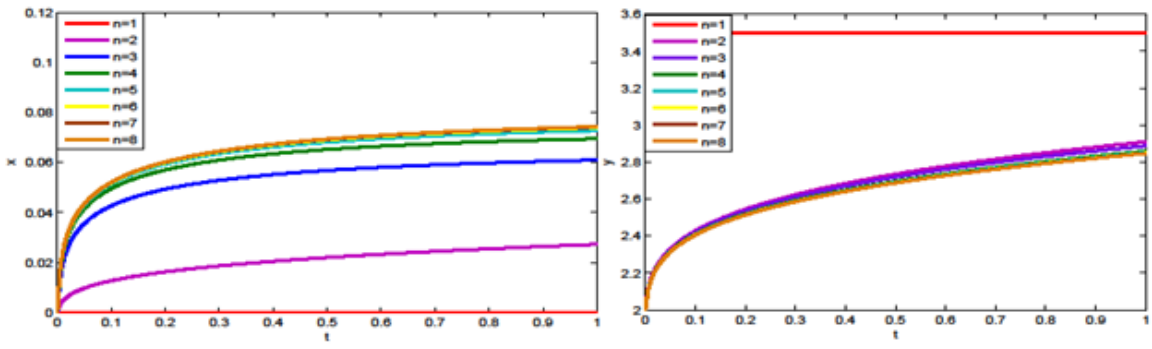


Figure 1. Graph of presented approximate solution of coupled systems hybrid fractional difference equation for $\alpha = 0.5$

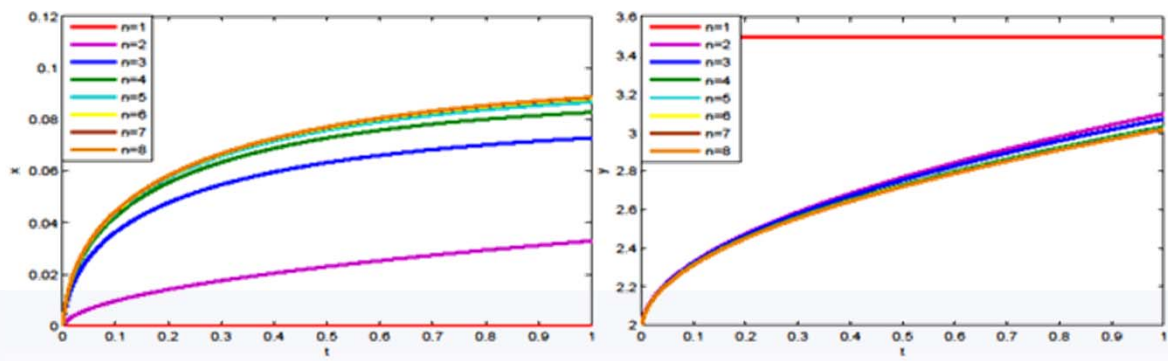


Figure 2. Graph of presented approximate solution of coupled systems hybrid fractional difference equation for $\alpha = 0.25$

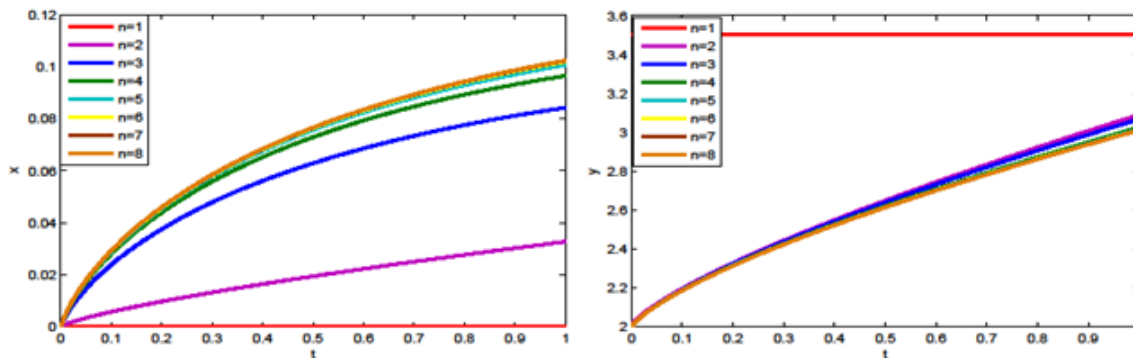
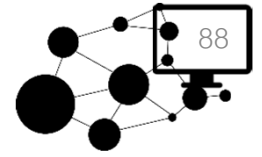


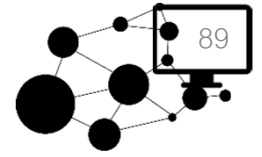
Figure 3. Graph of presented approximate solution of coupled systems hybrid fractional difference equation for $\alpha = 0.75$

REFERENCES

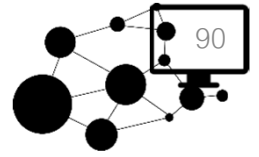
- [1] Arqub, O.A., El-Ajou, A., Solution of the fractional epidemic model by homotopy analysis method. *Journal of King Saud University - Science* **25**, 73–81 (2013)
- [2] El-Saka, H.A.A., The fractional-order sis epidemic model with variable population size. *Journal of the Egyptian Mathematical Society* **22**, 50–54 (2014)
- [3] Ameen, I., Novati, P., The solution of fractional order epidemic model by implicit adams methods. *Applied Mathematical Modelling*, 1–13 (2016)
- [4] Arenas, A.J., Gonz'alez-Parra, G., Chen-Charpentier, B.M., Construction of nonstandard finite difference schemes for the si and sir epidemic models of fractional order. *Mathematics and Computers in Simulation* **121**, 48–63 (2016)
- [5] Pinto, C.M.A., Carvalho, A.R.M., A latency fractional order model for hiv dynamics. *Journal of Computational and Applied Mathematics* **312**, 240–256 (2016)
- [6] Angstmann, C.N., Henry, B.I., McGann, A.V., A fractional-order infectivity sir model. *Physica A: Statistical Mechanics and its Applications* **452**, 86–93 (2016)
- [7] Huo, J., Zhao, H., Dynamical analysis of a fractional sir model with birth and death on heterogeneous complex networks. *Physica A: Statistical Mechanics and its Applications* **448**, 41–56 (2016)
- [8] Butera, S., Paola, M.D., A physically based connection between fractional calculus and fractal geometry. *Annals of Physics* **350**, 146–158 (2014)
- [9] Feng, Q., A new analytical method for seeking traveling wave solutions of space–time fractional partial differential equations arising in mathematical physics. *Optik - International Journal for Light and Electron Optics*, 1–19 (2016)
- [10] Feng, Q., Meng, F., Explicit solutions for space-time fractional partial differential equations in mathematical physics by a new generalized fractional jacobi elliptic equation-based sub-equation method. *Optik - International Journal for Light and Electron Optics* **127**, 1–19 (2016)
- [11] Butera, S., Paola, M.D., A physically based connection between fractional calculus and fractal geometry. *Annals of Physics* **350**, 146–158 (2014)
- [12] Wang, Z., Huang, X., Shen, H., Control of an uncertain fractional order economic system via adaptive sliding model. *Neurocomputing* **83**, 83–88 (2012)



- [13] Machado, J.A.T., Mata, M.E., Pseudo phase plane and fractional calculus modeling of western global economic downturn. *Communications in Nonlinear Science and Numerical Simulation* **22**, 396–406 (2015)
- [14] Hu, Z., Tu, X., A new discrete economic model involving generalized fractal derivative. *Advances in Difference Equations*, 1–11 (2015)
- [15] Toledo-Hernandez, R., Rico-Ramirez, V., Iglesias-Silva, G.A., Diwekar, U.M., A fractional calculus approach to the dynamic optimization of biological reactive systems. part i: Fractional models for biological reactions. *Chemical Engineering Science* **117**, 217–228 (2014)
- [16] Rihan, F.A., Numerical modeling of fractional-order biological systems. *Abstract and Applied Analysis*, 1–11 (2013)
- [17] Kumar, S., A new fractional modeling arising in engineering sciences and its analytical approximate solution. *Alexandria Engineering Journal* **52**, 813–819 (2013)
- [18] Dhage, B.C., Quadratic perturbations of periodic boundary value problems of second order ordinary differential equations. *Differential Equation and Applications* **2**(4), 465–486 (2010)
- [19] Noroozi, H., Ansari, A., Basic results on distributed order fractional hybrid differential equations with linear perturbations. *Journal of Mathematical Modeling* **2**(1), 55–73 (2014)
- [20] Sun, S., Zhao, Y., Han, Z., Li, Y., The existence of solutions for boundary value problem of fractional hybrid differential equations. *Commun Nonlinear Sci Numer Simulat* **17**, 4961–4967 (2012)
- [21] Ahmad, B., An existence theorem for fractional hybrid differential inclusions of hadamard type. *Differential Inclusions, Control and Optimization* **34**, 207–218 (2014)
- [22] Darwish, M.A., Sadarangani, K., Existence of solutions for hybrid fractional pantograph equation. *Applicable Analysis and Discrete Mathematics* **9**, 150–167 (2015)
- [23] E.T., K., K., L.B.a.S., About the existence of solutions for a hybrid nonlinear generalized fractional pantograph equation. *Fractional Differential Calculus*, 1–15 (2016)
- [24] Zhao, Y., Sun, S., Han, Z., Li, Q., Theory of fractional hybrid differential equations. *Computers and Mathematics with Applications* **62**, 1312–1324 (2011)
- [25] Somjaiwang, D., Sa Ngiamsunthorn, P., Existence and approximation of solutions to fractional order hybrid differential equations. *Advances in Difference Equations*, 1–11 (2016)
- [26] Ahmad, B., An existence theorem for fractional hybrid differential inclusions of hadamard type. *Differential Inclusions, Control and Optimization* **34**, 207–218 (2014)
- [27] Baleanu, D., Khan, H., Jafari, H., Khan, R.A., Alipour, M.: On existence results for solutions of a coupled system of hybrid boundary value problems with hybrid conditions. *Advances in Difference Equations*, 1–14 (2015)

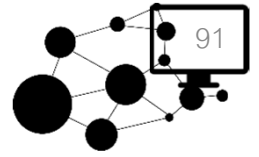


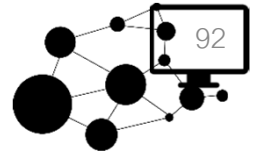
- [28] Bashiri, T., Mansour, S., Vaezpour, Park, C., A coupled fixed point theorem and application to fractional hybrid differential problems. *Advances in Difference Equations*, 1–11 (2016)
- [29] Dhage, B.C., Dhage, S.B., Ntouyas, S.K., Approximating solutions of nonlinear hybrid differential equations. *Applied Mathematics Letters* **34**, 76–80 (2014)
- [30] Dhage, B.C., Hybrid fixed point theory in partially ordered normed linear spaces and applications to fractional integral equations. *Differential Equations & Applications* **5**(2), 155–184 (2013)
- [31] Dhage, B., Partially condensing mappings in partially ordered normed linear spaces and applications to functional integral equations. *Tamkang Journal of Mathematics* **45**(4), 397–426 (2014)
- [32] Dhage, B.C., The dhage iteration principle for coupled pbvps of nonlinear second order differential equations. *International Journal of Analysis and Applications* **8**(1), 53–62 (2015)

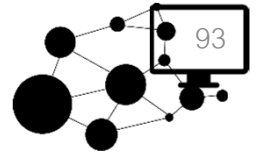


ANSCSE22 SPONSORED BY



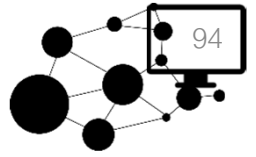


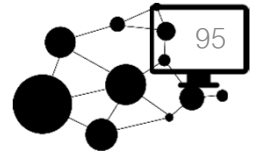




**Hewlett Packard
Enterprise**

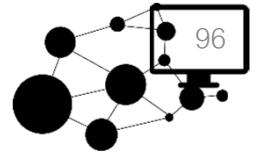






DELL EMC





wise life

